

Supporting Information

Umpolung Cyclization Reaction of *N*-Cinnamoylthioureas in the Presence of DBU

Rei Saito,^a Naohiro Uemura,^a Hiroki Ishikawa,^a Akina Magara,^a Yasushi Yoshida,^{a,b} Takashi Mino,^{a,b} Yoshio Kasashima,^c and Masami Sakamoto^{*a,b}

^aDepartment of Applied Chemistry and Biotechnology, Graduate School of Engineering, Yayoi-cho, Inage-ku, Chiba 265-8522, Japan

^bMolecular Chirality Research Center, Yayoi-cho, Inage-ku, Chiba 265-8522, Japan

^cEducation Center, Faculty of Creative Engineering, Chiba Institute of Technology, Shibazono, Narashino, Chiba 275-0023, Japan.

Contents

General	-----	S3
Single crystal X-Ray single crystallographic analysis of 2h	-----	S4
Single crystal X-Ray single crystallographic analysis of 2i	-----	S5
Single crystal X-Ray single crystallographic analysis of 2j	-----	S6
Single crystal X-Ray single crystallographic analysis of 3i	-----	S7
Single crystal X-Ray single crystallographic analysis of 3j	-----	S8
Single crystal X-Ray single crystallographic analysis of 4j	-----	S9
Single crystal X-Ray single crystallographic analysis of 5c	-----	S10
¹ H and ¹³ C NMR spectral chart of 1a-1j	-----	S11
¹ H and ¹³ C NMR spectral chart of 2a-2j	-----	S21
¹ H and ¹³ C NMR spectral chart of 3-5	-----	S31

General.

NMR spectra were recorded in CDCl_3 solutions on Bruker 300 and 400 spectrometers for ^1H - and ^{13}C -NMR. Chemical shifts are reported in parts per million (ppm) relative to TMS as an internal standard. IR spectra were recorded on a JASCO FT/IR-230 spectrometer. High-resolution mass spectra (HRMS) were performed on an Orbitrap ThermoFisher Exactive ion trap mass spectrometer. X-ray single crystallographic analysis was conducted using a SMART APEX II (Bruker AXS) and APEX II ULTRA (Bruker AXS). Commercially available reagents and solvents were used without further purification.

Single crystal X-Ray crystallographic analysis of 2h (CCDC 1859352)

Colorless prism ($0.20 \times 0.10 \times 0.05$ mm 3), monoclinic space group $P2_1/c$, $a = 12.8458(5)$ Å, $b = 5.3427(2)$ Å, $c = 24.6144(10)$ Å, $\beta = 101.767(3)$ °, $V = 1653.82(11)$ Å 3 , $Z = 4$, λ (CuK α) = 1.54178 Å, $\rho = 1.303$ g/cm 3 , μ (CuK α) = 1.776 mm $^{-1}$, 10898 reflections measured ($T = 173$ K, $3.514^\circ < \theta < 68.341^\circ$), nb of independent data collected: 3012, nb of independent data used for refinement: 2264 in the final least-squares refinement cycles on F^2 , the model converged at $R_1 = 0.0495$, $wR_2 = 0.1324$ [$|I| > 2s(I)$], $R_1 = 0.0696$, $wR_2 = 0.1416$ (all data), and GOF = 1.007, H-atom parameters constrained.

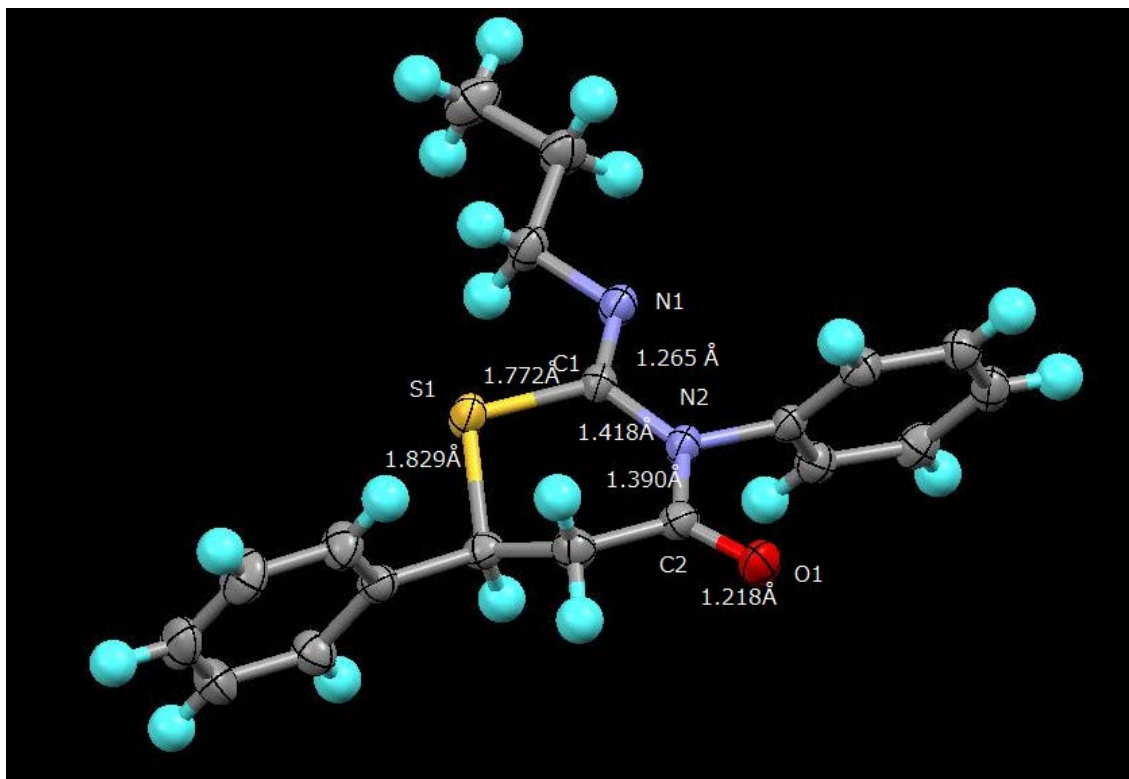


Figure S1. Perspective view of **2h**. Ellipsoids were drawn in 50% probability. Torsional angles: S-C1-N1-C2: 4.09 °, S-C1-N2-C2: 11.13 °, C1-N2-C1-O1: 5.29 °, C2-N1-C1-N1: 11.5 °.

Single crystal X-Ray structure analysis of **2i (CCDC 1859353)**

Colorless prism ($0.20 \times 0.05 \times 0.05 \text{ mm}^3$), monoclinic space group $P2_1/c$, $a = 13.0104(7) \text{ \AA}$, $b = 5.4301(3) \text{ \AA}$, $c = 24.2997(15) \text{ \AA}$, $\beta = 101.772(4)^\circ$, $V = 1680.61(17) \text{ \AA}^3$, $Z = 4$, $\lambda (\text{CuK}\alpha) = 1.54178 \text{ \AA}$, $\rho = 1.282 \text{ g/cm}^3$, $\mu (\text{CuK}\alpha) = 1.747 \text{ mm}^{-1}$, 11611 reflections measured ($T = 173 \text{ K}$, $3.470^\circ < \theta < 68.239^\circ$), nb of independent data collected: 3051, nb of independent data used for refinement: 2600 in the final least-squares refinement cycles on F^2 , the model converged at $R_1 = 0.0468$, $wR_2 = 0.1307 [I > 2s(I)]$, $R_1 = 0.0545$, $wR_2 = 0.1367$ (all data), and GOF = 1.029, H-atom parameters constrained.

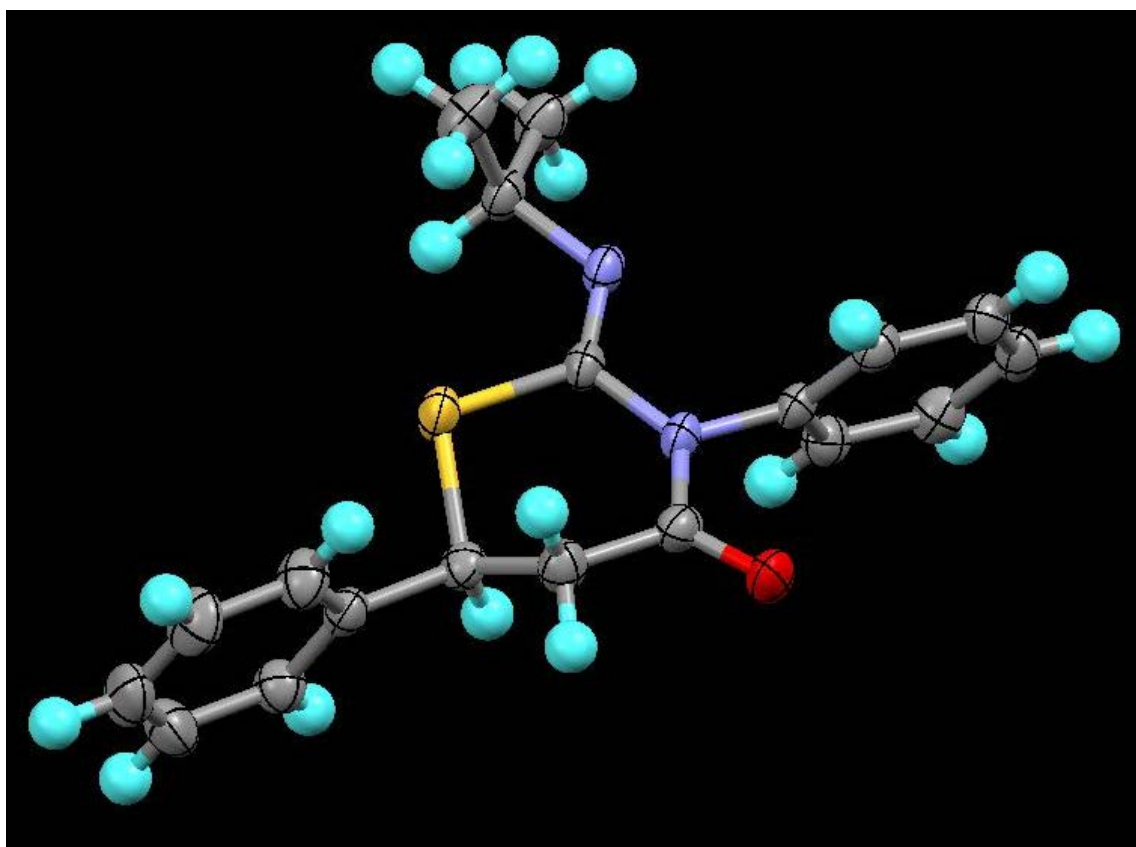


Figure S2. Perspective view of **2i**. Ellipsoids were drawn in 50% probability.

Single crystal X-Ray structure analysis of 2j (CCDC 1859354)

Colorless prism ($0.50 \times 0.20 \times 0.10 \text{ mm}^3$), monoclinic space group $P2_1/c$, $a = 13.613(2) \text{ \AA}$, $b = 5.3251(9) \text{ \AA}$, $c = 26.026(4) \text{ \AA}$, $\beta = 95.958(3)^\circ$, $V = 1876.4(6) \text{ \AA}^3$, $Z = 4$, $\lambda(\text{MoK}\alpha) = 0.71073 \text{ \AA}$, $\rho = 1.318 \text{ g/cm}^3$, $\mu(\text{MoK}\alpha) = 0.188 \text{ mm}^{-1}$, 10165 reflections measured ($T = 173 \text{ K}$, $1.504^\circ < \theta < 27.502^\circ$), nb of independent data collected: 4244, nb of independent data used for refinement: 2649 in the final least-squares refinement cycles on F^2 , the model converged at $R_1 = 0.0521$, $wR_2 = 0.1235 [I > 2s(I)]$, $R_1 = 0.0974$, $wR_2 = 0.1579$ (all data), and GOF = 0.966, H-atom parameters constrained.

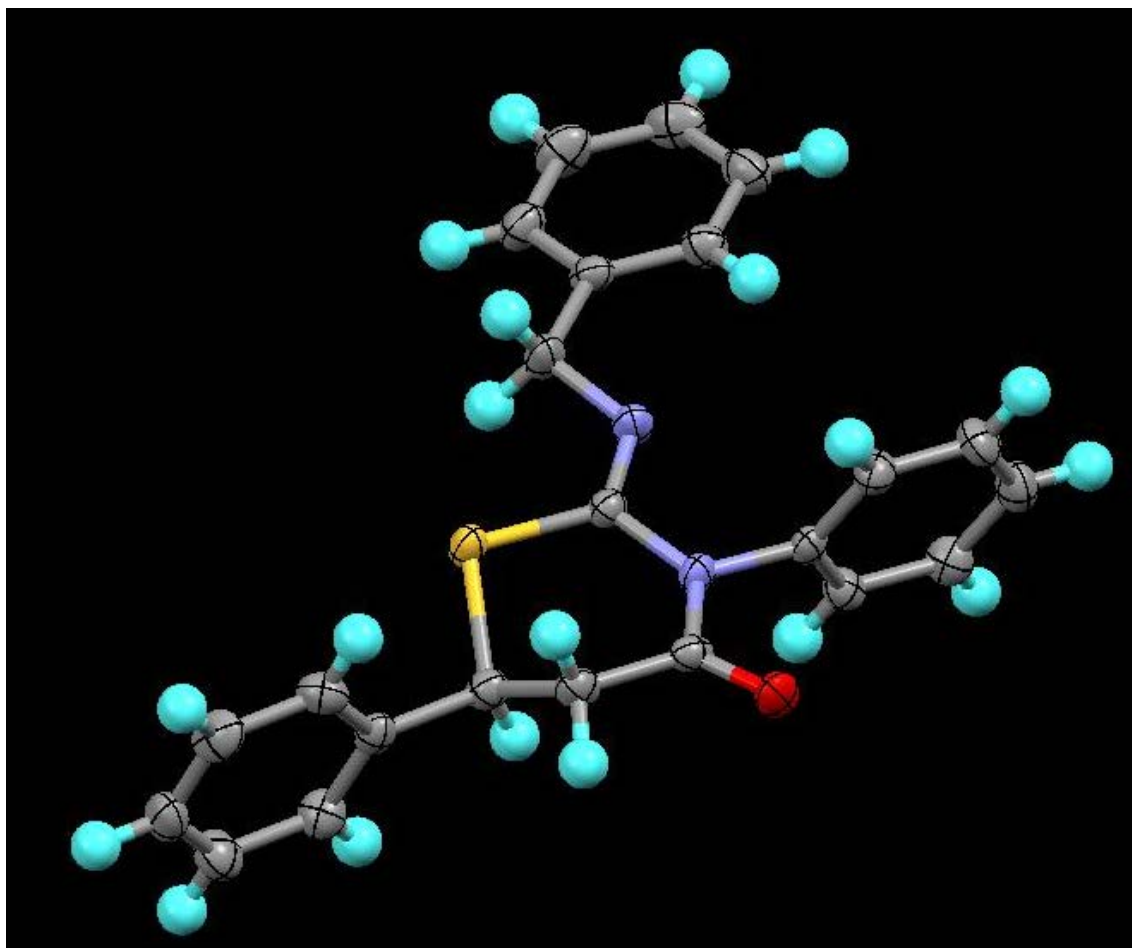


Figure S3. Perspective view of **2j**. Ellipsoids were drawn in 50% probability.

Single crystal X-Ray structure analysis of 3i (CCDC 1859407)

Colorless prism ($0.30 \times 0.20 \times 0.10 \text{ mm}^3$), monoclinic space group $P2_1/c$, $a = 12.4130(15) \text{ \AA}$, $b = 17.816(2) \text{ \AA}$, $c = 7.9085(10) \text{ \AA}$, $\beta = 106.841(2)^\circ$, $V = 1674.0(4) \text{ \AA}^3$, $Z = 4$, $\lambda (\text{MoK}\alpha) = 0.71073 \text{ \AA}$, $\rho = 1.287 \text{ g/cm}^3$, $\mu (\text{MoK}\alpha) = 0.199 \text{ mm}^{-1}$, 9554 reflections measured ($T = 173 \text{ K}$, $2.5558^\circ < \square < 27.5219^\circ$), nb of independent data collected: 3838, nb of independent data used for refinement: 2379 in the final least-squares refinement cycles on F^2 , the model converged at $R_1 = 0.0512$, $wR_2 = 0.1170$ [$I > 2s(I)$], $R_1 = 0.0924$, $wR_2 = 0.1447$ (all data), and GOF = 0.929, H-atom parameters constrained.

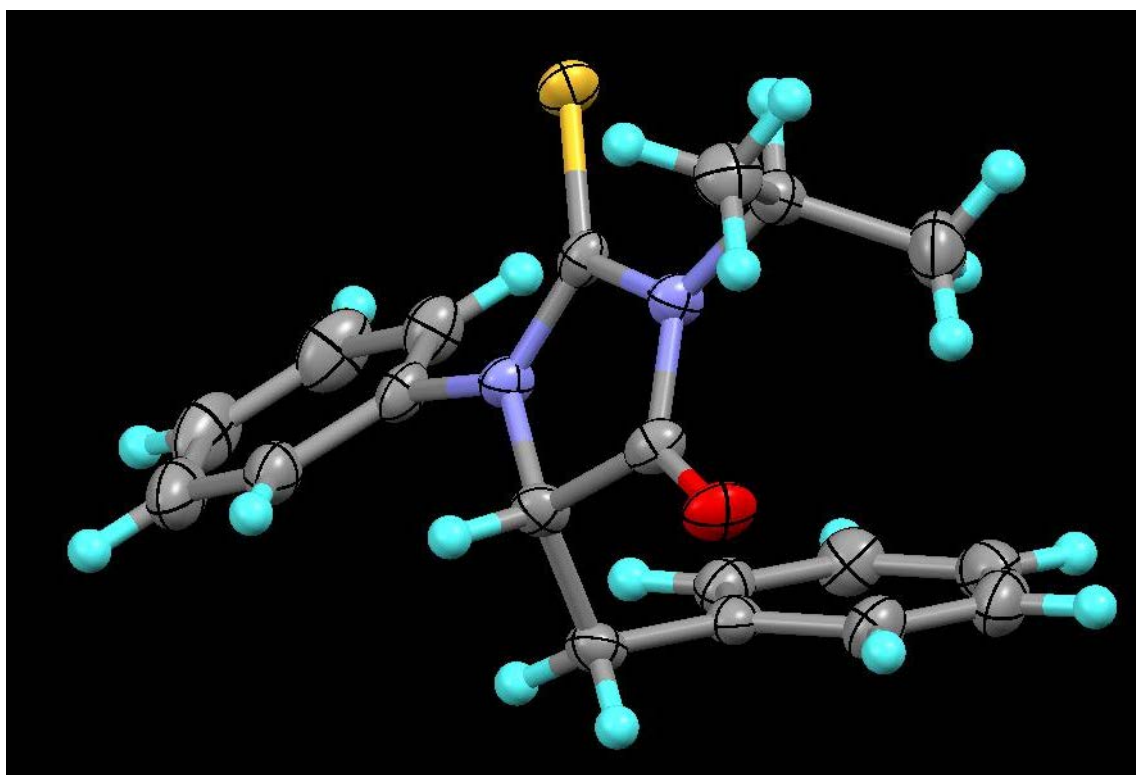


Figure S4. Perspective view of **3i**. Ellipsoids were drawn in 50% probability.

Single crystal X-Ray structure analysis of 3j (CCDC 1859355)

Colorless prism ($0.50 \times 0.50 \times 0.10 \text{ mm}^3$), triclinic space group $P\bar{1}$, $a = 8.887(2) \text{ \AA}$, $b = 9.348(2) \text{ \AA}$, $c = 12.182(3) \text{ \AA}$, $\alpha = 80.025(3)^\circ$, $\beta = 72.125(3)^\circ$, $\gamma = 88.273(3)^\circ$, $V = 948.3(4) \text{ \AA}^3$, $Z = 2$, $\lambda (\text{MoK}\alpha) = 0.71073 \text{ \AA}$, $\rho = 1.304 \text{ g/cm}^3$, $\mu (\text{MoK}\alpha) = 0.186 \text{ mm}^{-1}$, 5472 reflections measured ($T = 173 \text{ K}$, $2.2128^\circ < \theta < 27.5491^\circ$), nb of independent data collected: 4141, nb of independent data used for refinement: 3585 in the final least-squares refinement cycles on F^2 , the model converged at $R_1 = 0.0365$ $wR_2 = 0.0914$ [$I > 2s(I)$], $R_1 = 0.0429$, $wR_2 = 0.0954$ (all data), and GOF = 1.065, H-atom parameters constrained.

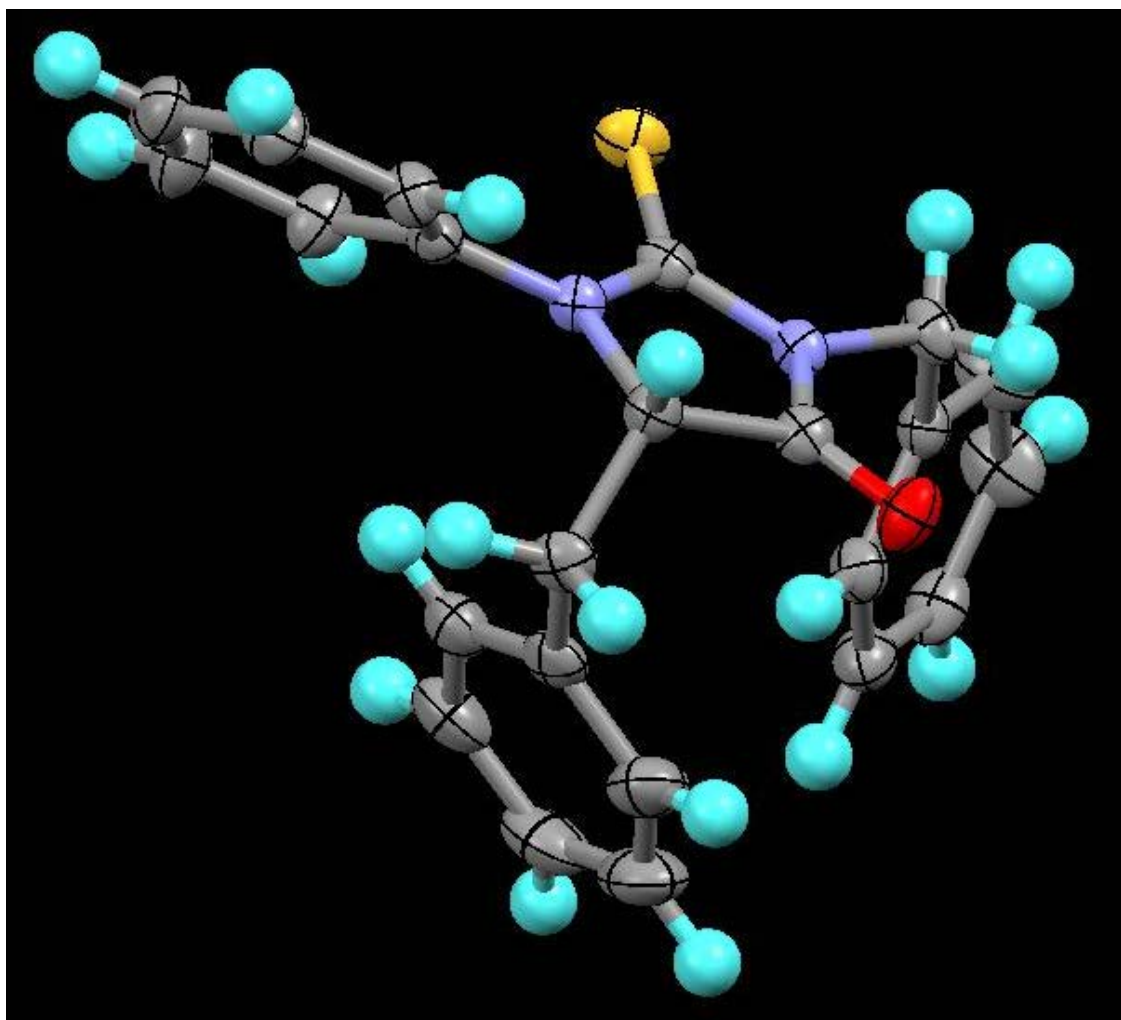


Figure S5. Perspective view of 3j. Ellipsoids were drawn in 50% probability.

Single crystal X-Ray structure analysis of 4g (CCDC 1859357)

Colorless prism ($0.50 \times 0.50 \times 0.10 \text{ mm}^3$), monoclinic space group $C2/c$, $a = 34.665(4) \text{ \AA}$, $b = 6.9265(9) \text{ \AA}$, $c = 14.4146(18) \text{ \AA}$, $\beta = 113.1370(10)^\circ$, $V = 3182.7(7) \text{ \AA}^3$, $Z = 8$, $\lambda (\text{MoK}\alpha) = 0.71073 \text{ \AA}$, $\rho = 1.296 \text{ g/cm}^3$, $\mu (\text{MoK}\alpha) = 0.207 \text{ mm}^{-1}$, 17622 reflections measured ($T = 173 \text{ K}$, $2.5558^\circ < \theta < 27.5219^\circ$), nb of independent data collected: 3651, nb of independent data used for refinement: 3146 in the final least-squares refinement cycles on F^2 , the model converged at $R_1 = 0.0310$, $wR_2 = 0.0789 [I > 2s(I)]$, $R_1 = 0.0380$, $wR_2 = 0.0871$ (all data), and GOF = 1.042, H-atom parameters constrained.

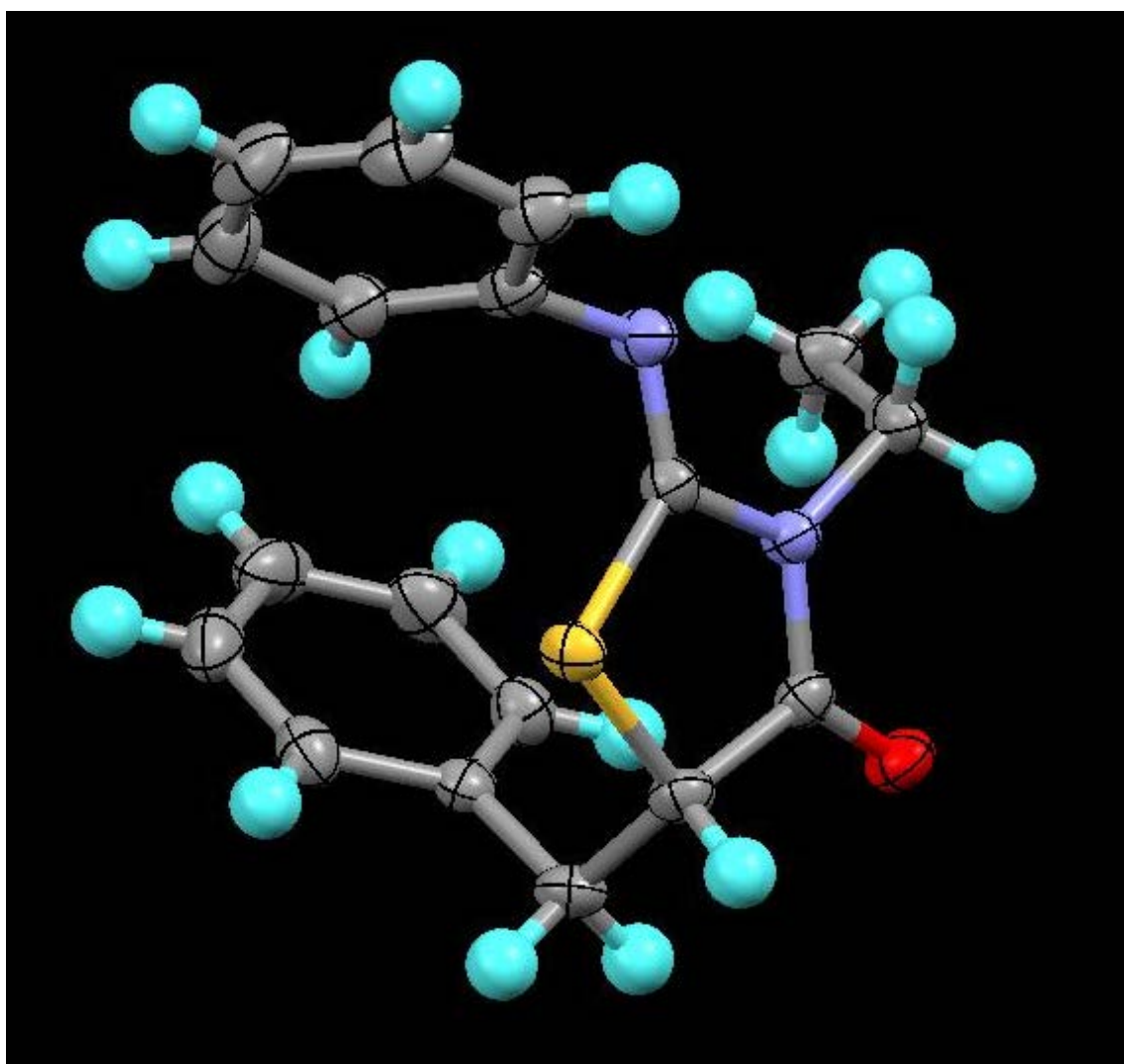


Figure S6. Perspective view of **4g**. Ellipsoids were drawn in 50% probability.

Single crystal X-Ray structure analysis of 5c (CCDC 1859359)

Colorless prism ($0.40 \times 0.30 \times 0.10 \text{ mm}^3$), triclinic space group $P\bar{1}$, $a = 8.7745(14) \text{ \AA}$, $b = 9.4352(16) \text{ \AA}$, $c = 20.409(3) \text{ \AA}$, $\alpha = 93.504(2)^\circ$, $\beta = 97.479(2)^\circ$, $\gamma = 90.918(2)^\circ$, $V = 1671.6(5) \text{ \AA}^3$, $Z = 4$, $\lambda (\text{MoK}\alpha) = 0.71073 \text{ \AA}$, $\rho = 1.218 \text{ g/cm}^3$, $\mu (\text{MoK}\alpha) = 0.200 \text{ mm}^{-1}$, 9602 reflections measured ($T = 173 \text{ K}$, $2.1632^\circ < \theta < 23.5028^\circ$), nb of independent data collected: 7319, nb of independent data used for refinement: 4764 in the final least-squares refinement cycles on F^2 , the model converged at $R_1 = 0.0538$, $wR_2 = 0.1302 [I > 2s(I)]$, $R_1 = 0.0851$, $wR_2 = 0.1602$ (all data), and GOF = 0.999, H-atom parameters constrained.

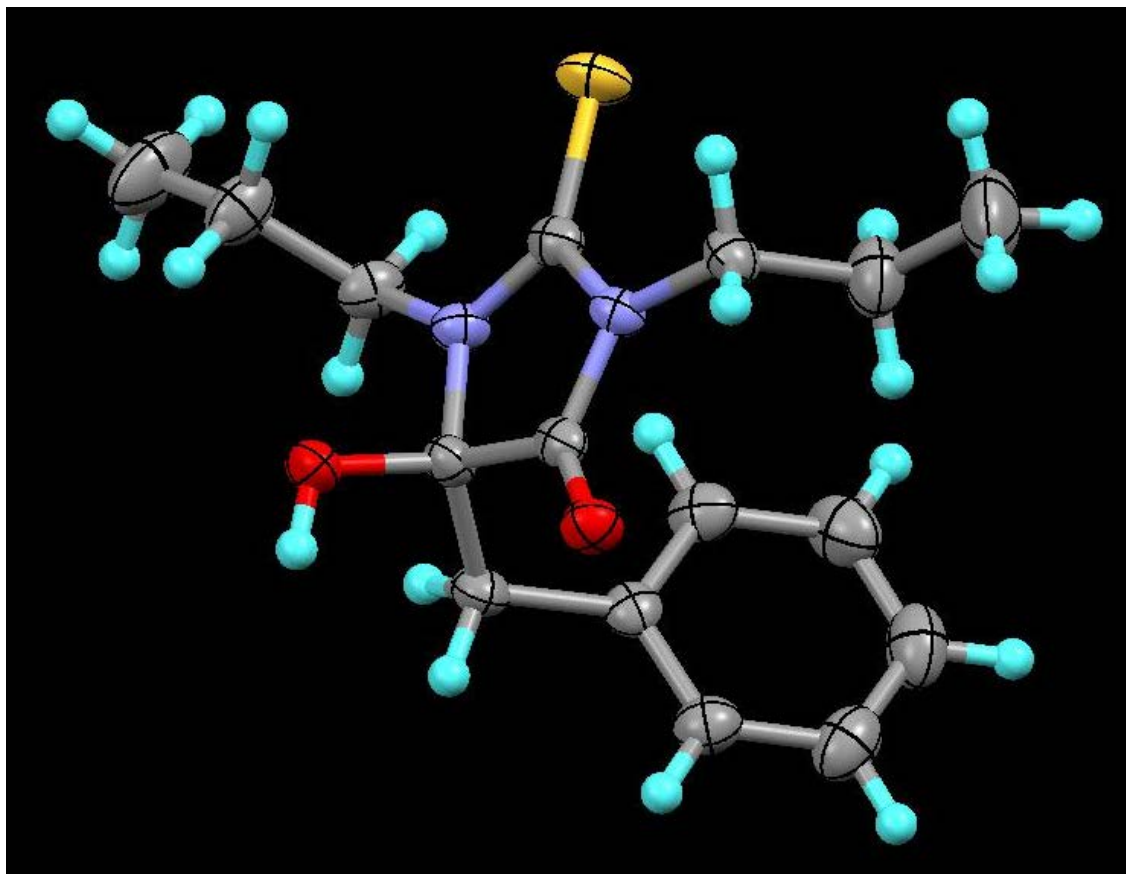


Figure S7. Perspective view of **5c**. Ellipsoids were drawn in 50% probability.

Figure S8. ^1H and ^{13}C NMR spectra of **1a**

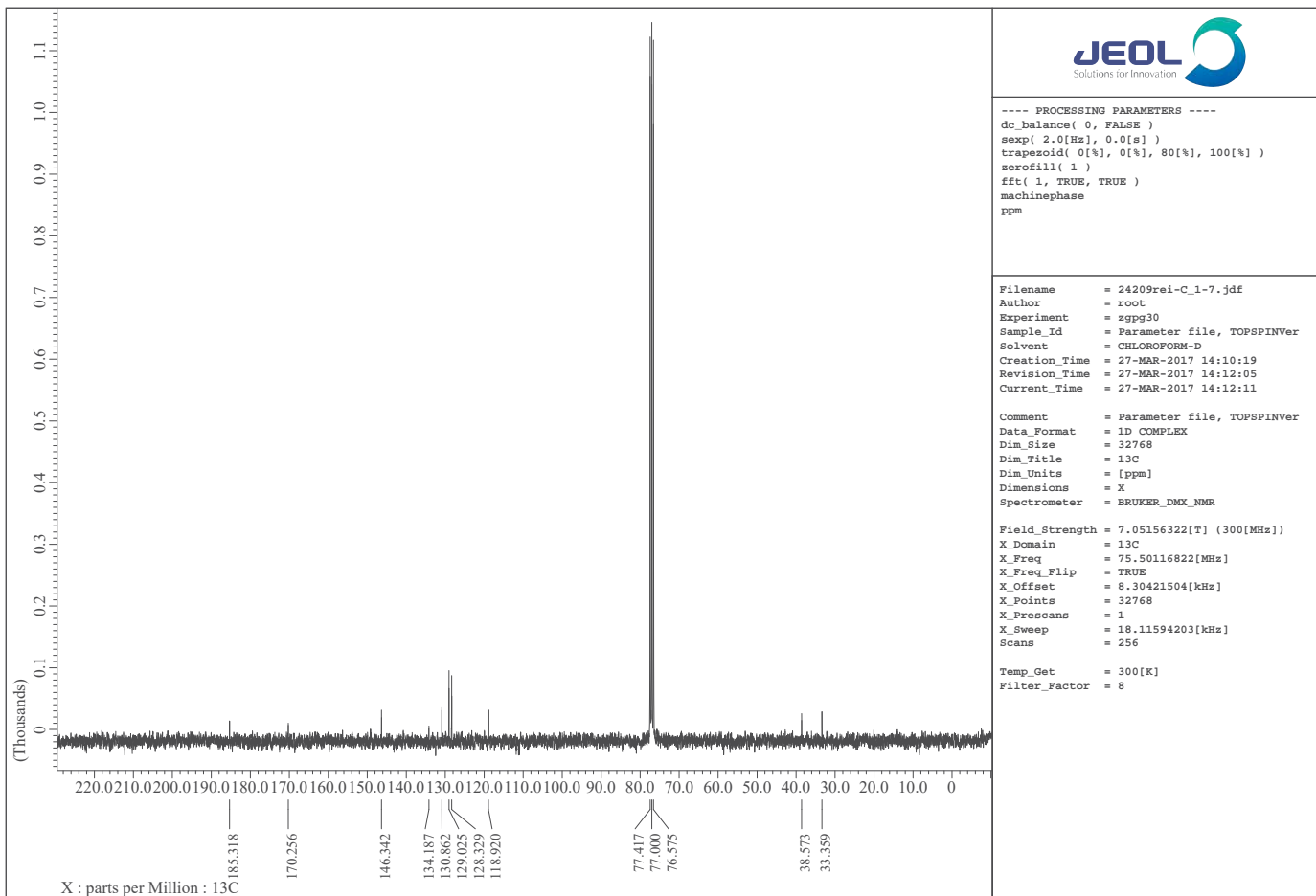
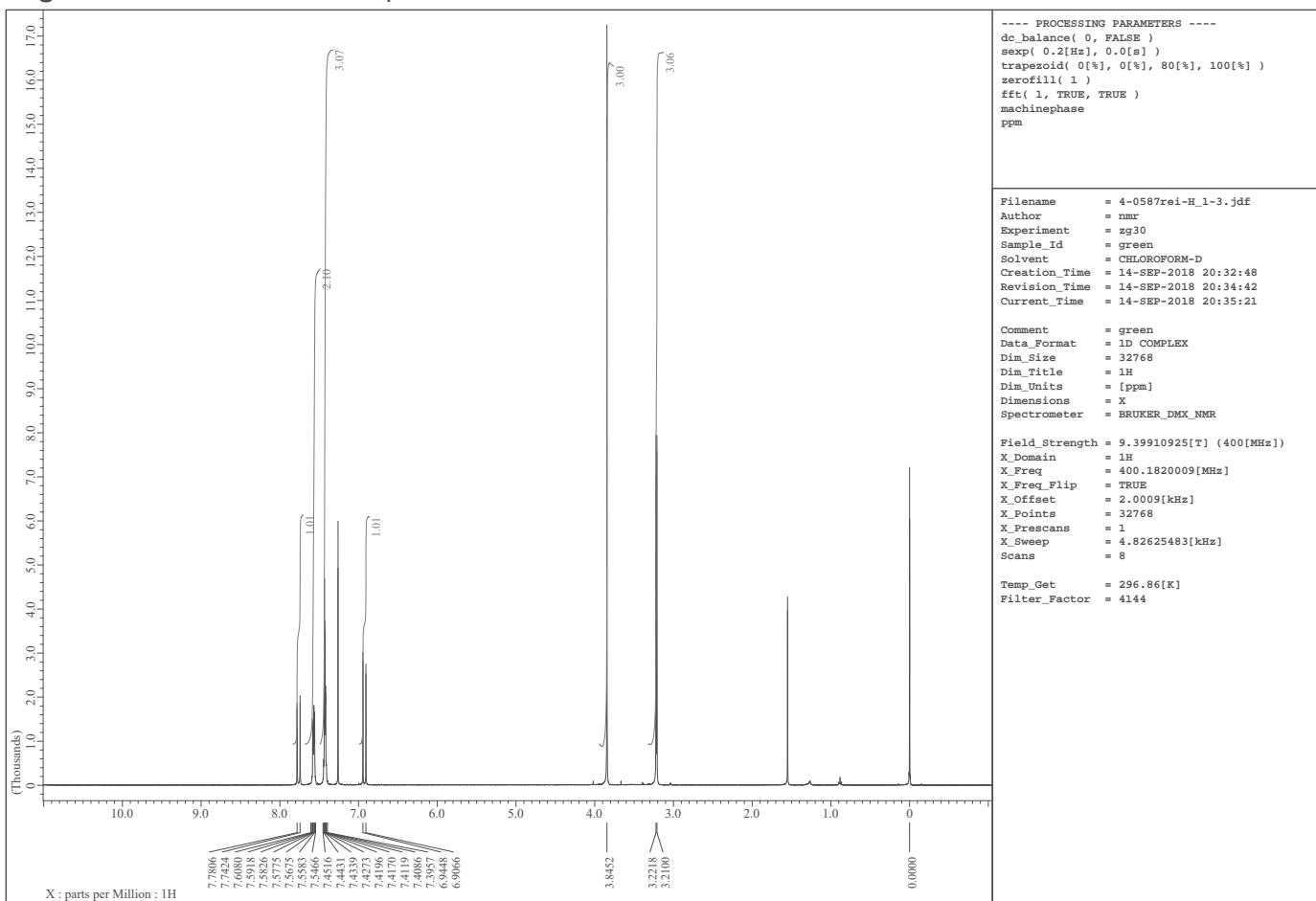
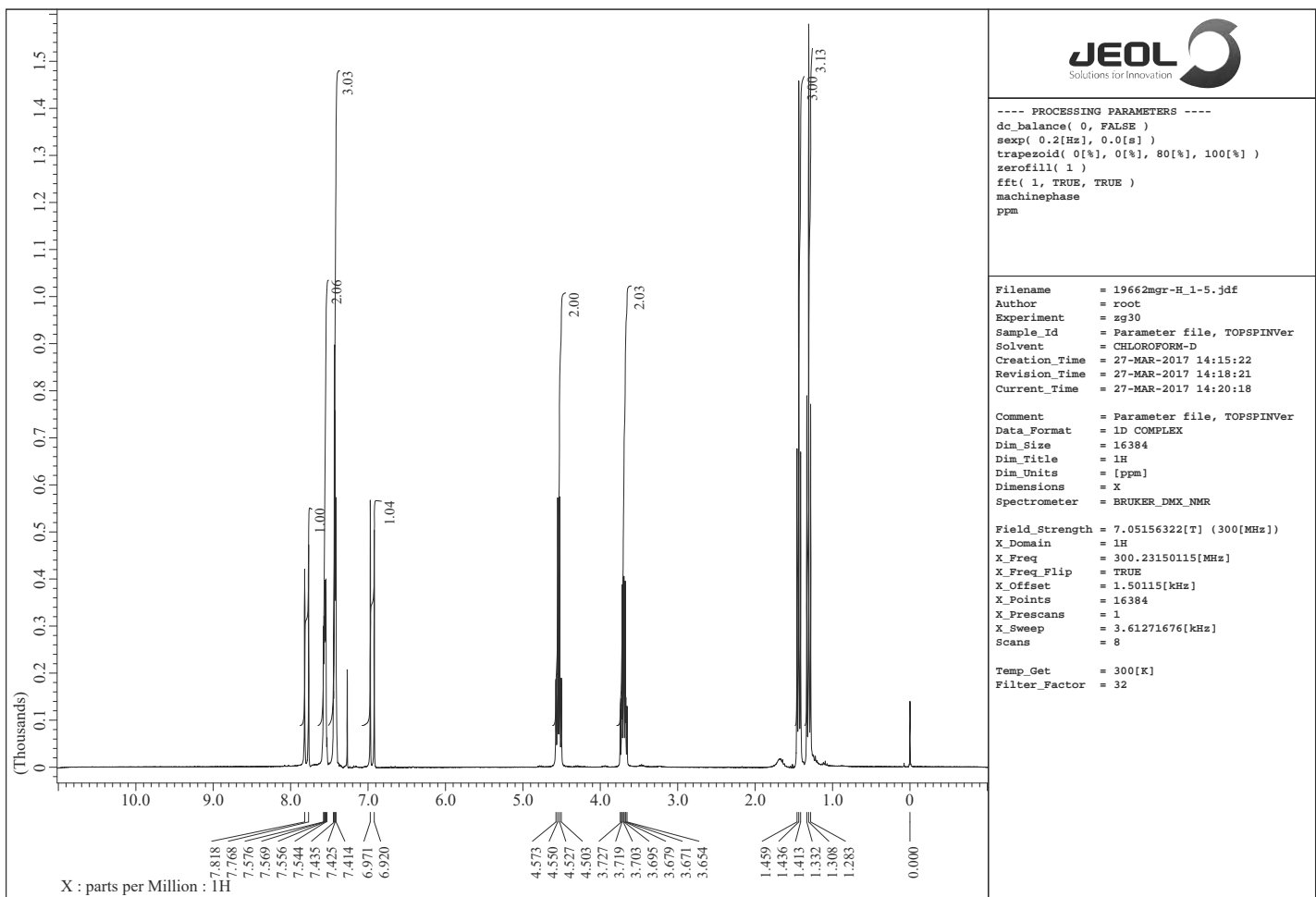
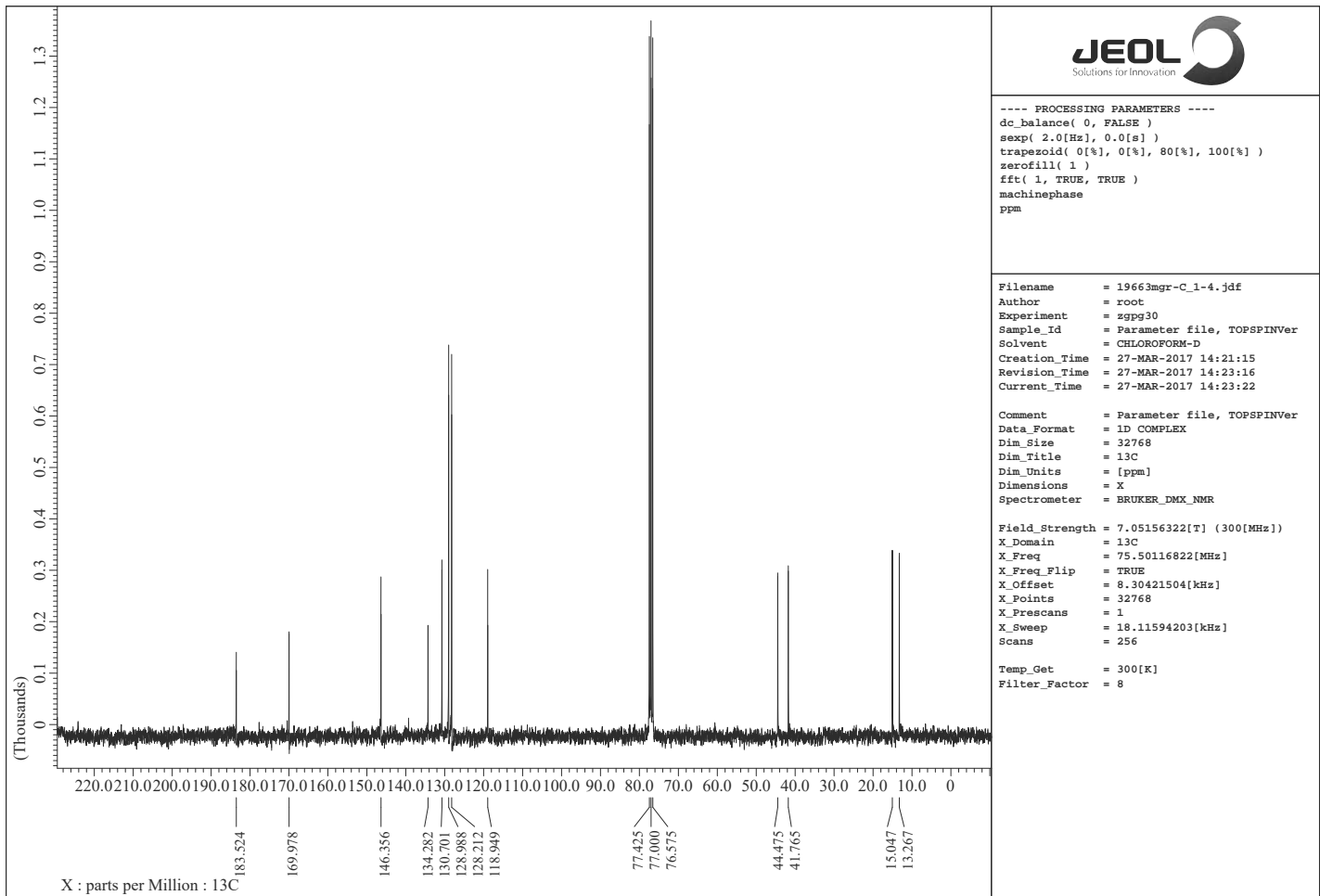


Figure S9. ^1H and ^{13}C NMR spectra of **1b**

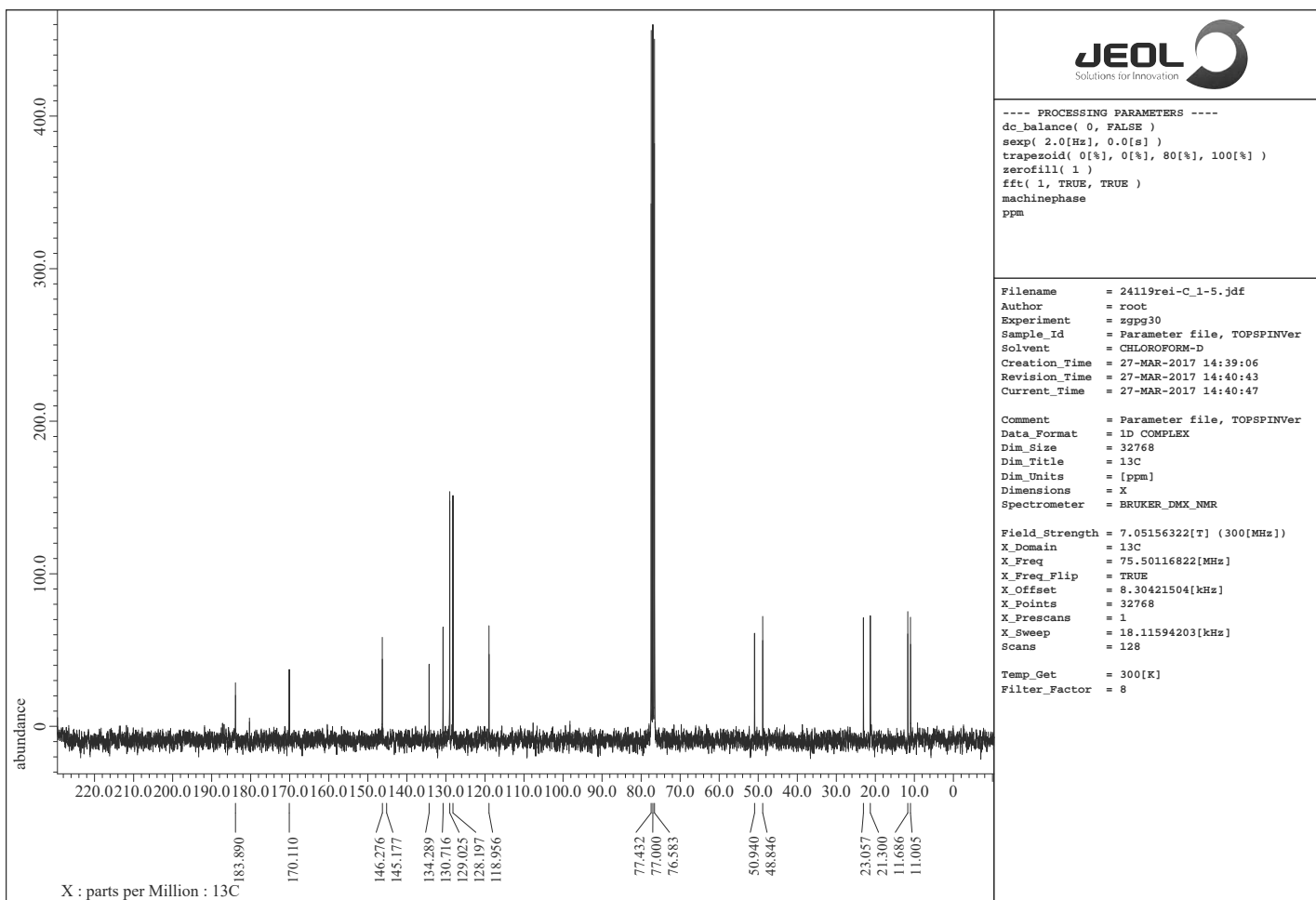
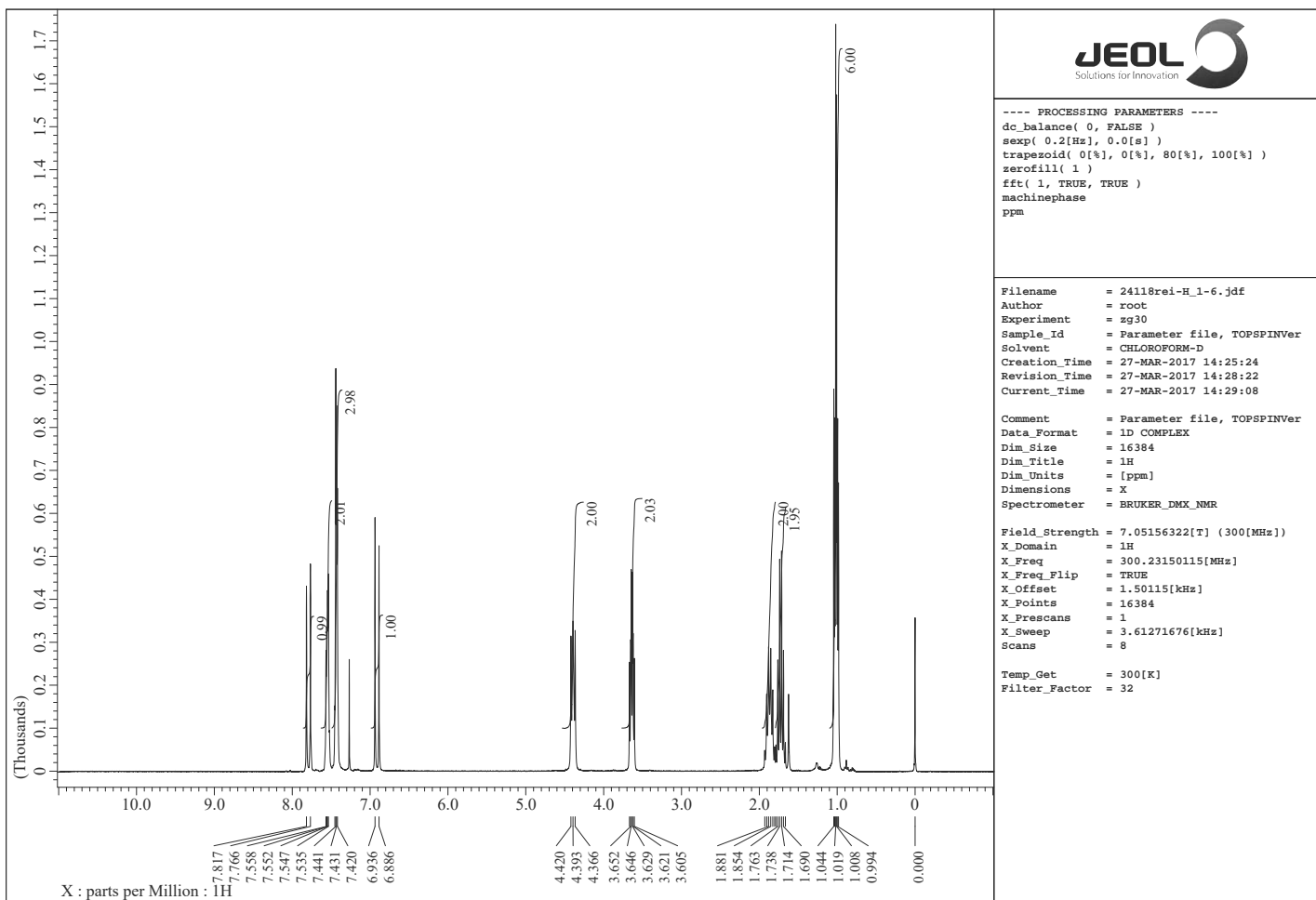


<<S11>>



<<S12>>

Figure S10. ^1H and ^{13}C NMR spectra of **1c**



<<S13>>

Figure S11. ^1H and ^{13}C NMR spectra of **1d**

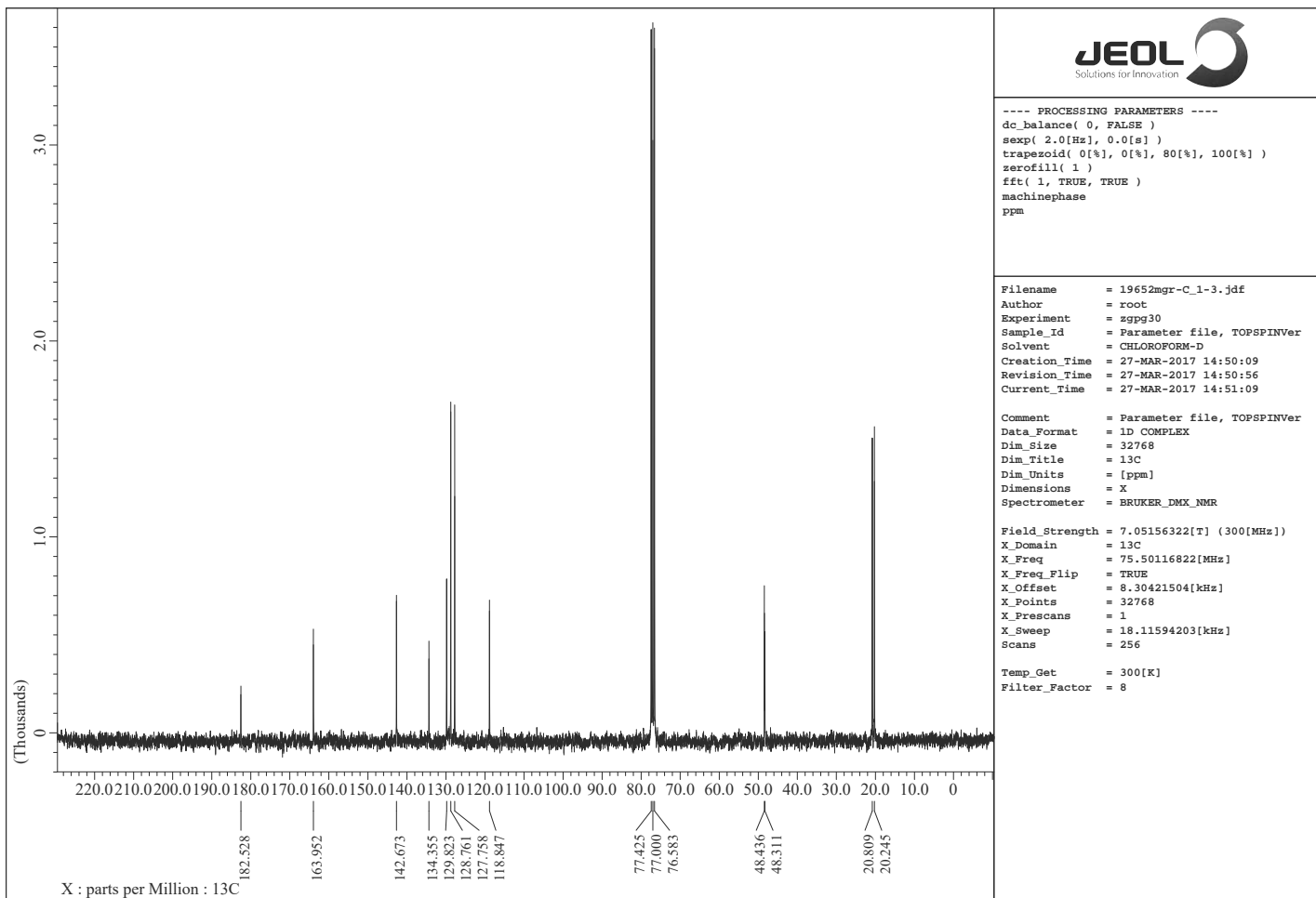
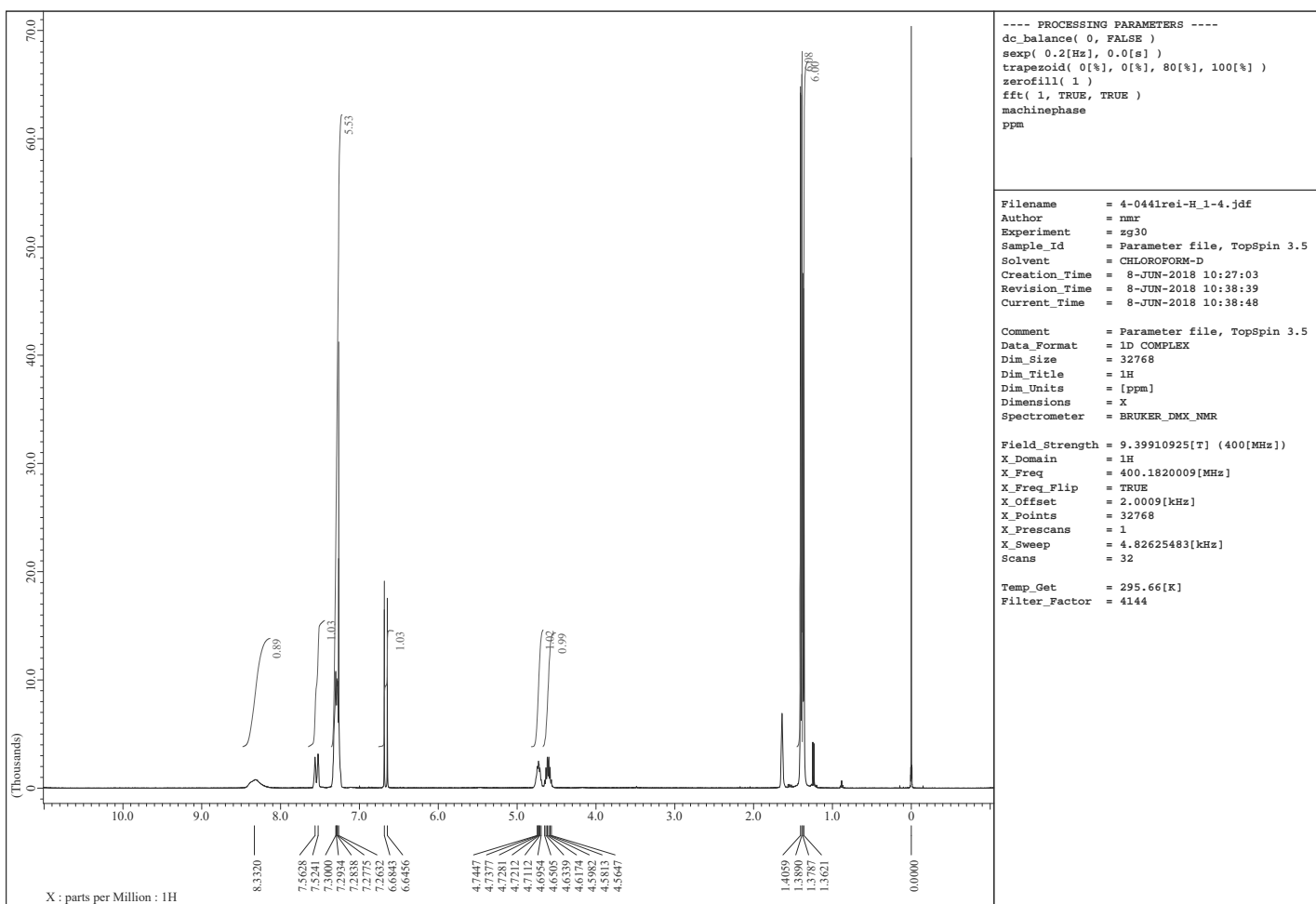
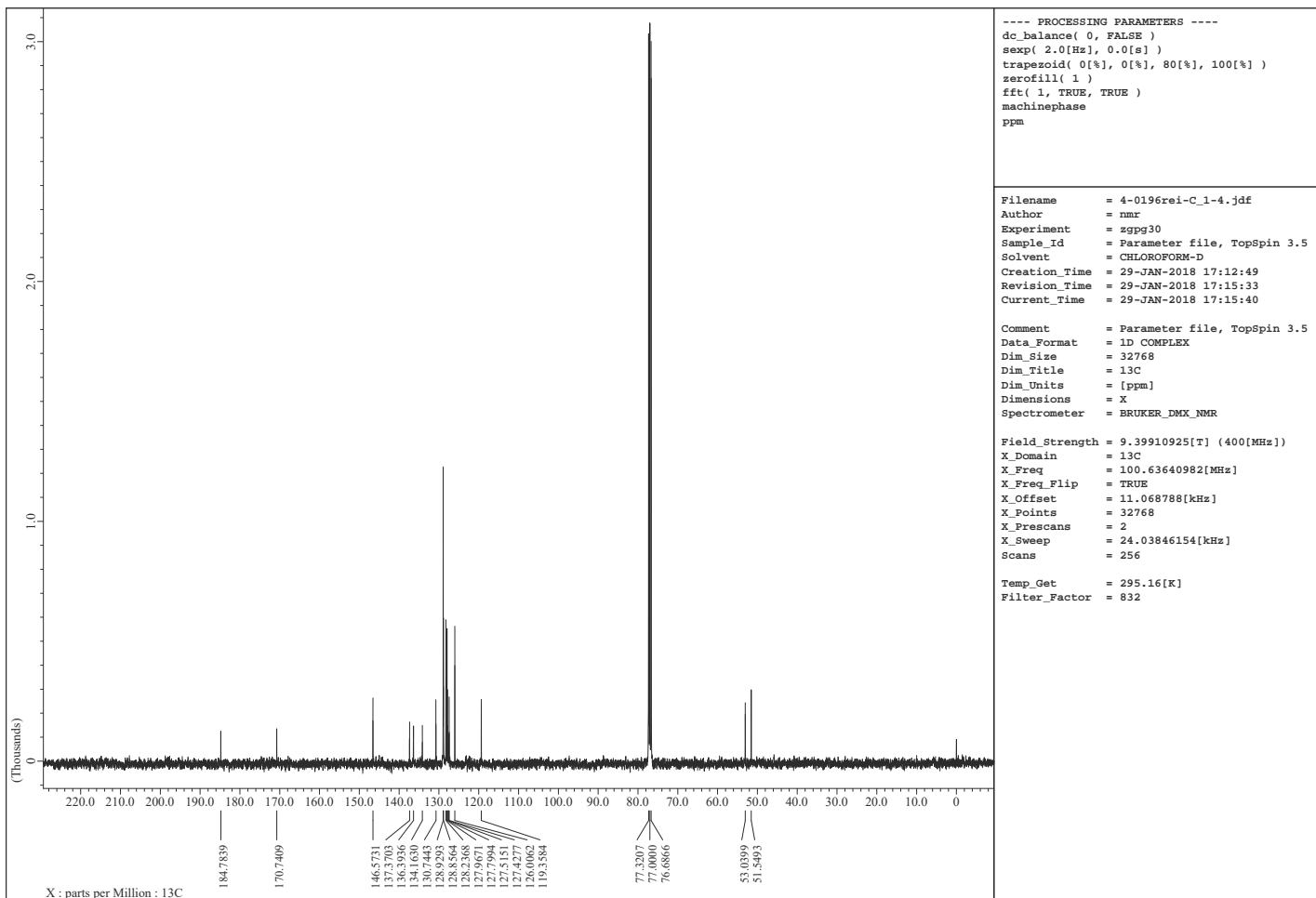
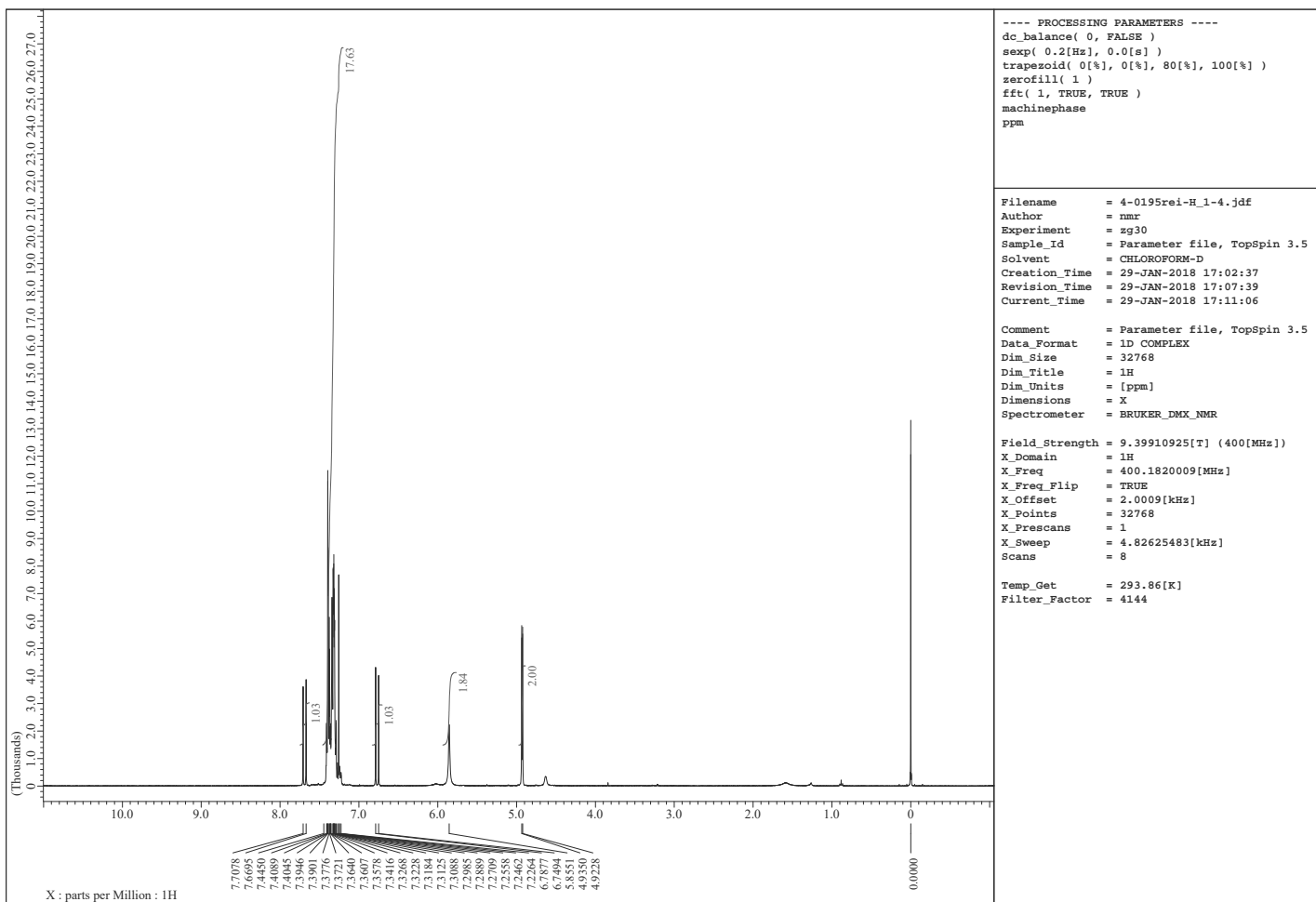


Figure S12. ^1H and ^{13}C NMR spectra of **1e**



<<S15>>

Figure S13. ^1H and ^{13}C NMR spectra of **1f**

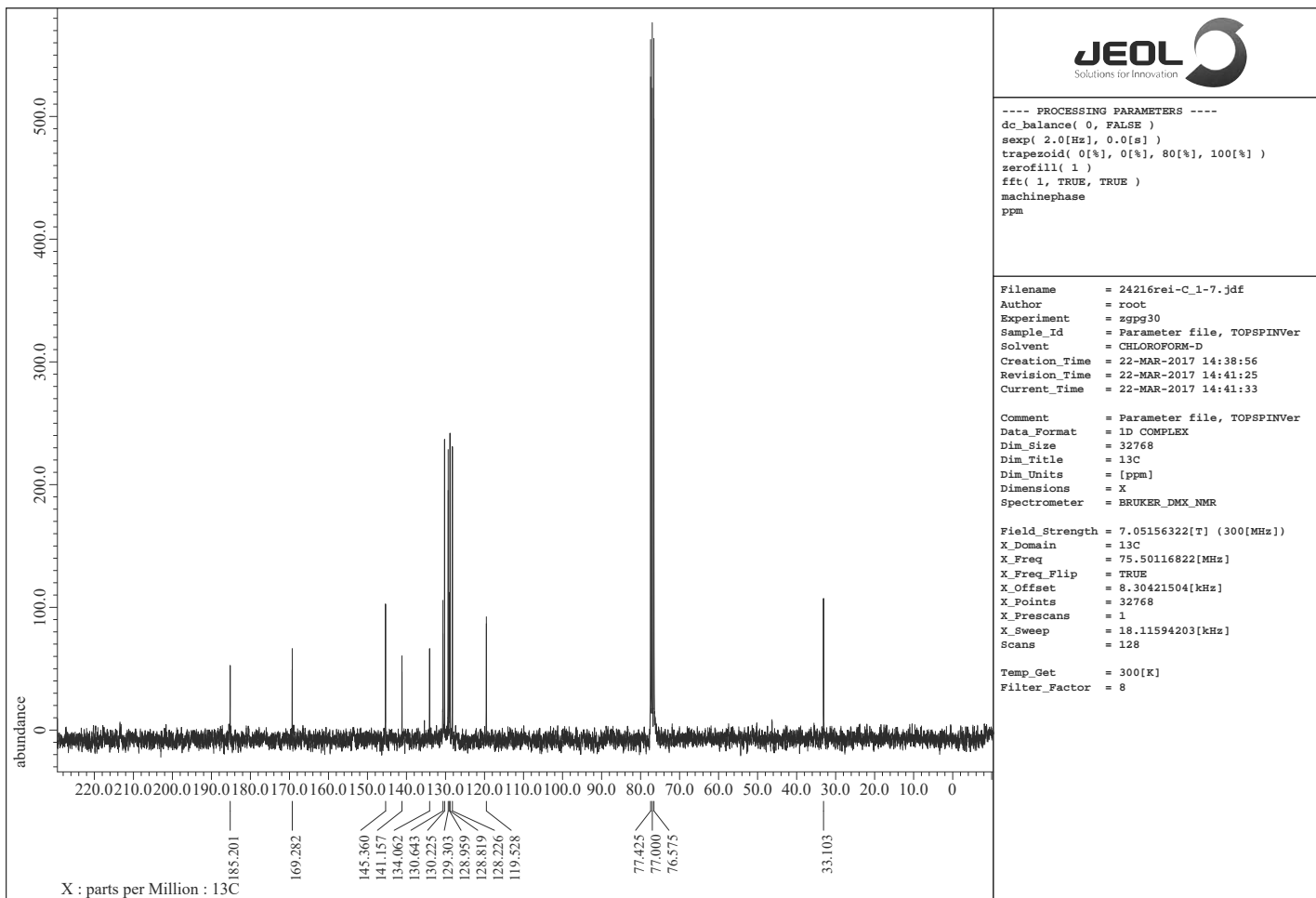
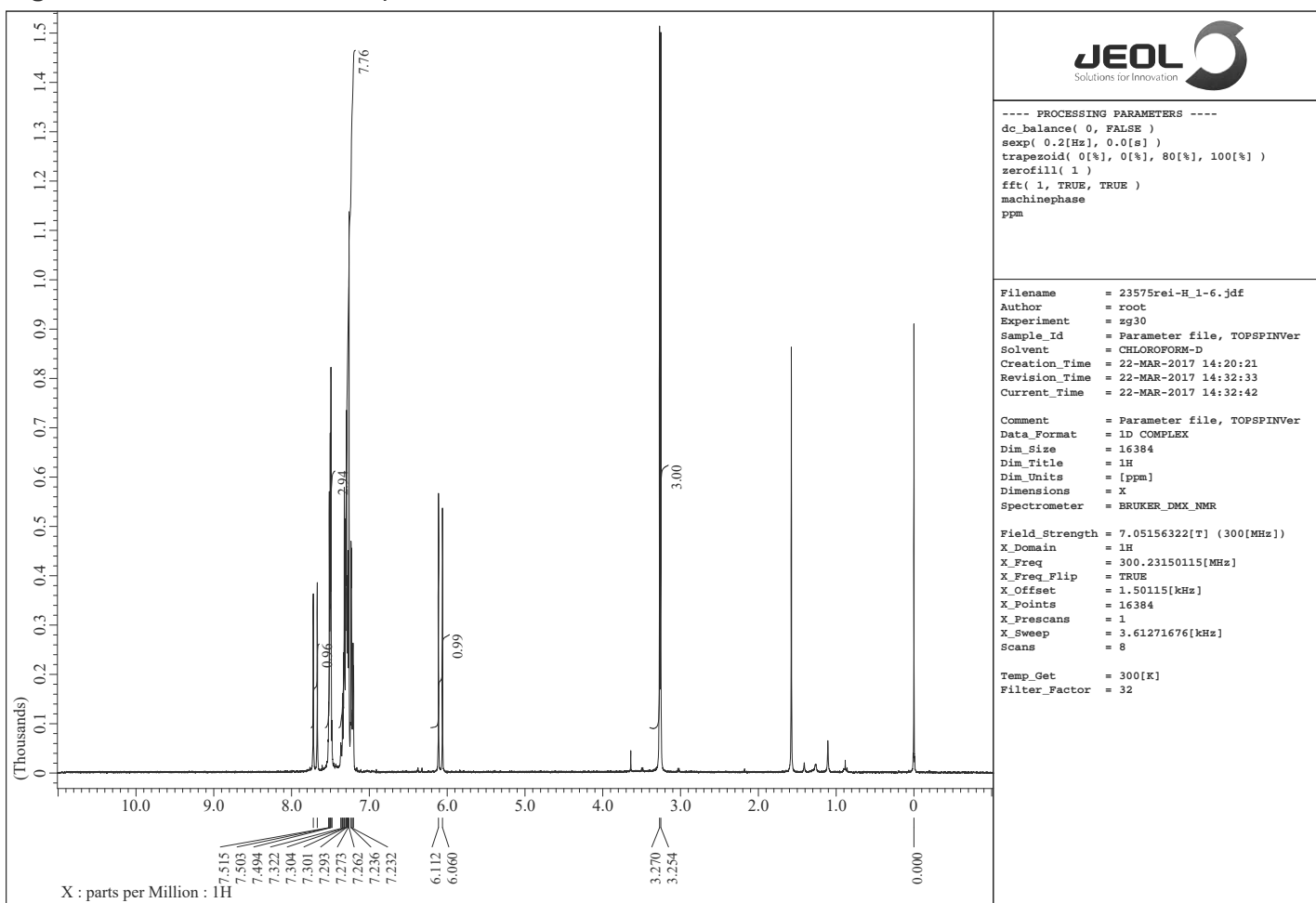
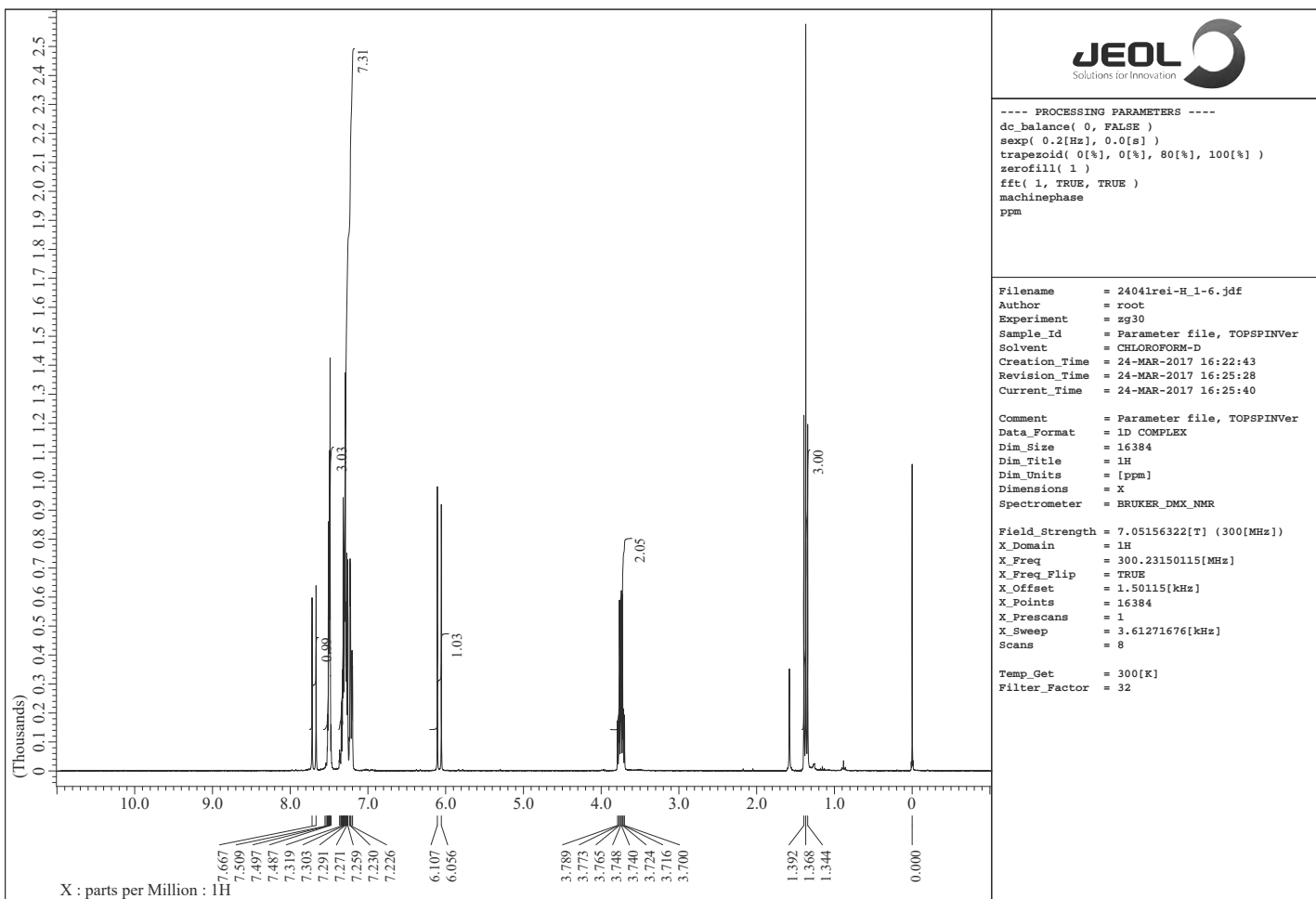
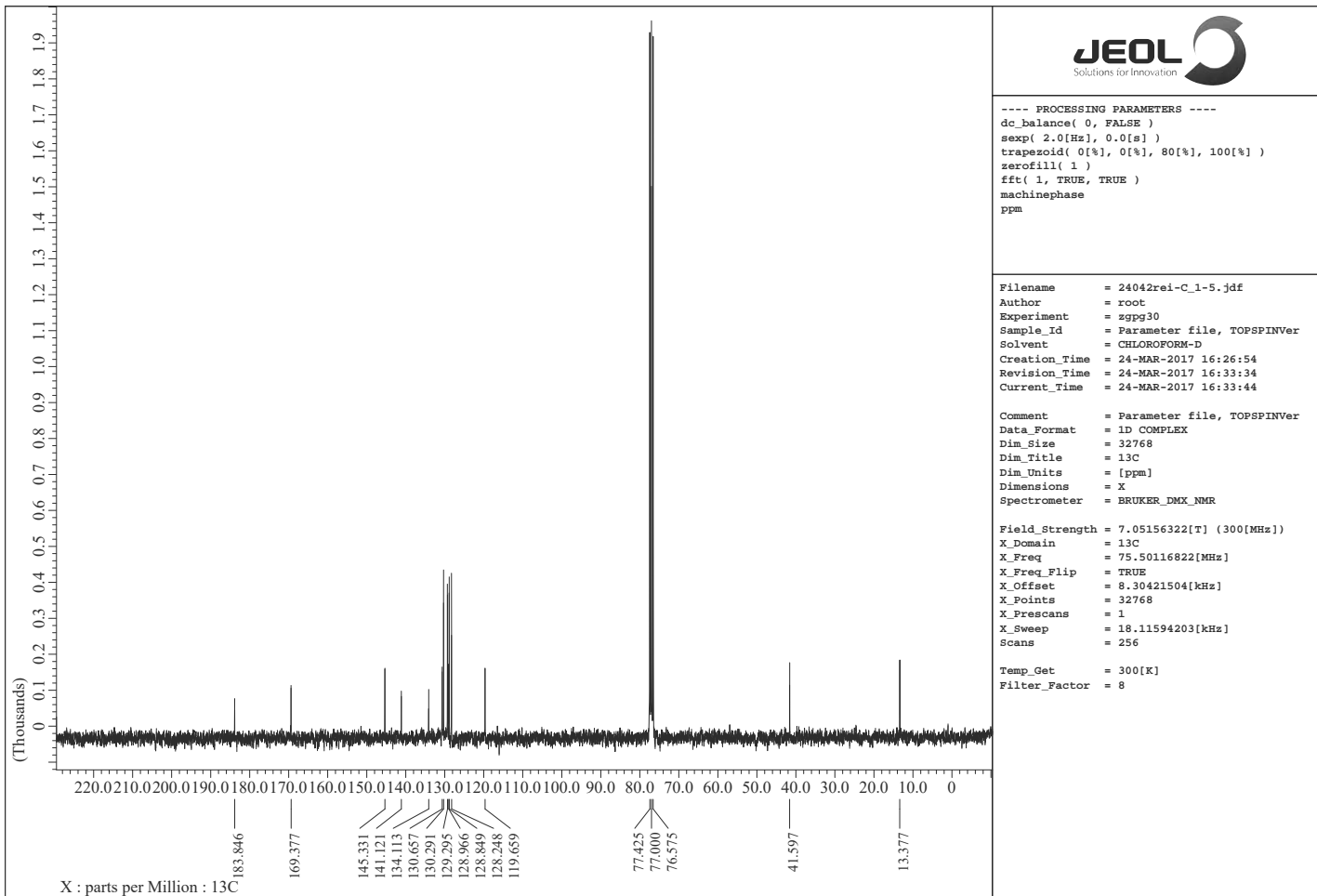


Figure S14. ^1H and ^{13}C NMR spectra of **1g**



N-Cinnamoyl-N-phenyl-N-ethylamine (1g)



N-Cinnamoyl-N-phenyl-N-ethylamine (1g)

Figure S15. ^1H and ^{13}C NMR spectra of **1h**

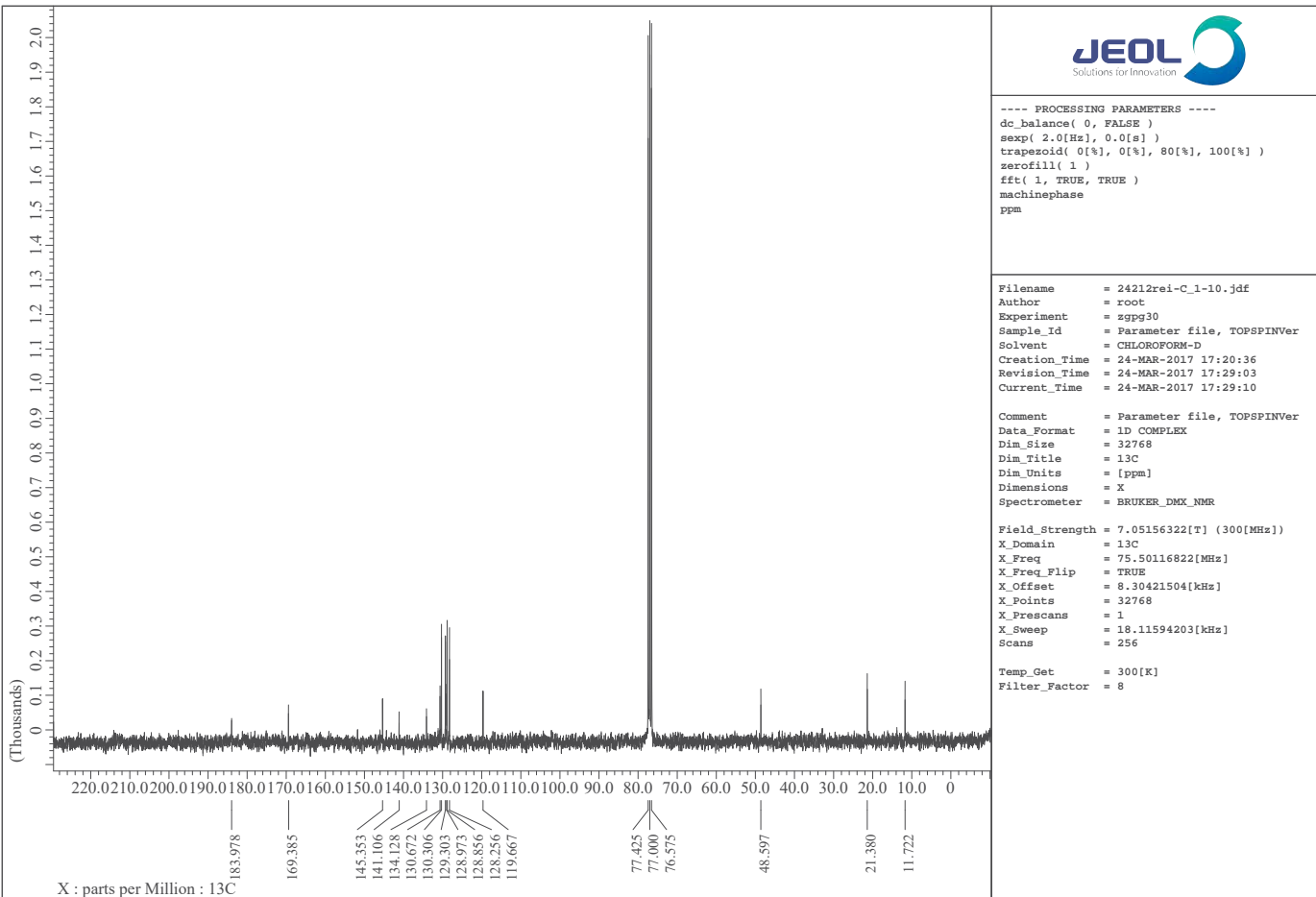
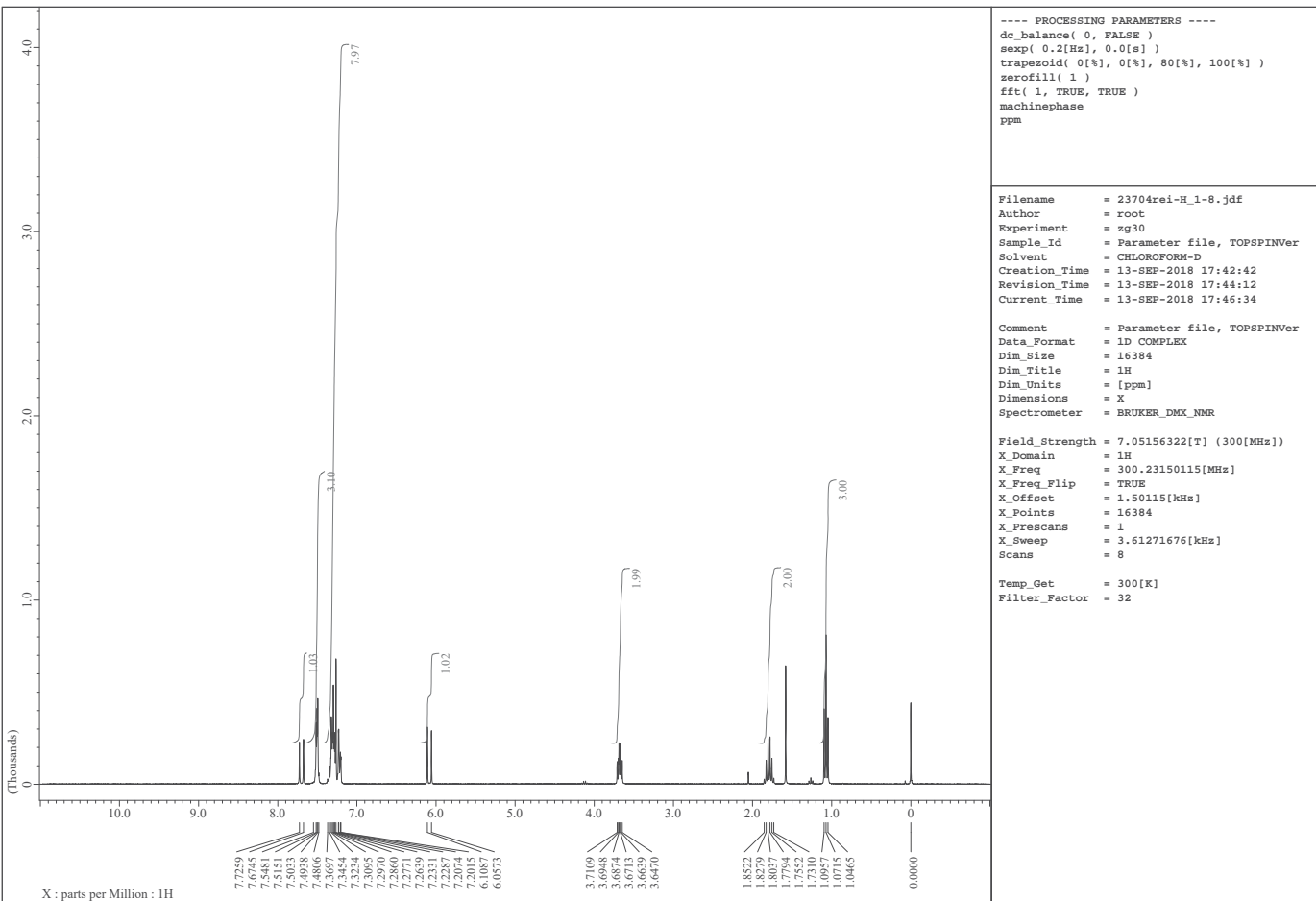


Figure S16. ^1H and ^{13}C NMR spectra of **1i**

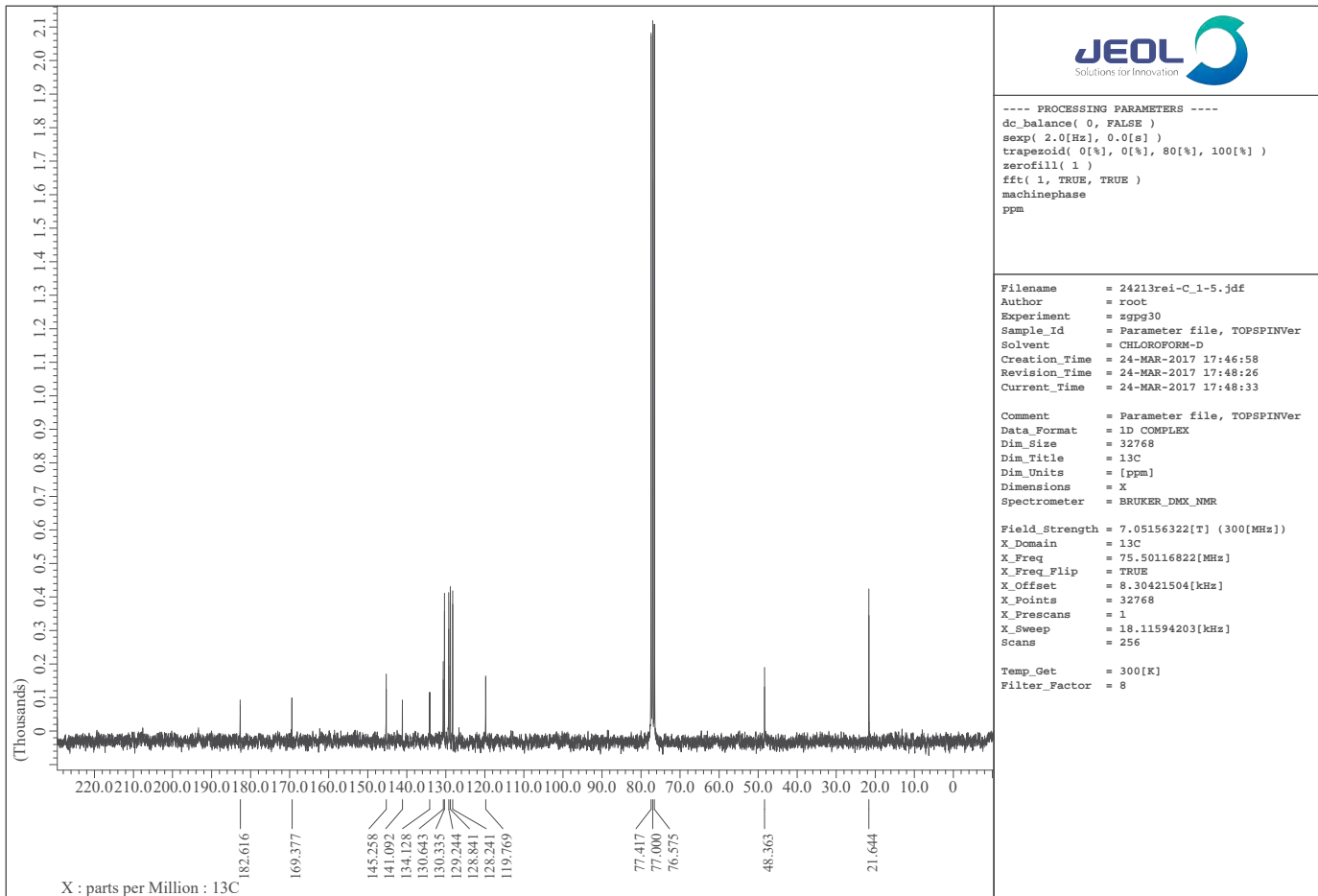
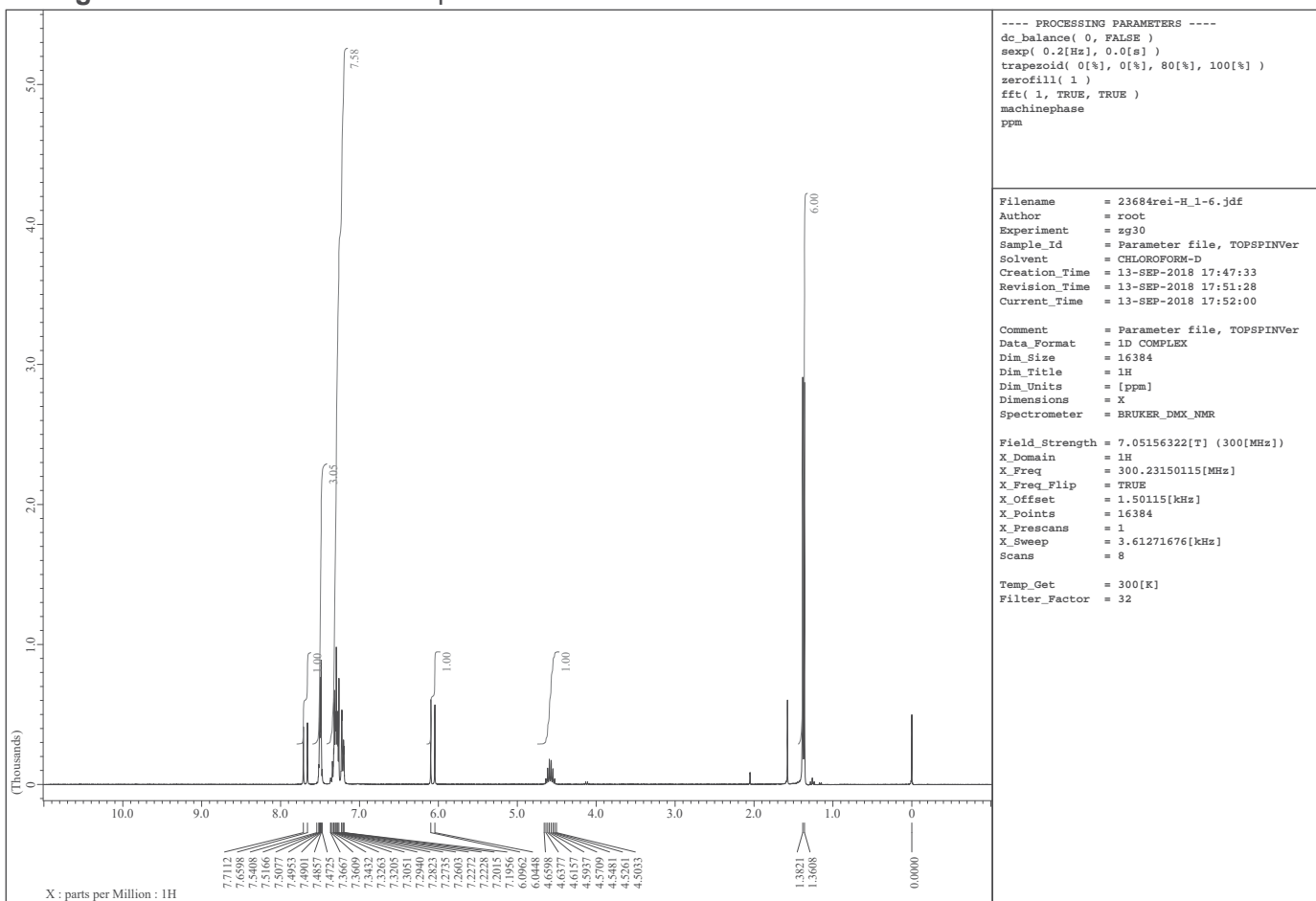


Figure S17. ^1H and ^{13}C NMR spectra of **1j**

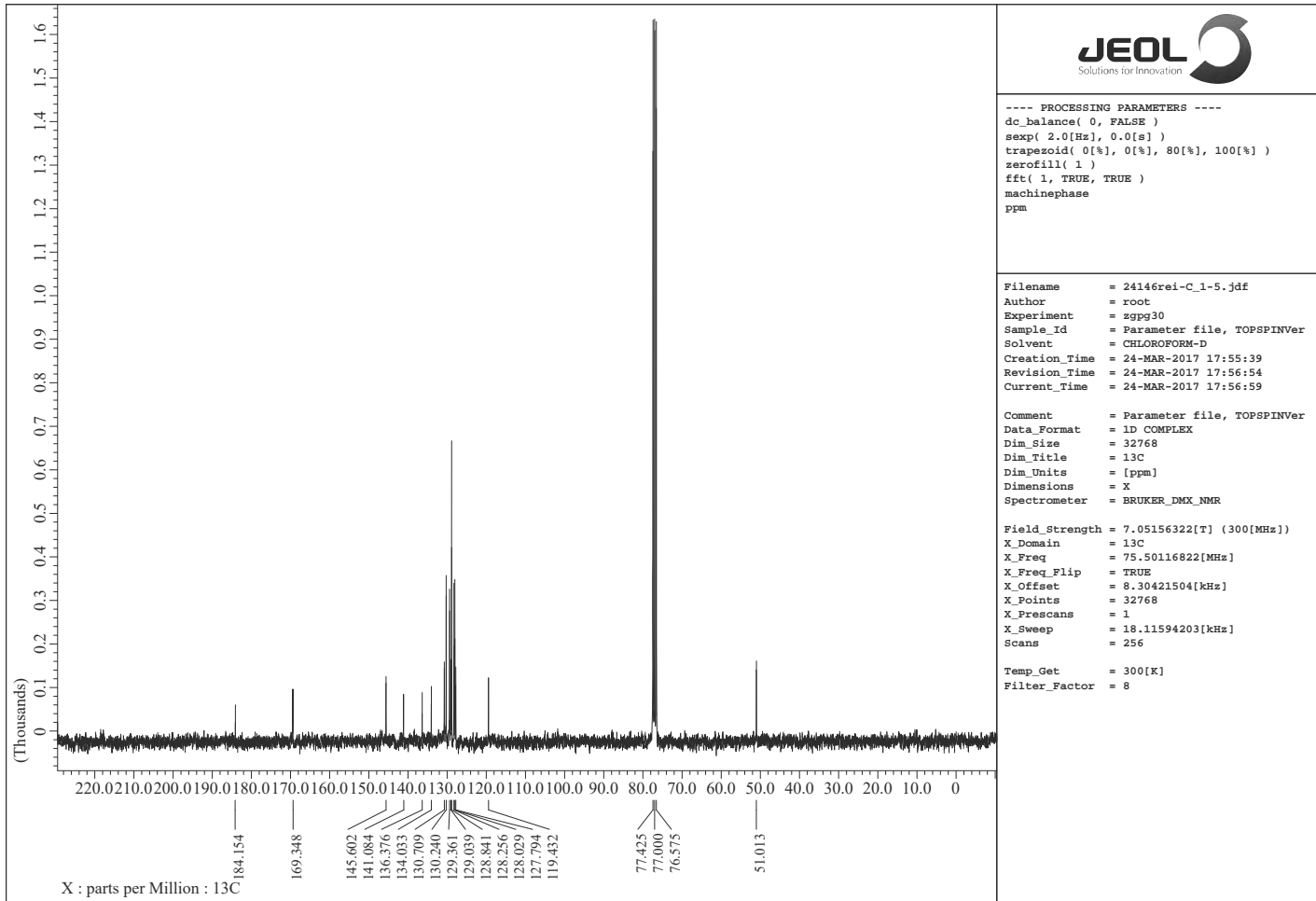
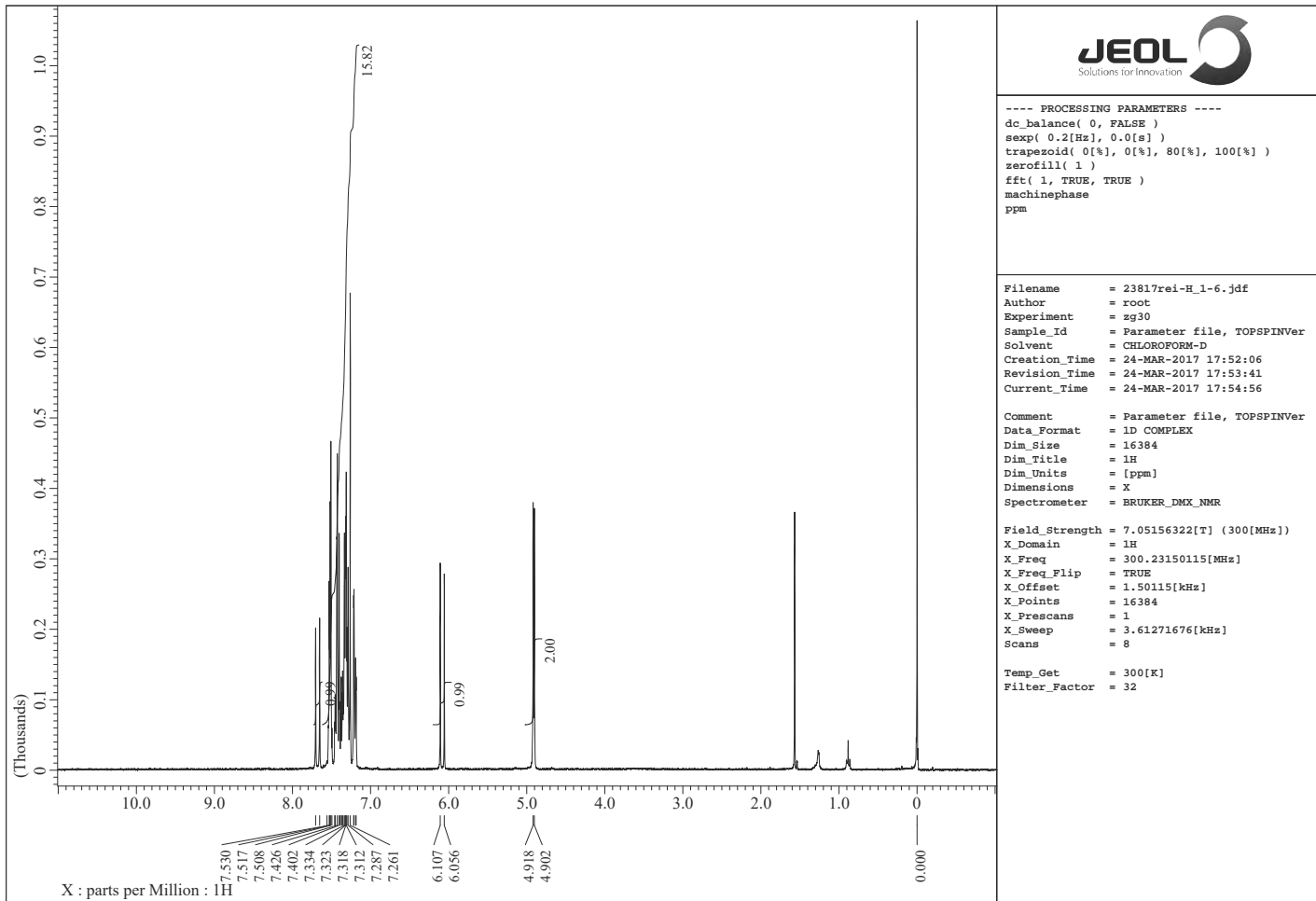
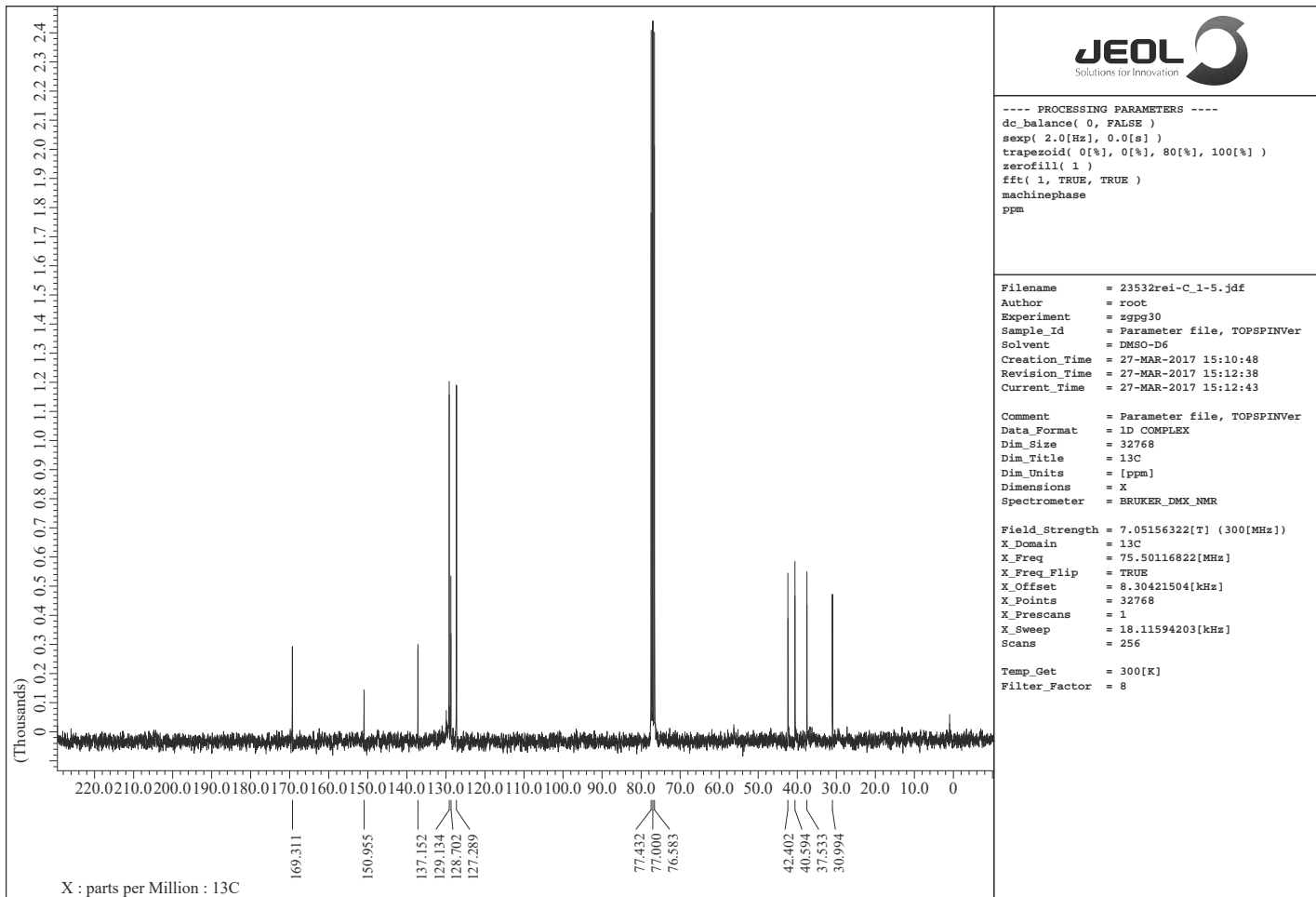
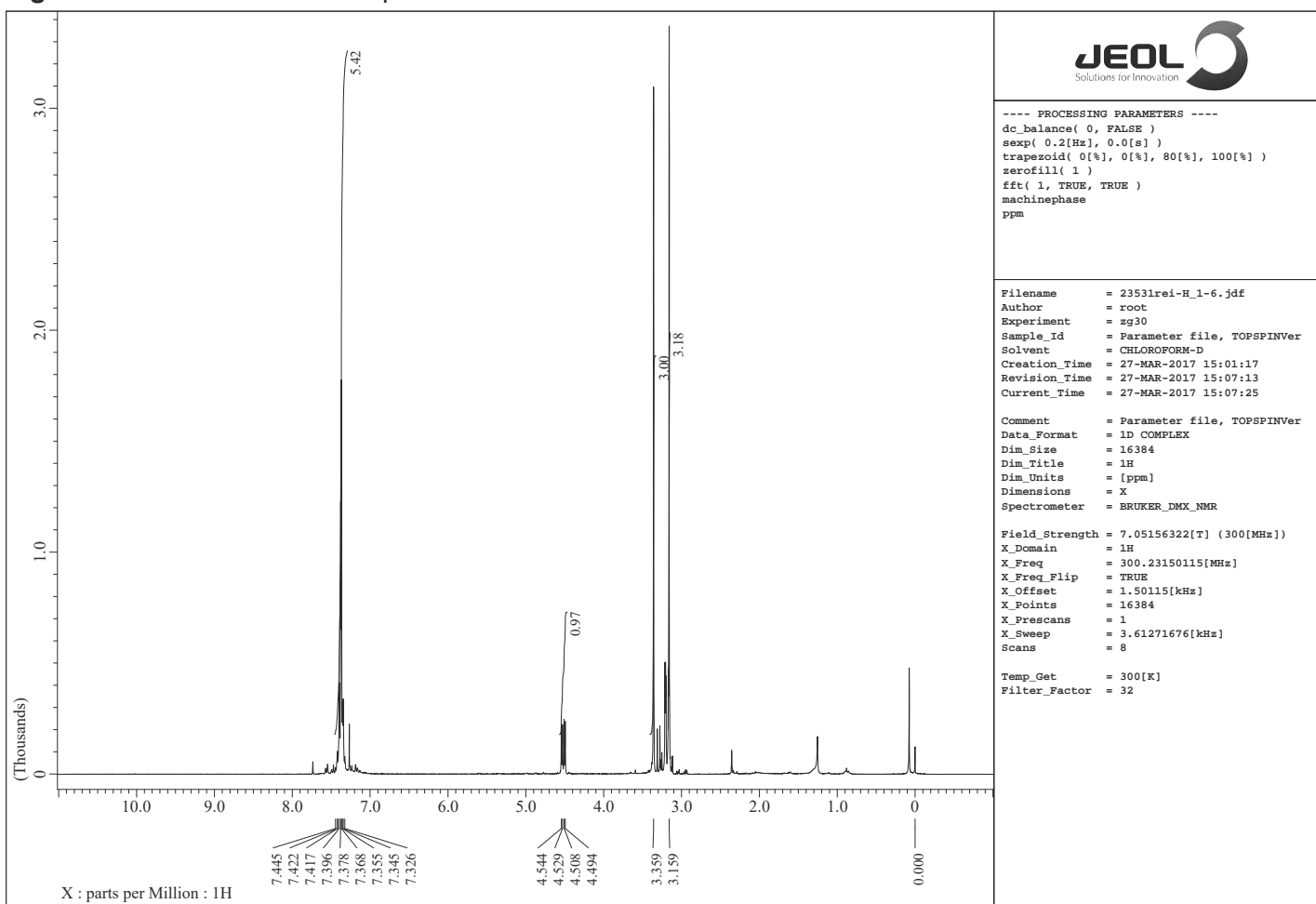
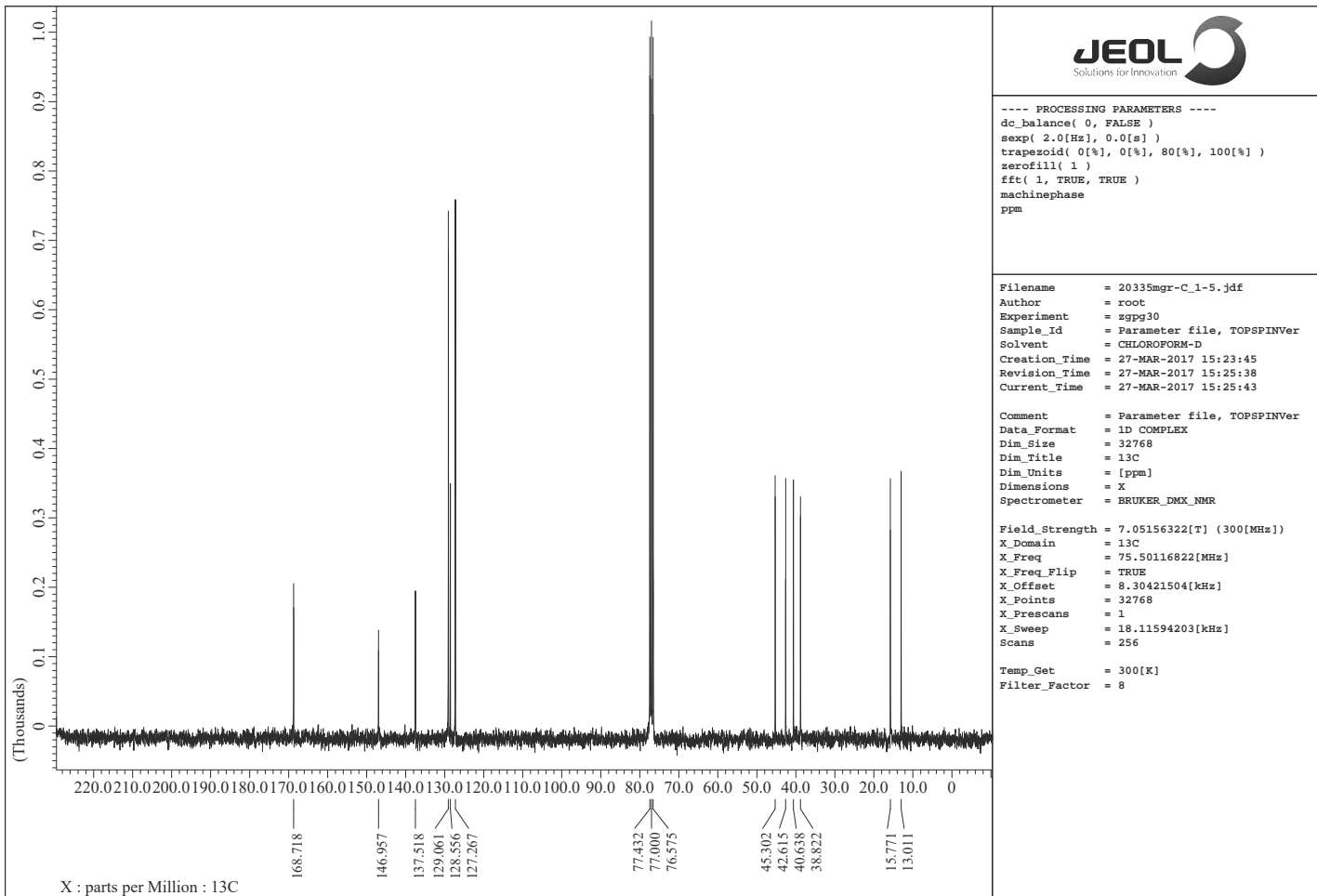
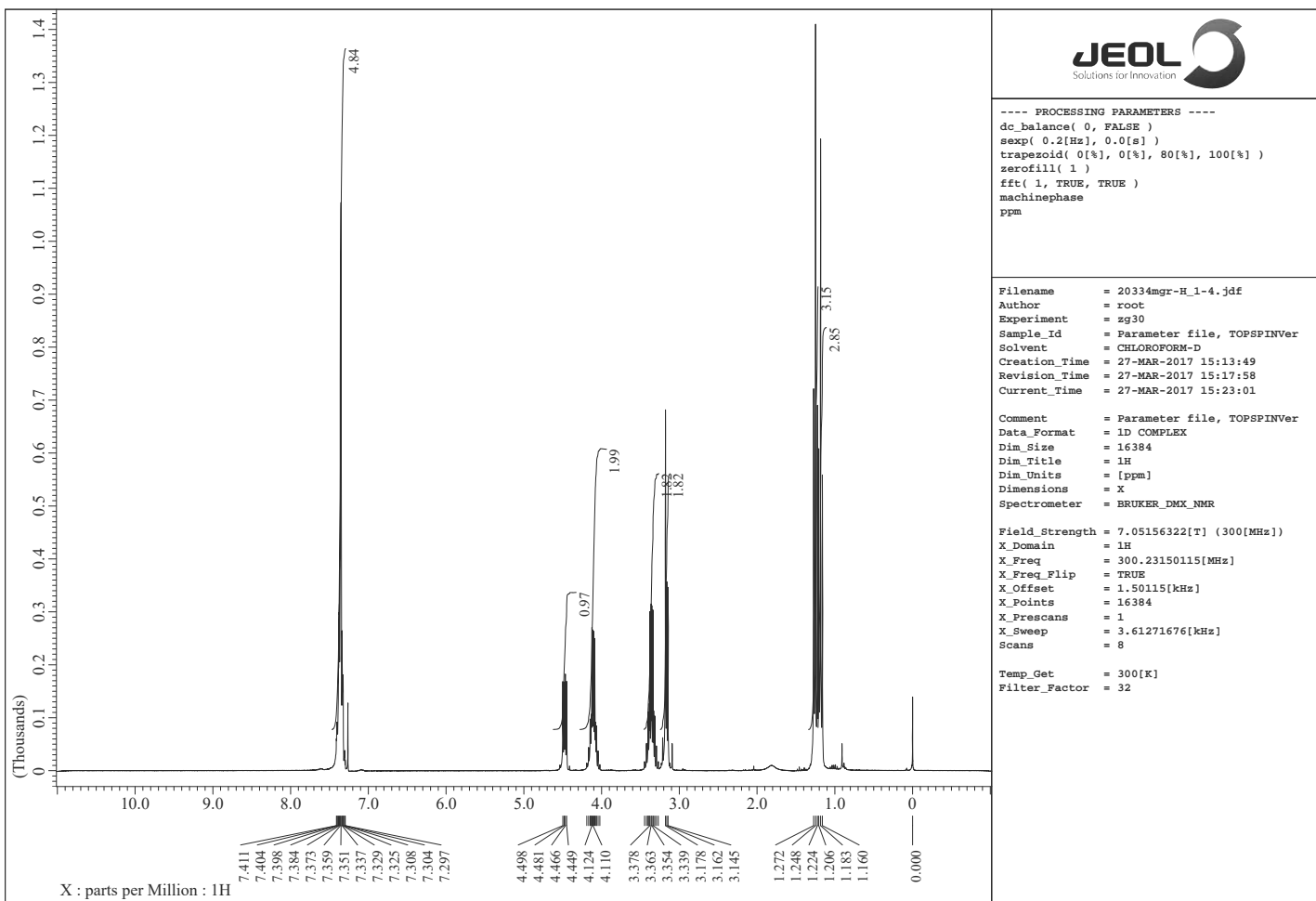


Figure S18. ^1H and ^{13}C NMR spectra of **2a**



<<S21>>

Figure S19. ^1H and ^{13}C NMR spectra of **2b**



<<S22>>

Figure S20. ^1H and ^{13}C NMR spectra of **2c**

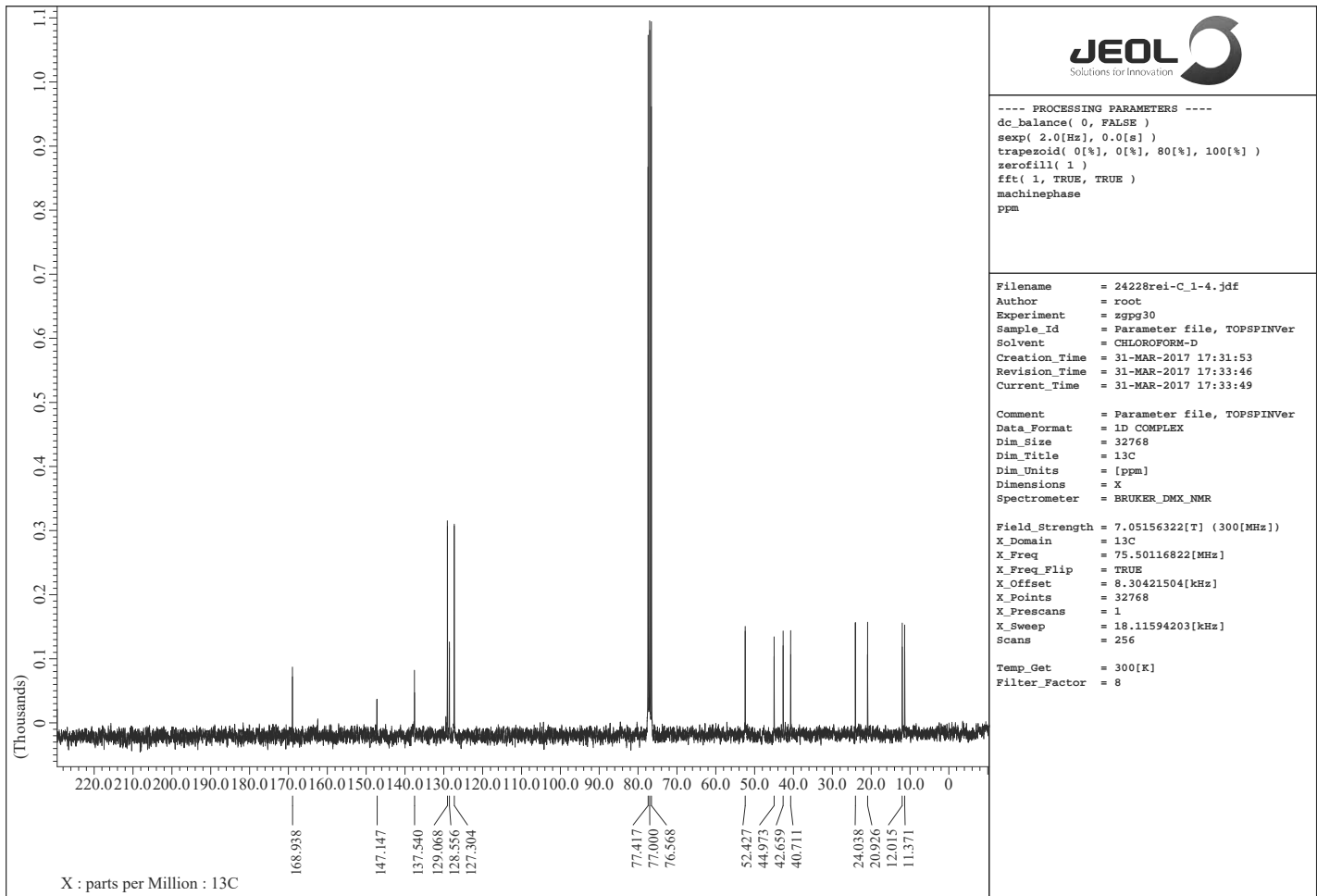
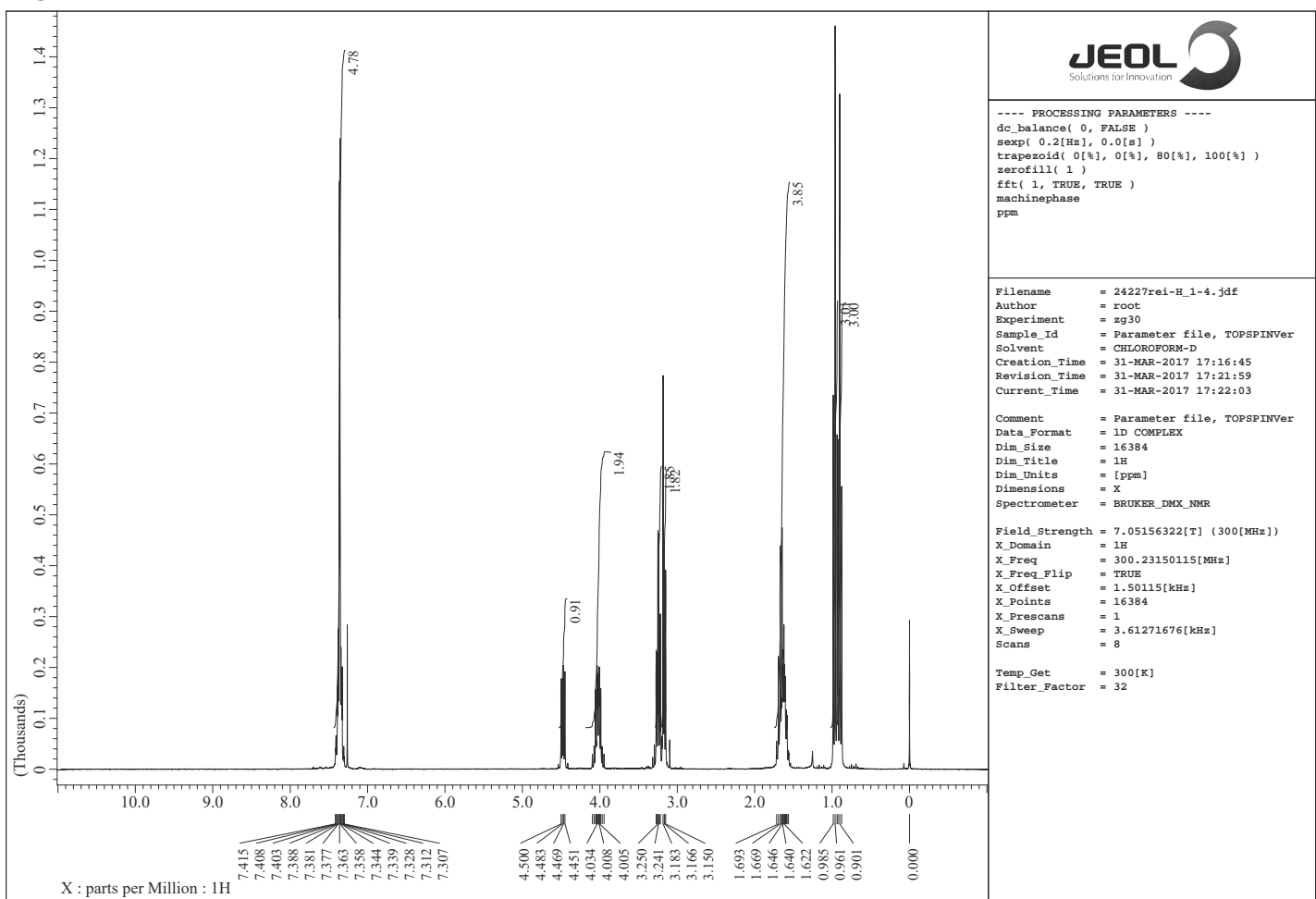


Figure S21. ^1H and ^{13}C NMR spectra of **2d**

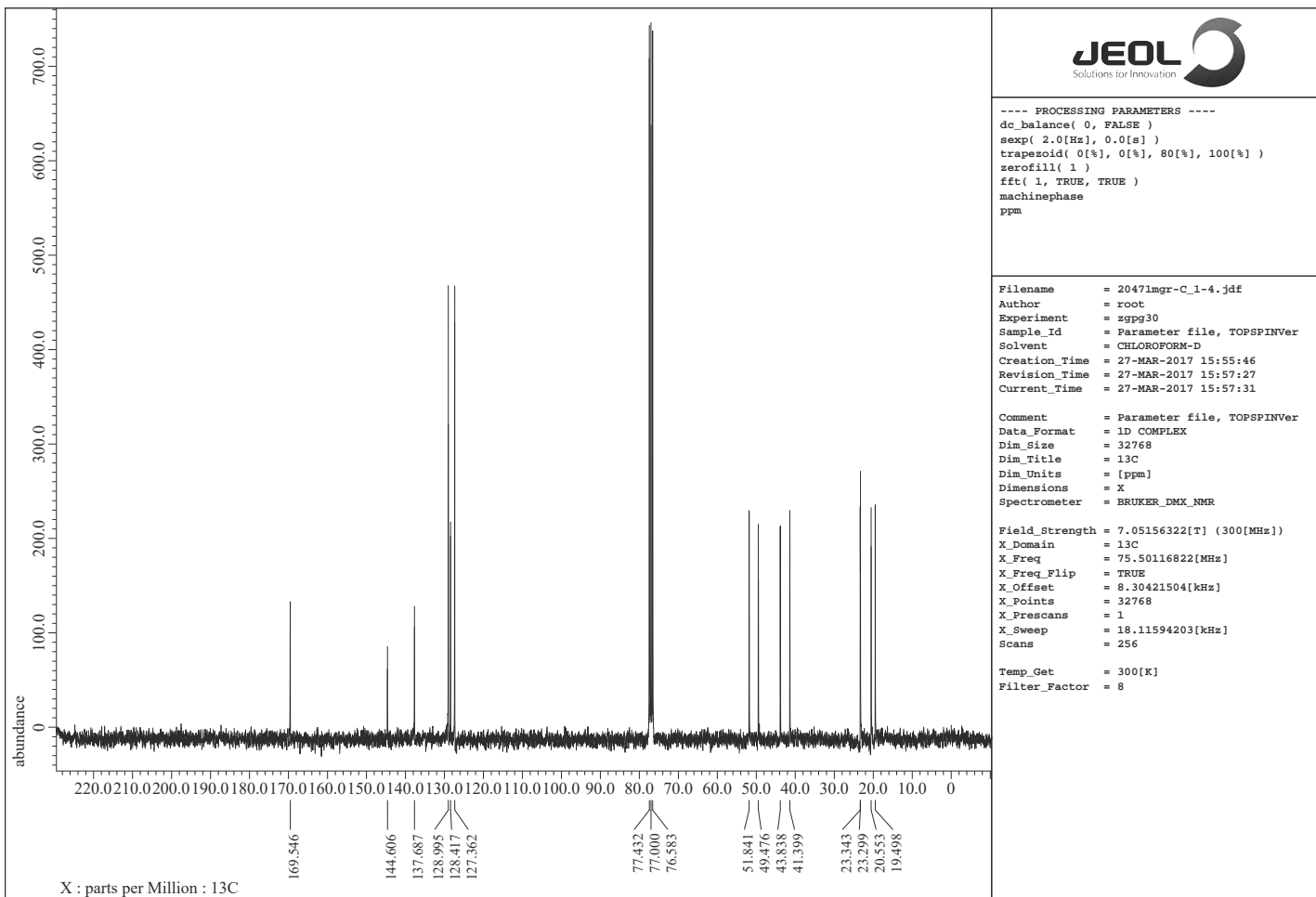
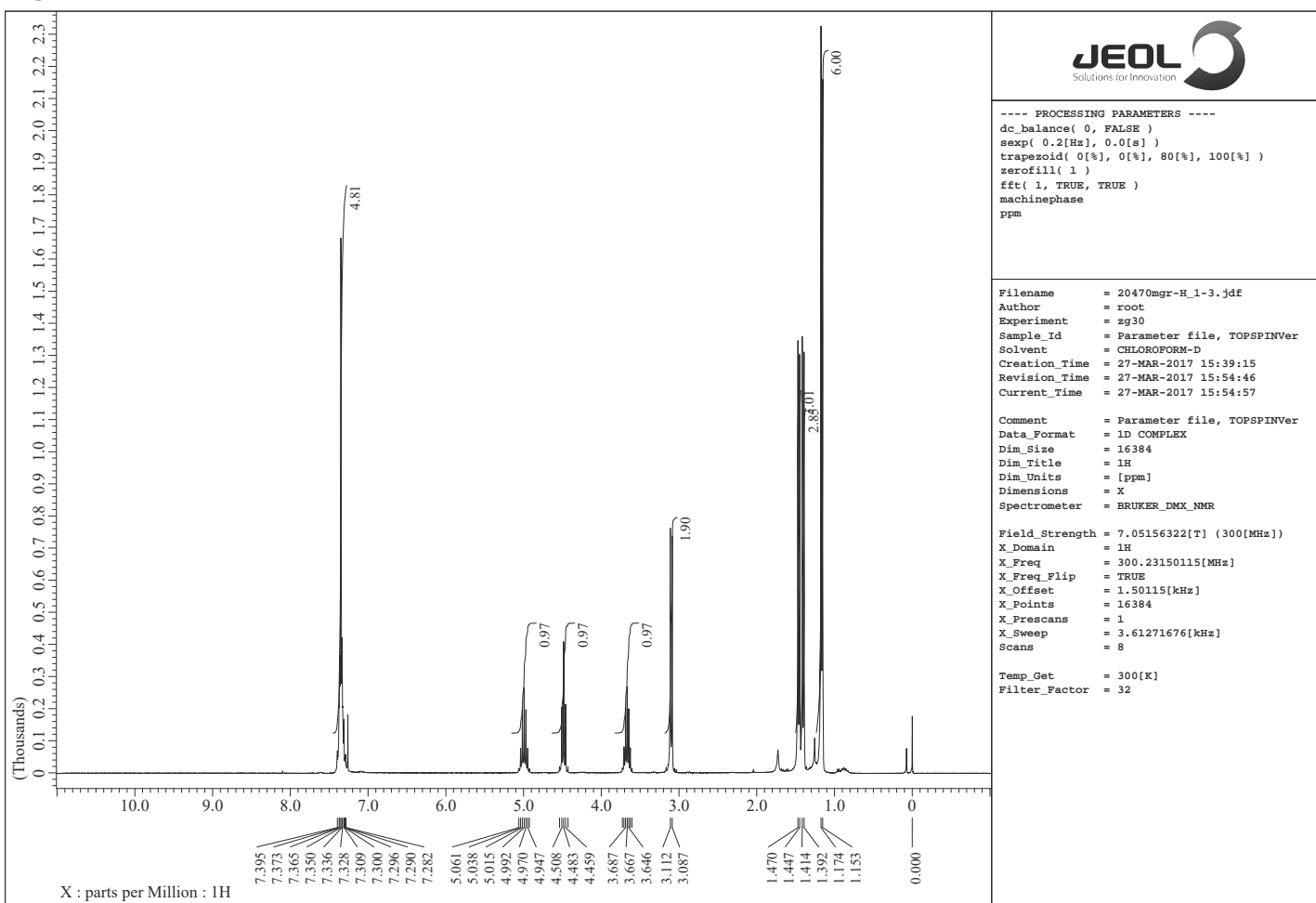


Figure S22. ^1H and ^{13}C NMR spectra of **2e**

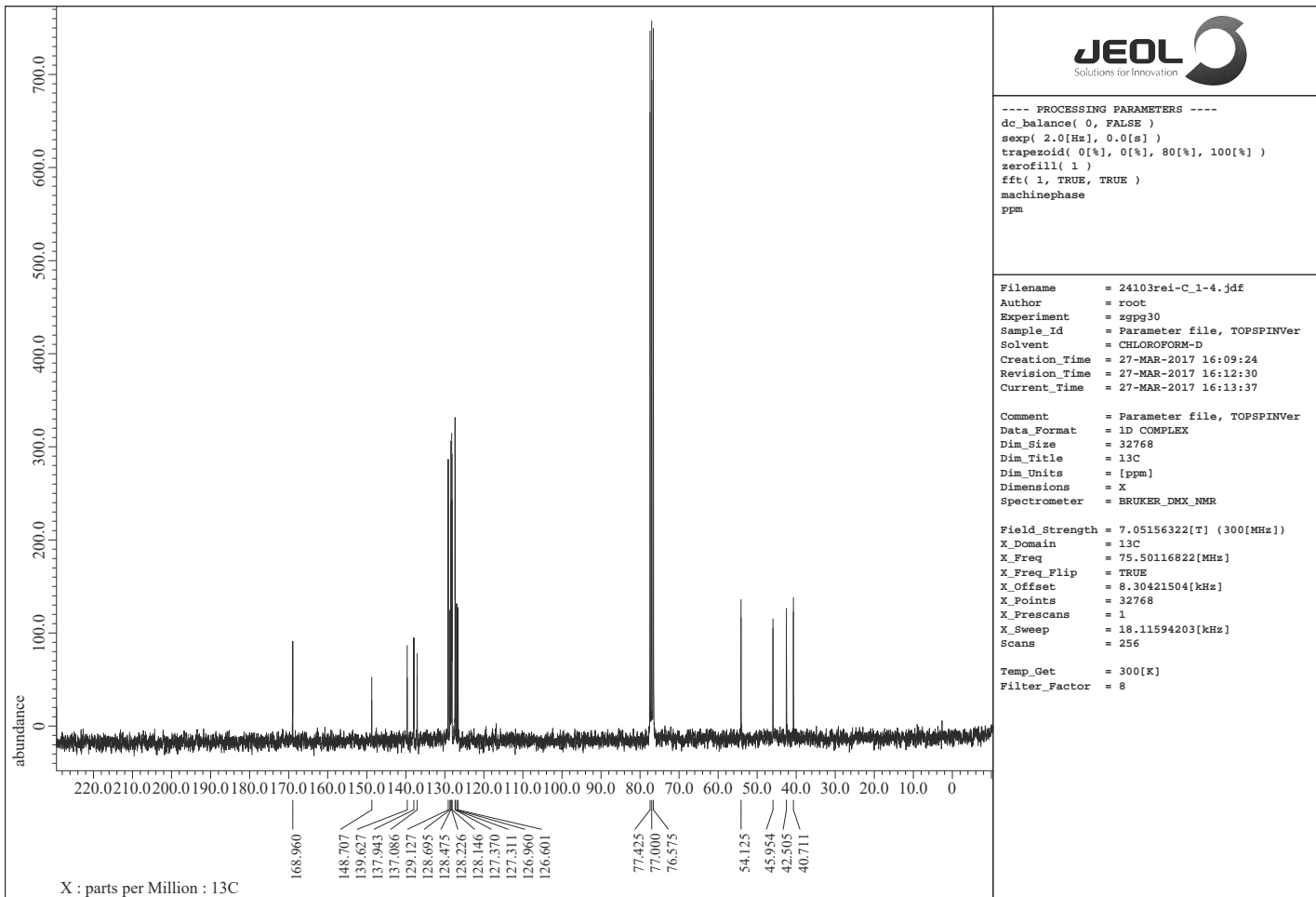
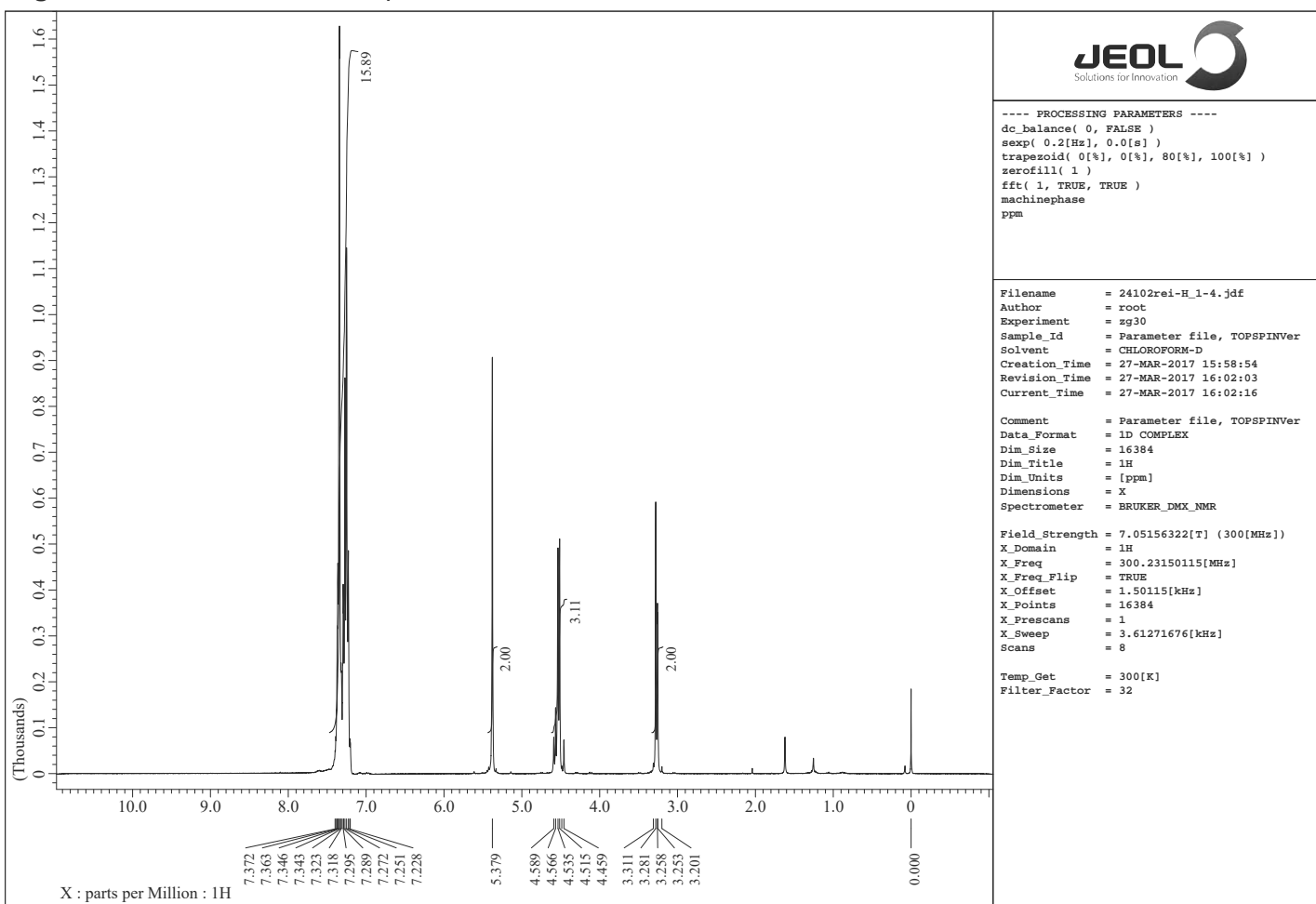


Figure S23. ^1H and ^{13}C NMR spectra of **2f**

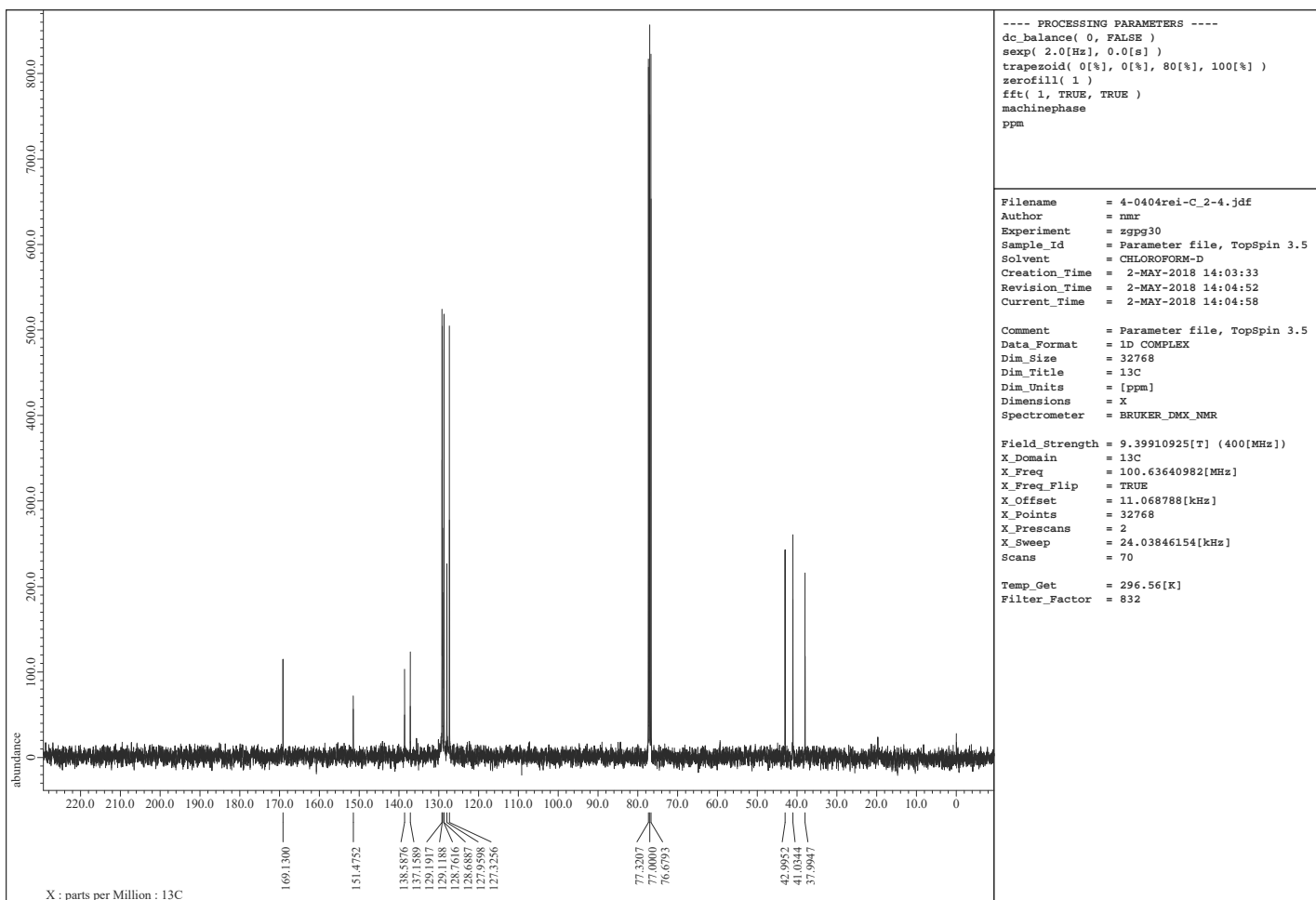
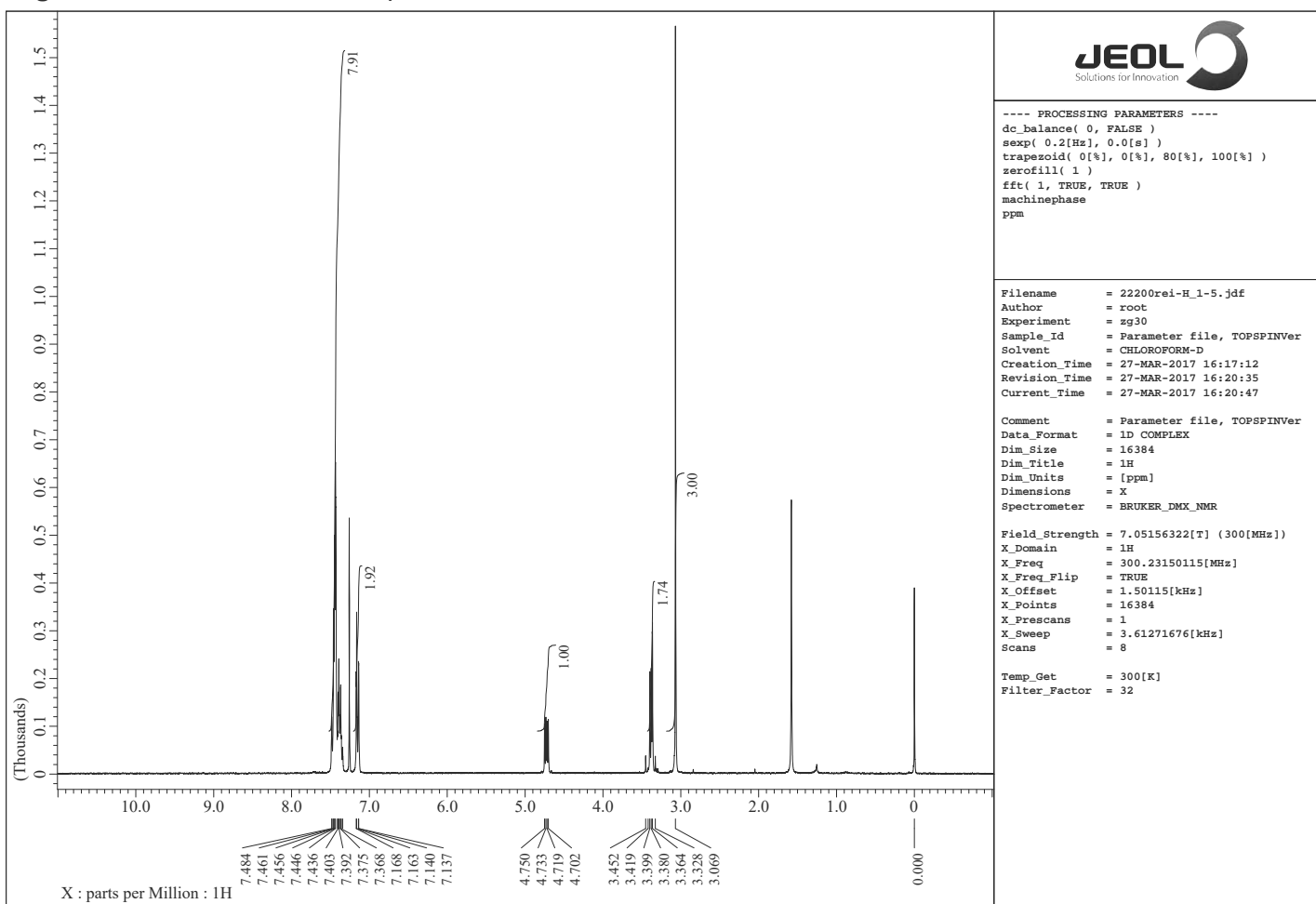


Figure S24. ^1H and ^{13}C NMR spectra of **2g**

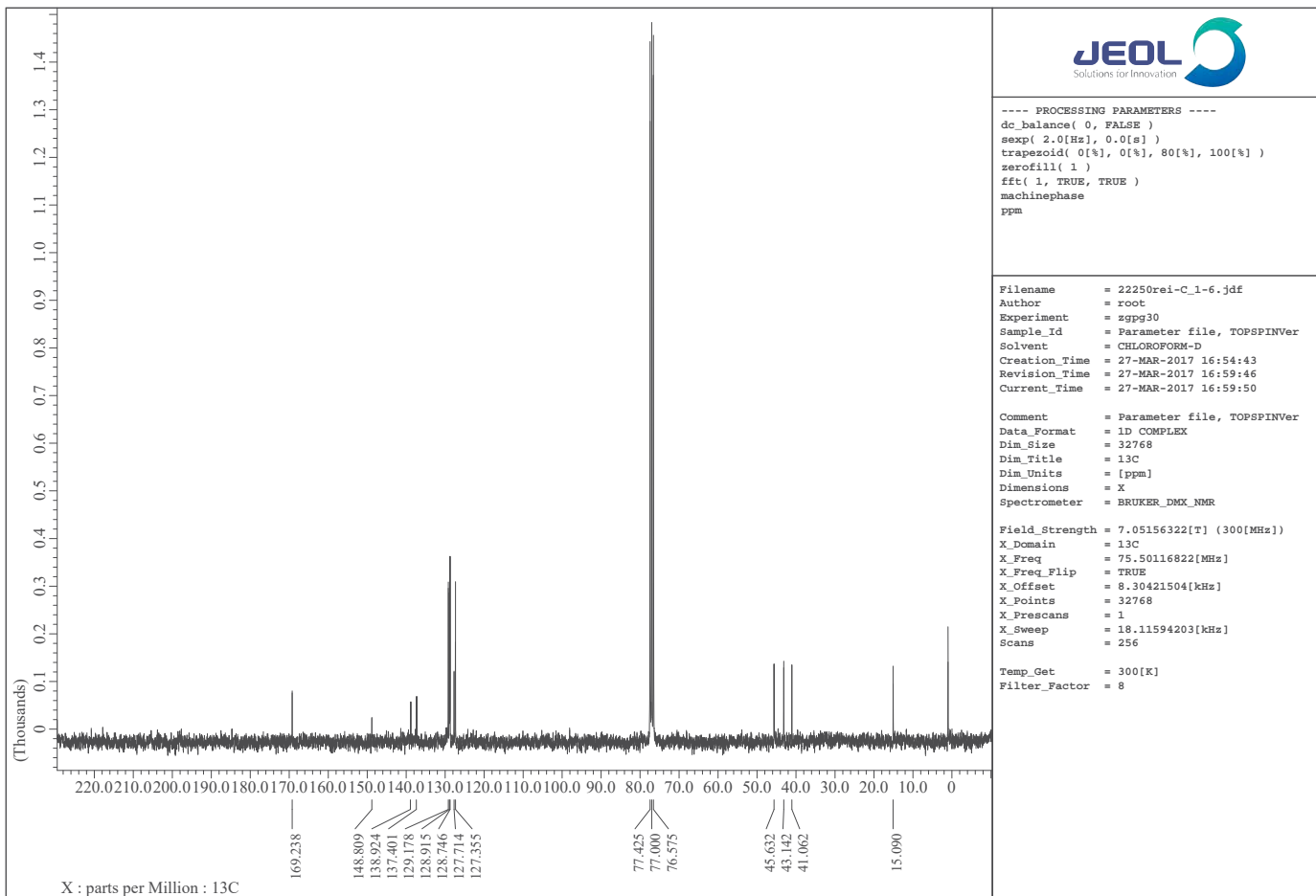
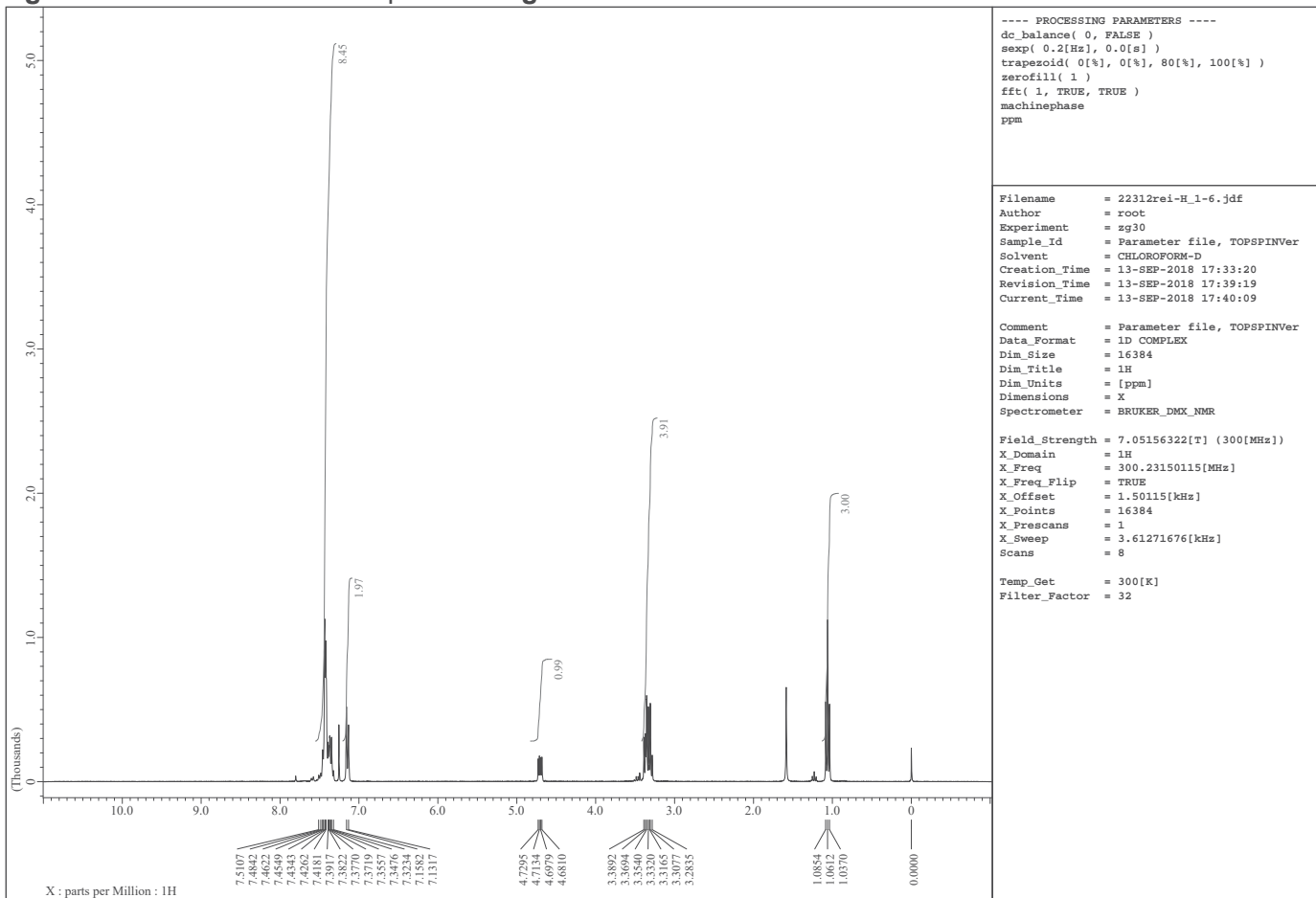


Figure S25. ^1H and ^{13}C NMR spectra of **2h**

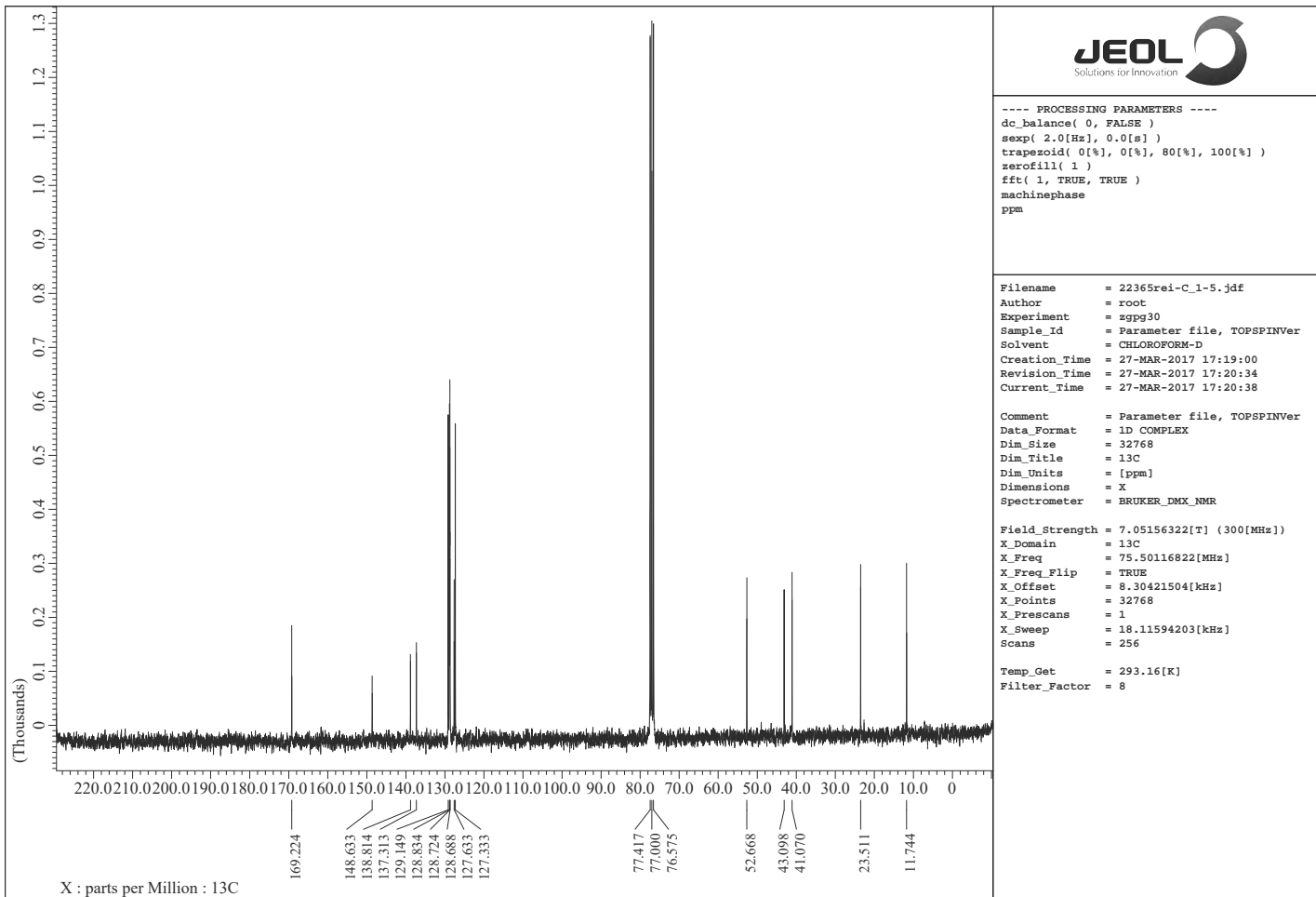
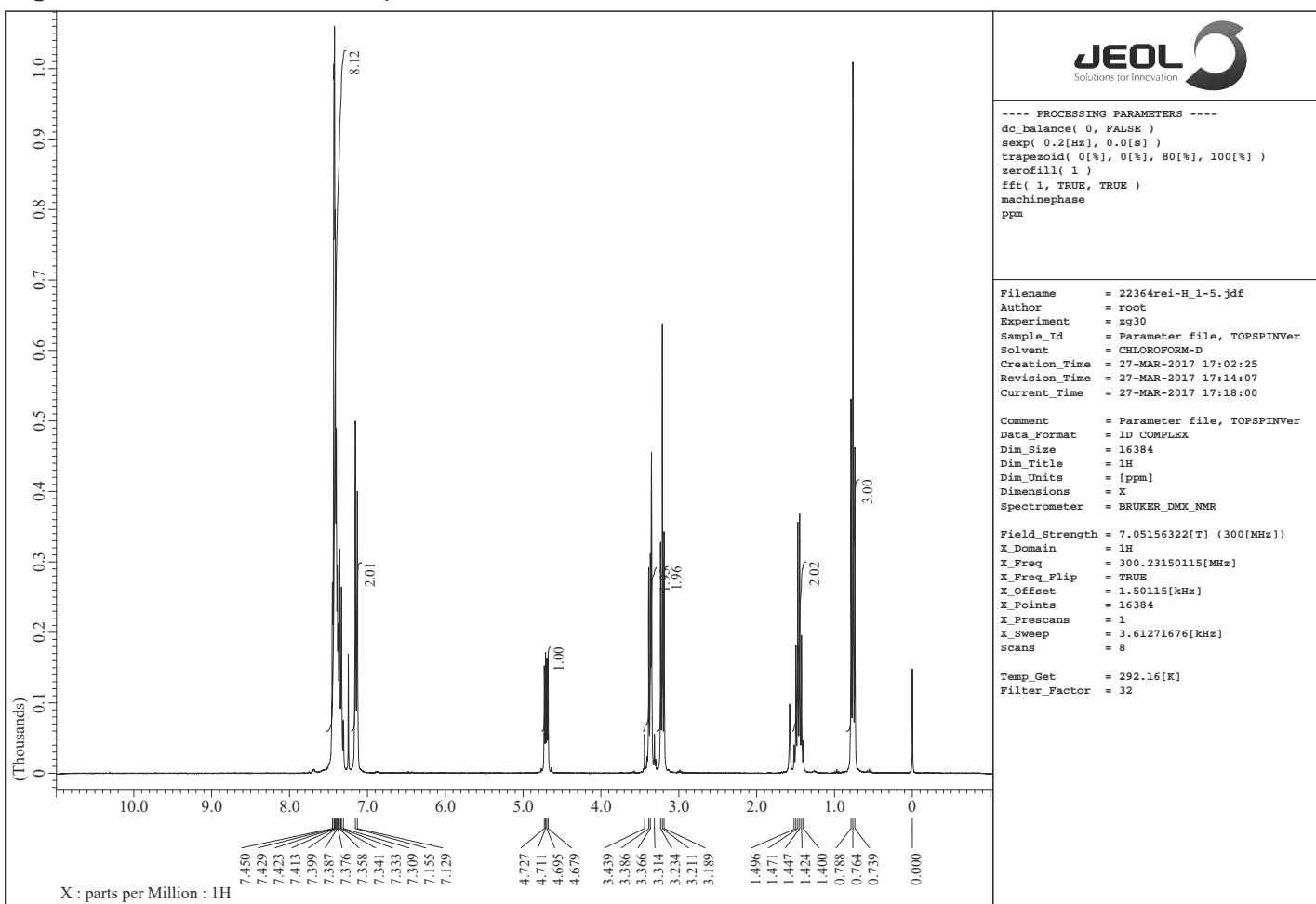
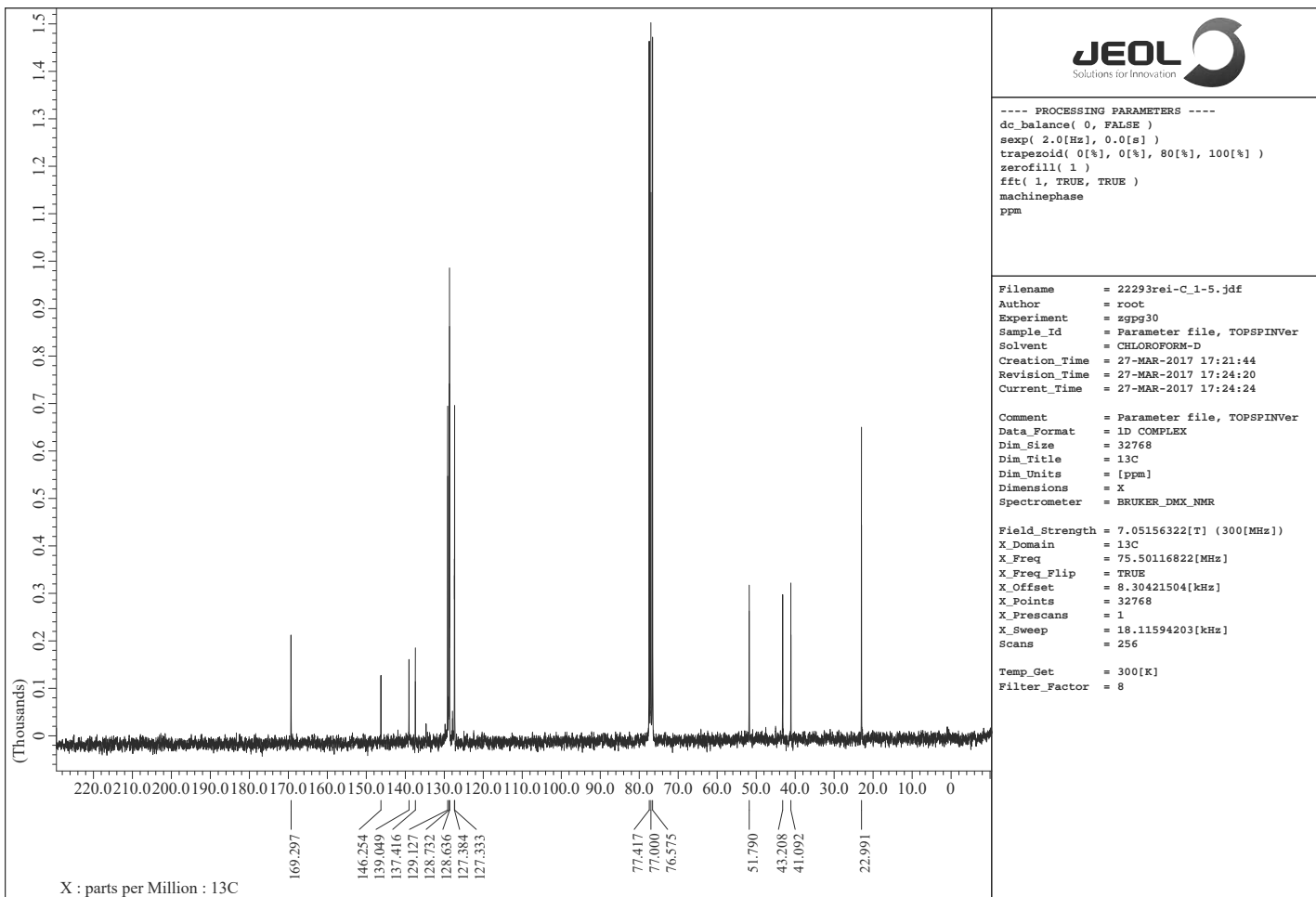
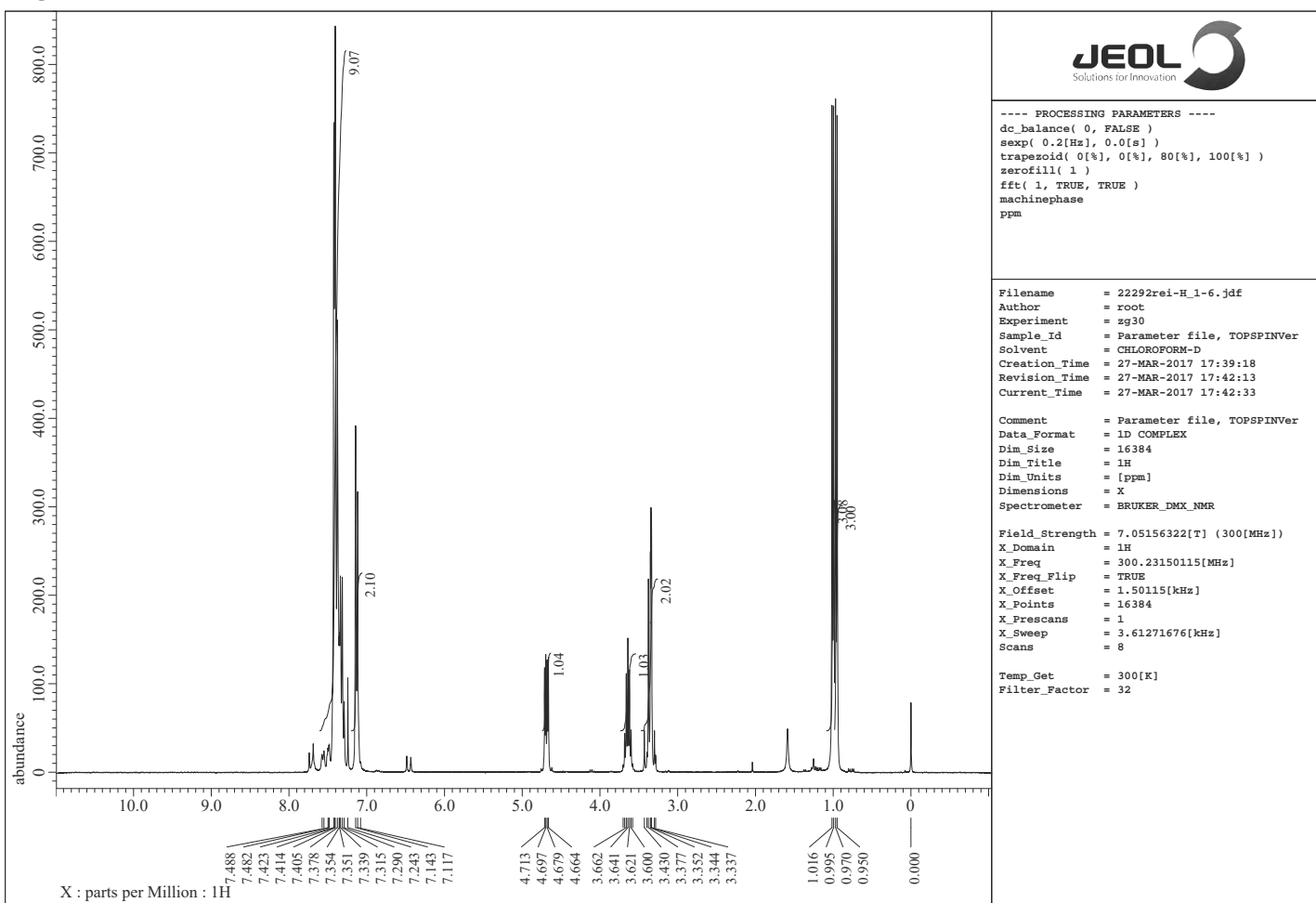
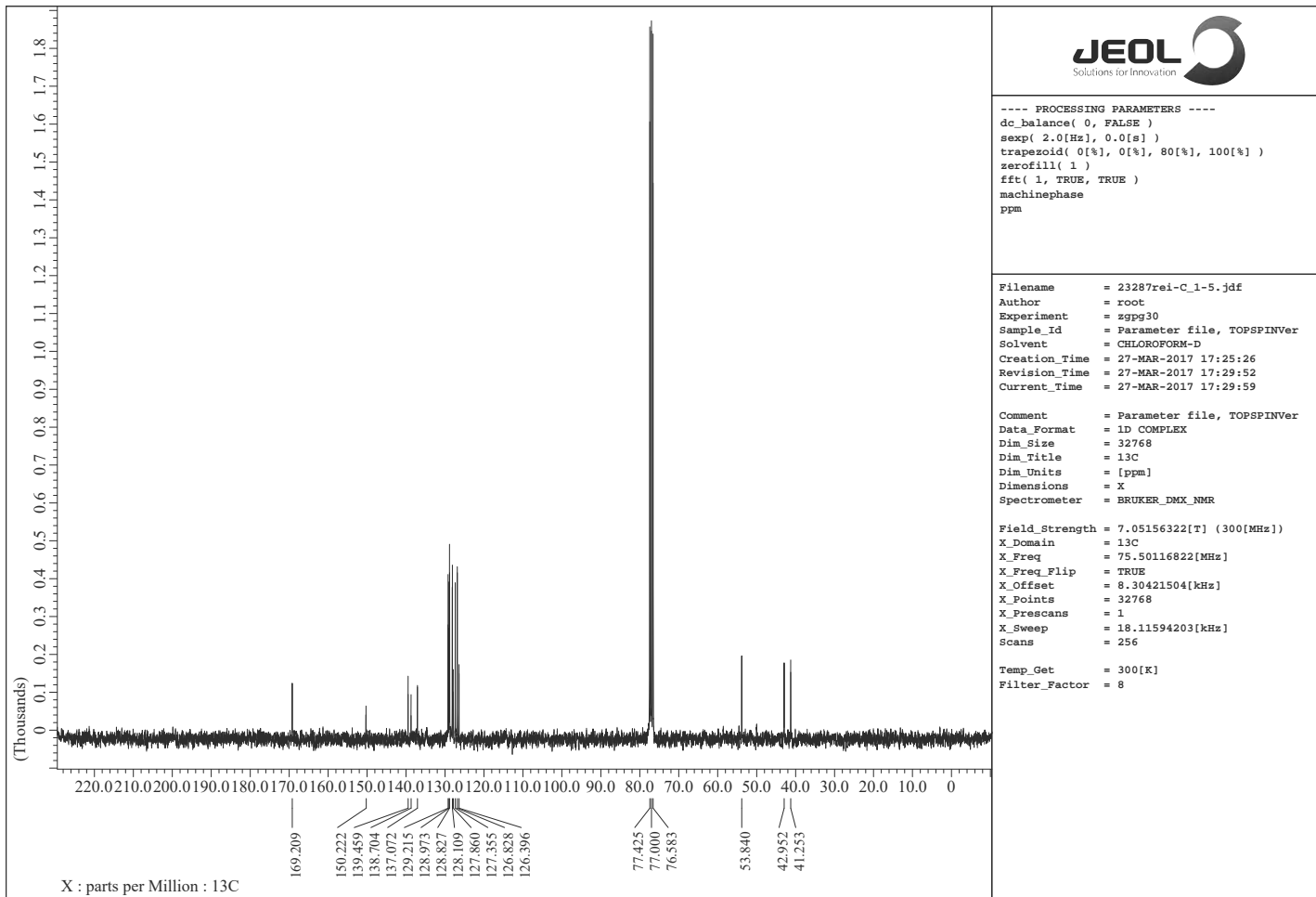
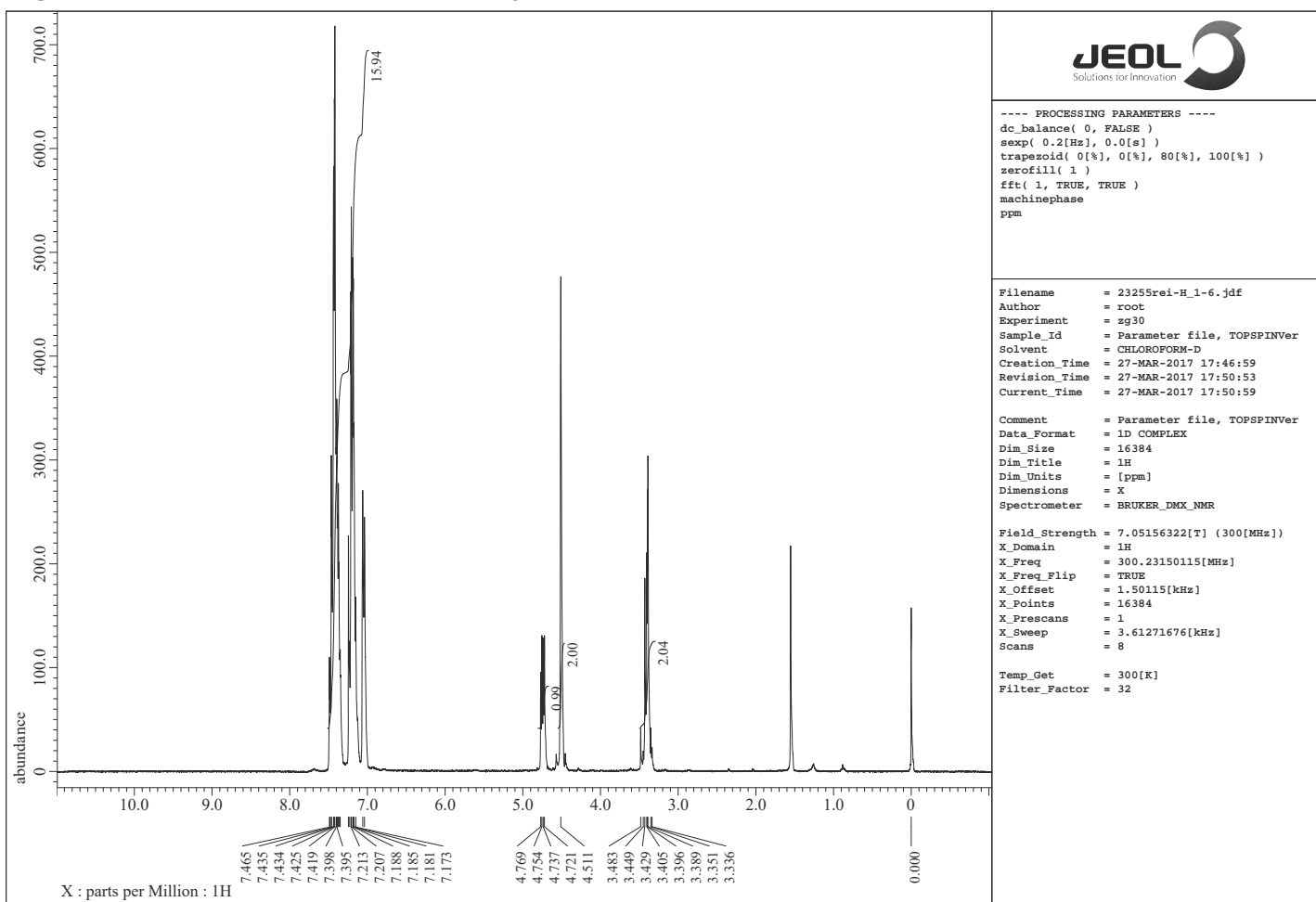


Figure S26. ^1H and ^{13}C NMR spectra of **2i**



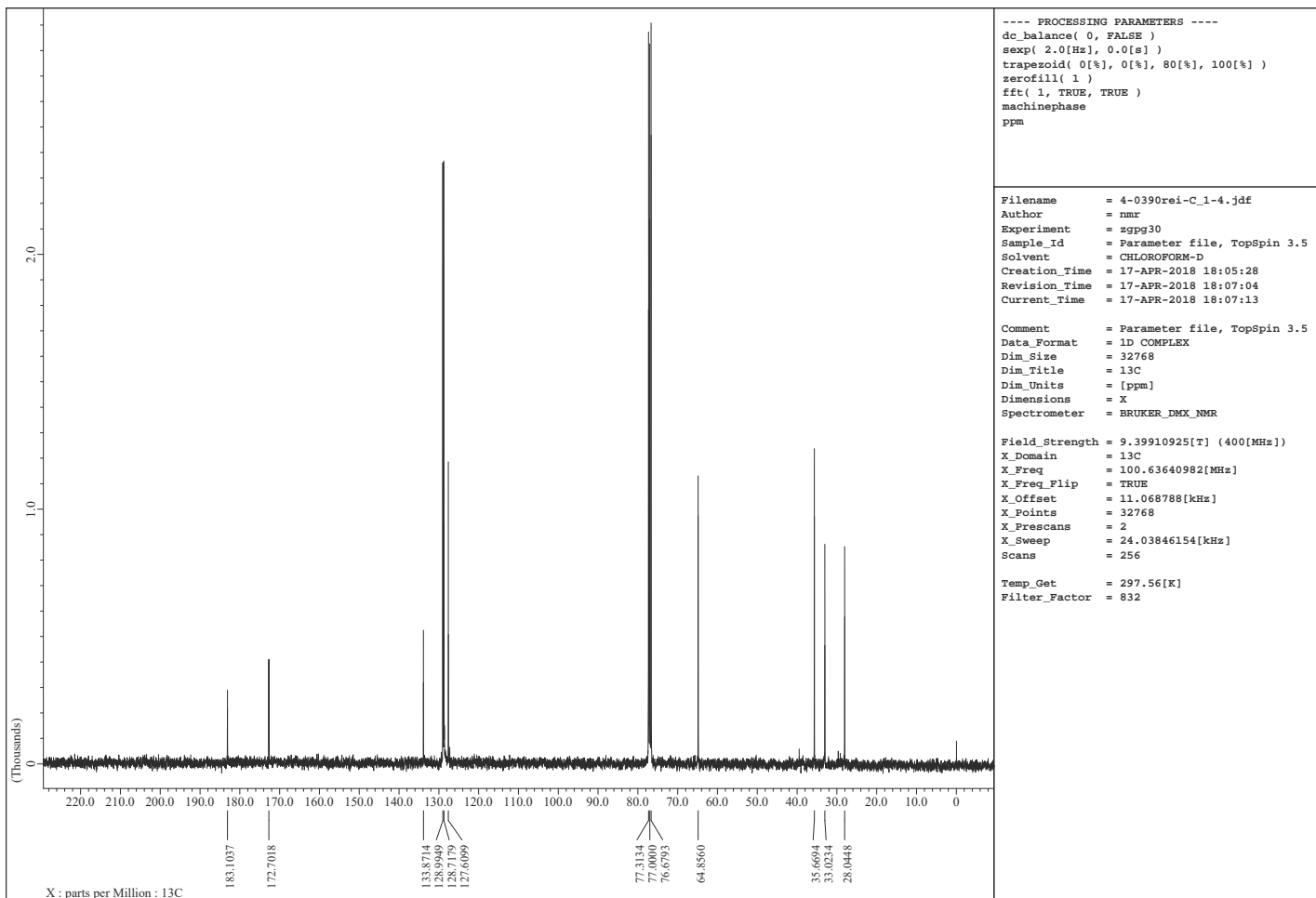
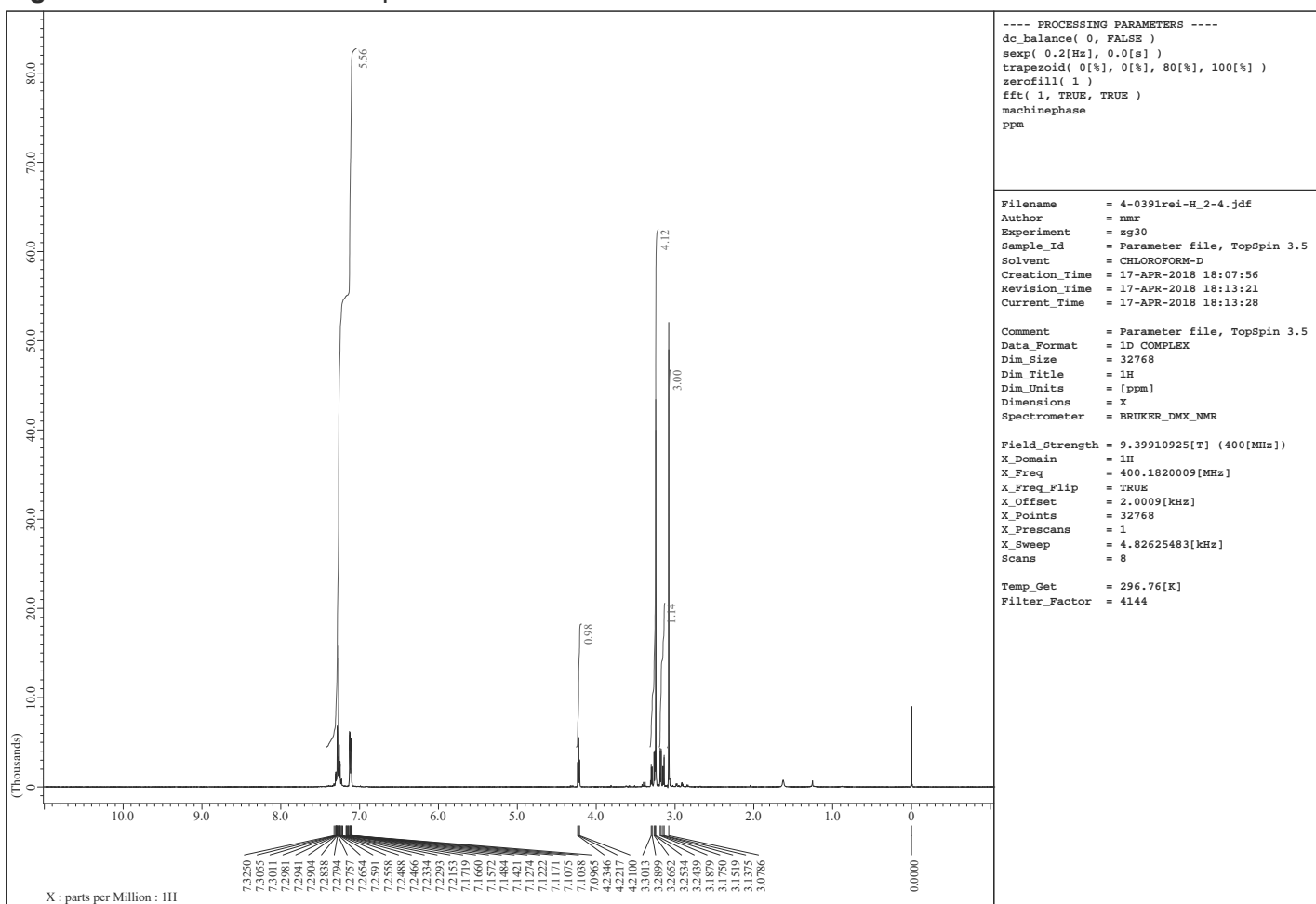
<<S29>>

Figure S27. ^1H and ^{13}C NMR spectra of **2j**



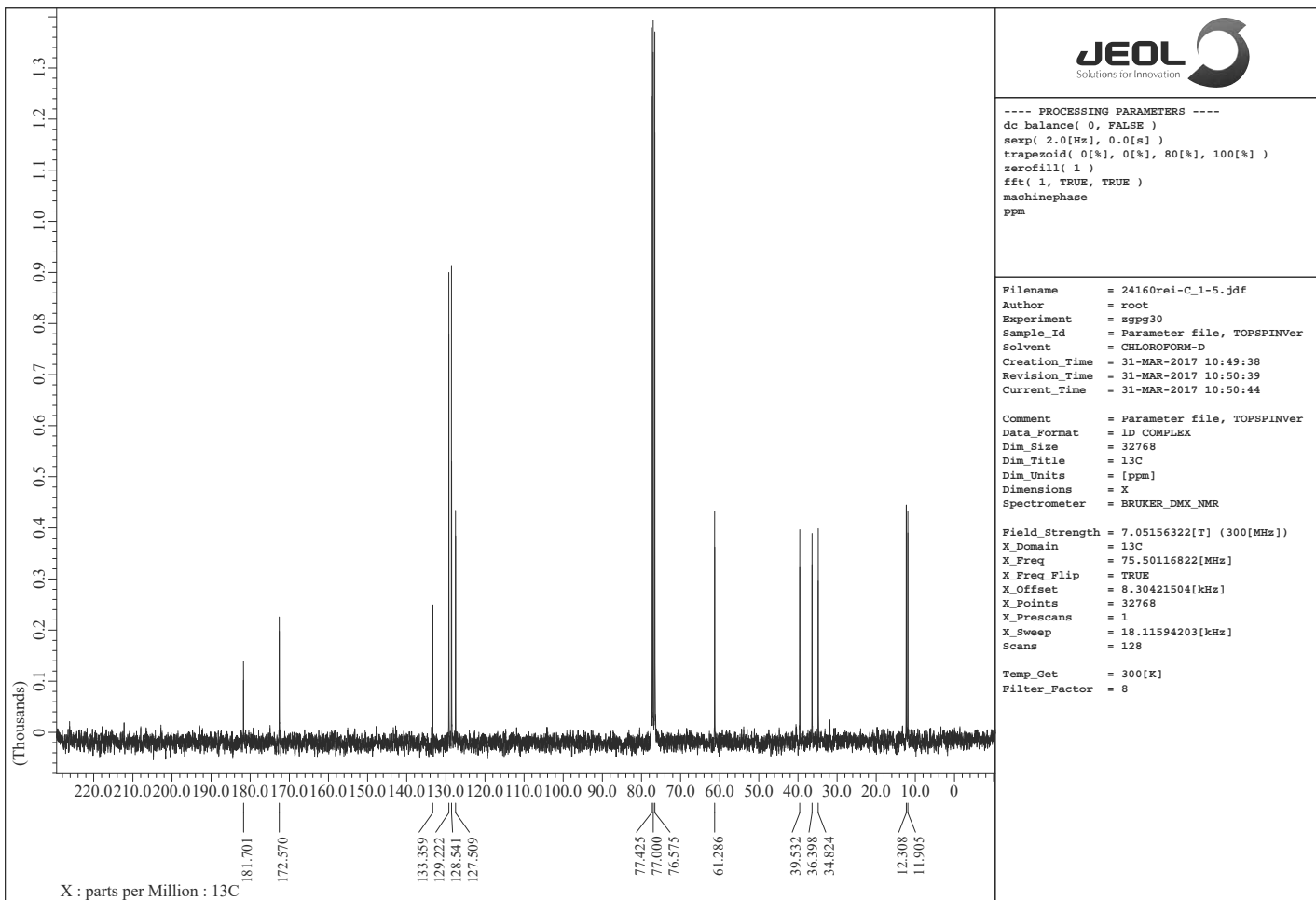
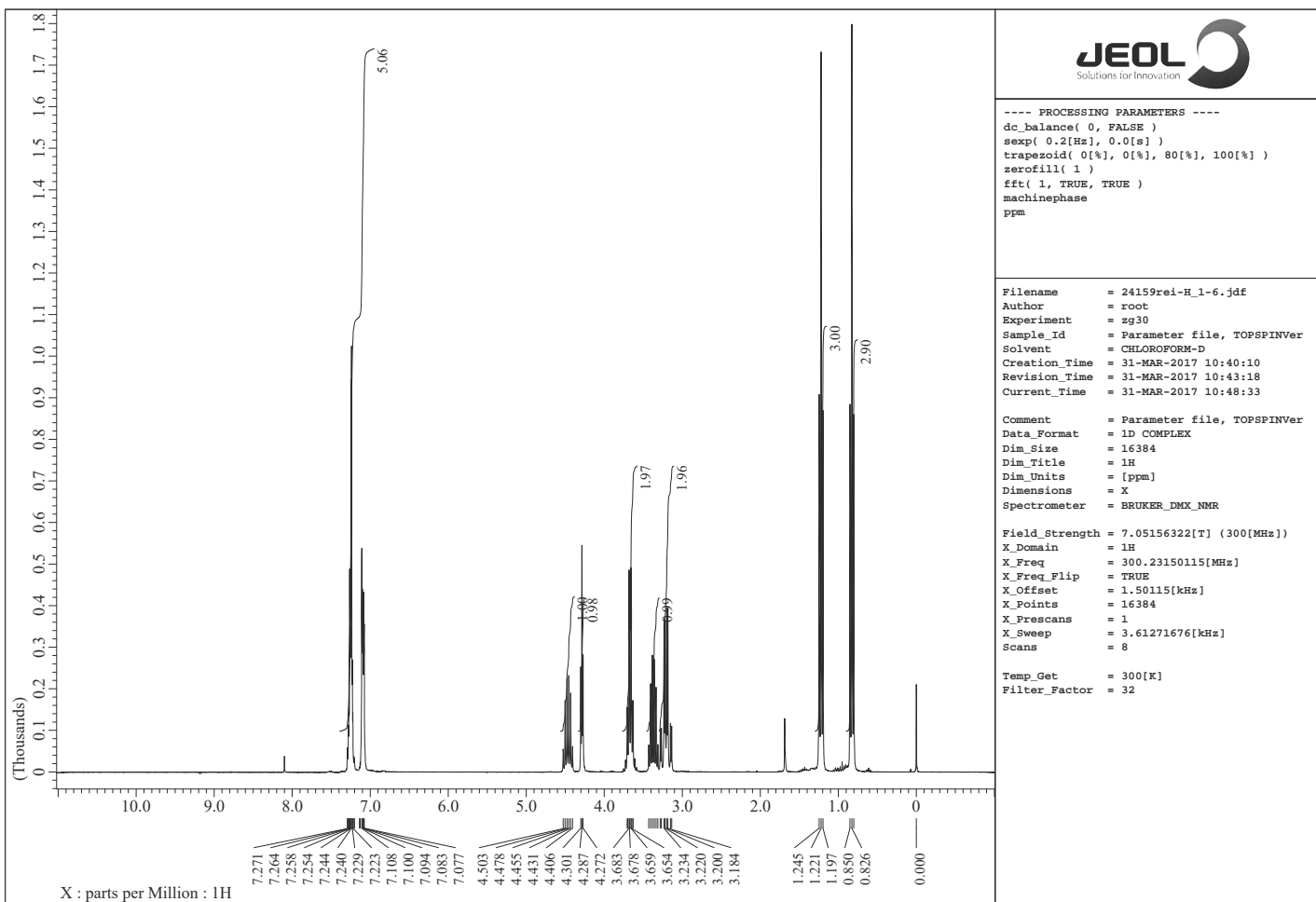
<<S30>>

Figure S28. ^1H and ^{13}C NMR spectra of **3a**



<<S31>>

Figure S29. ^1H and ^{13}C NMR spectra of **3b**



<<S32>>

Figure S30. ^1H and ^{13}C NMR spectra of **3c**

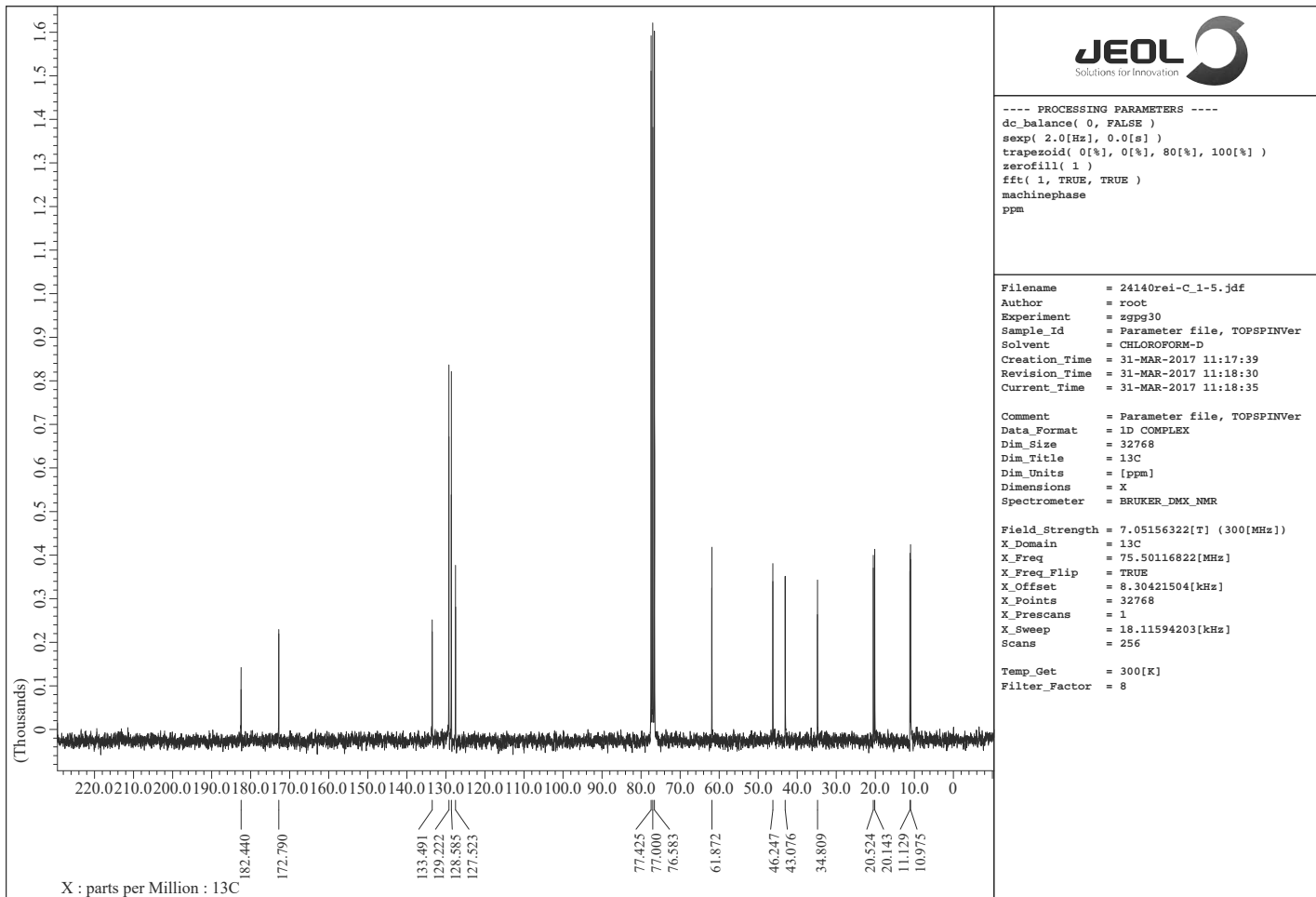
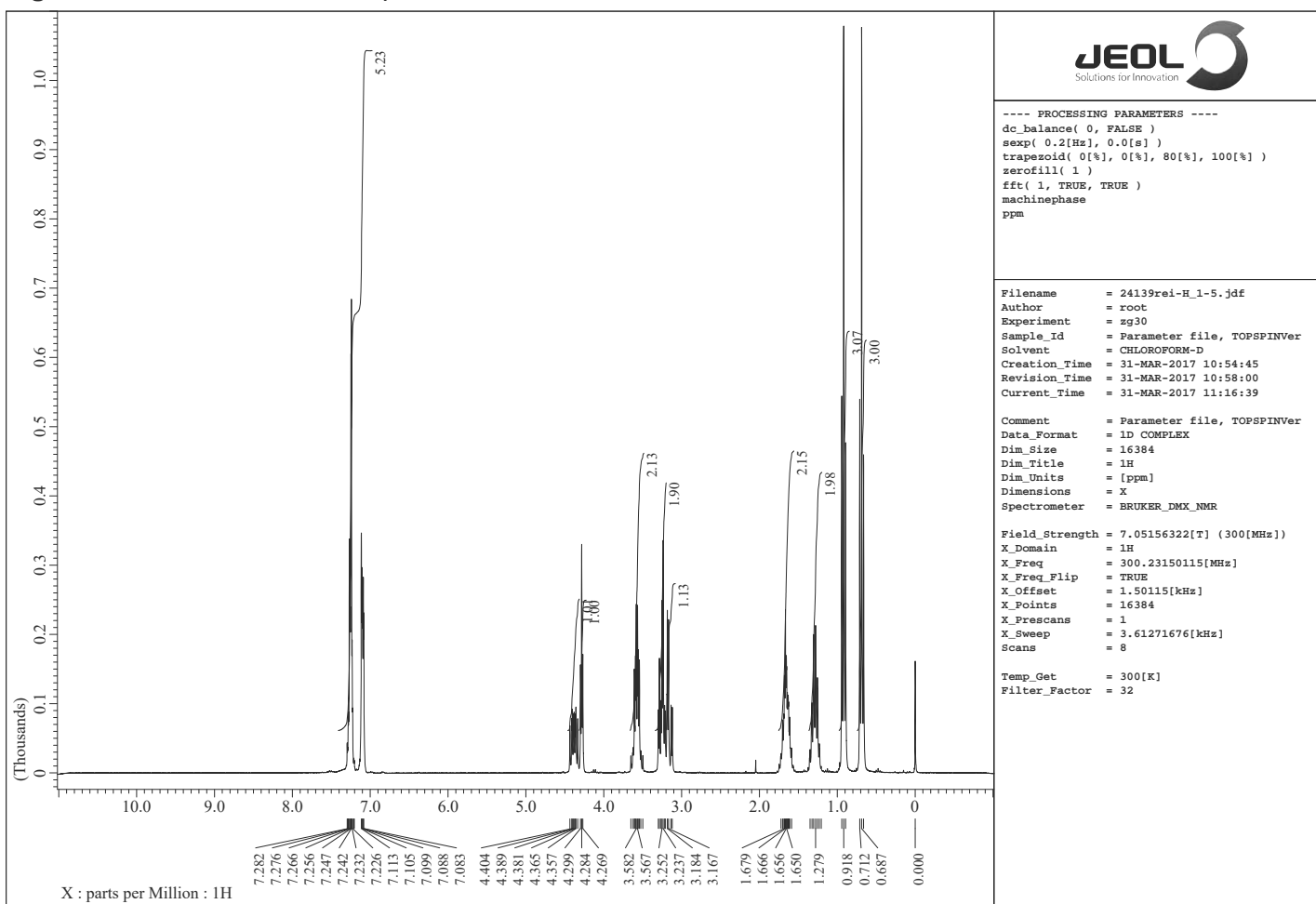


Figure S31. ^1H and ^{13}C NMR spectra of **3d**

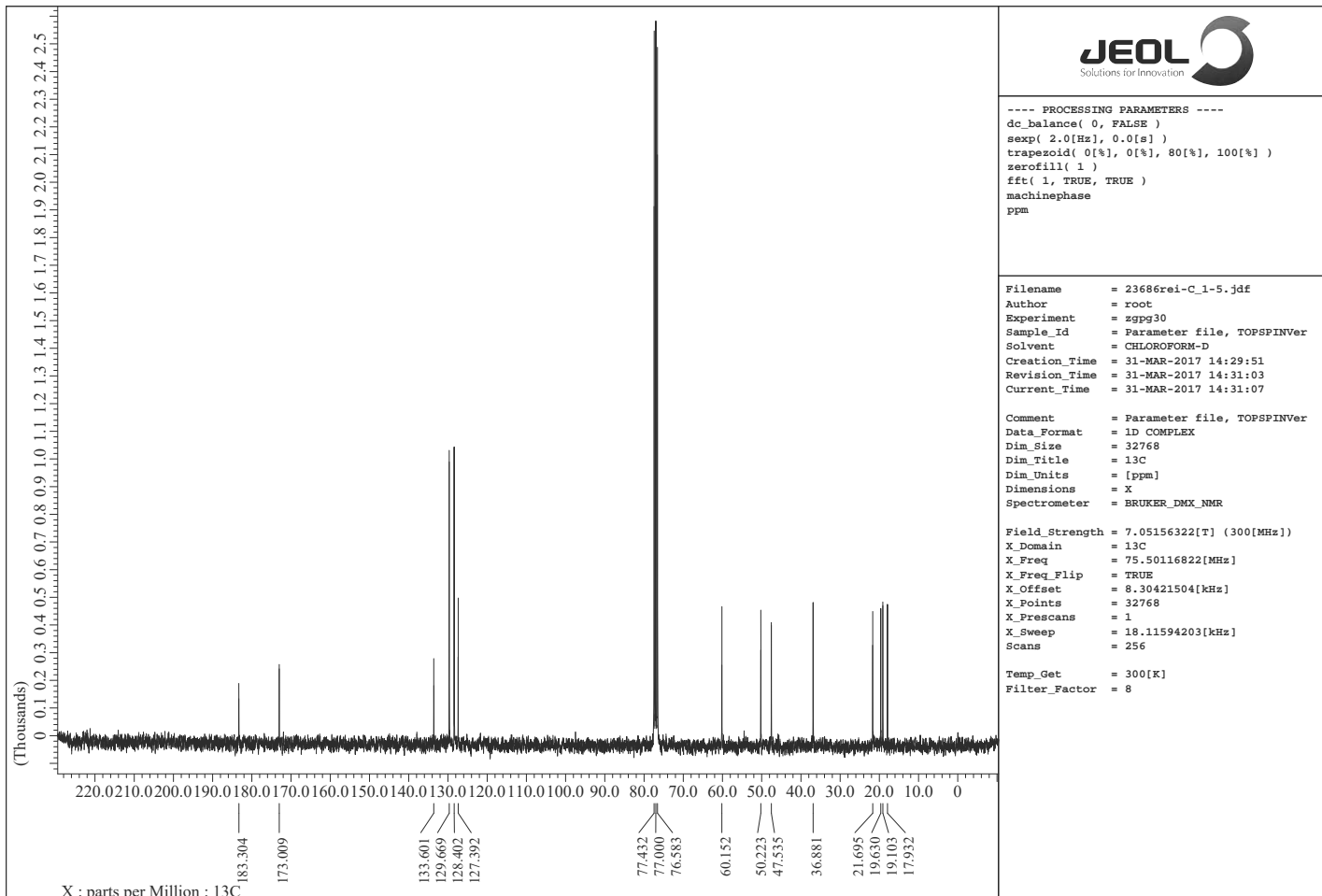
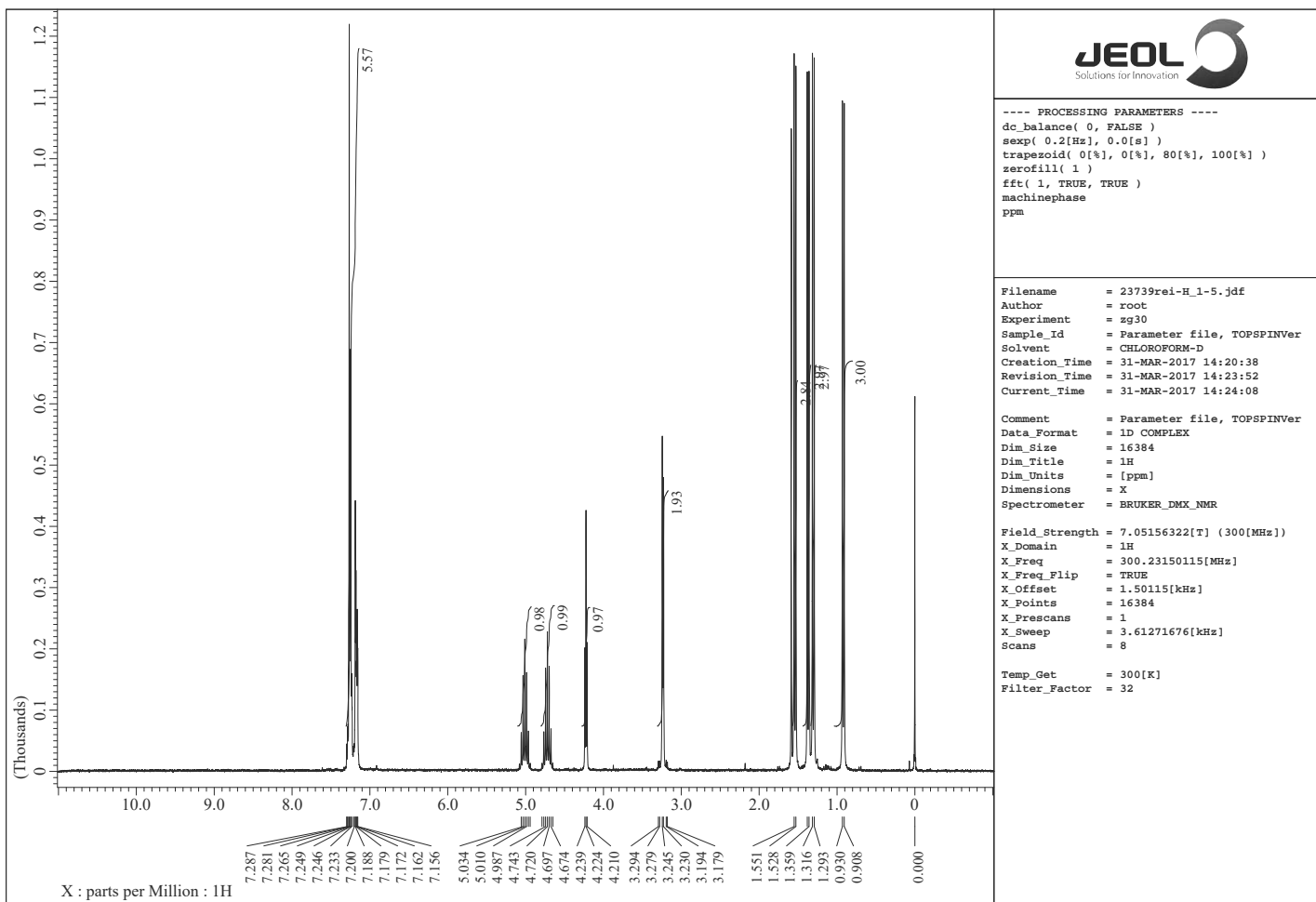


Figure S32. ^1H and ^{13}C NMR spectra of **3e**

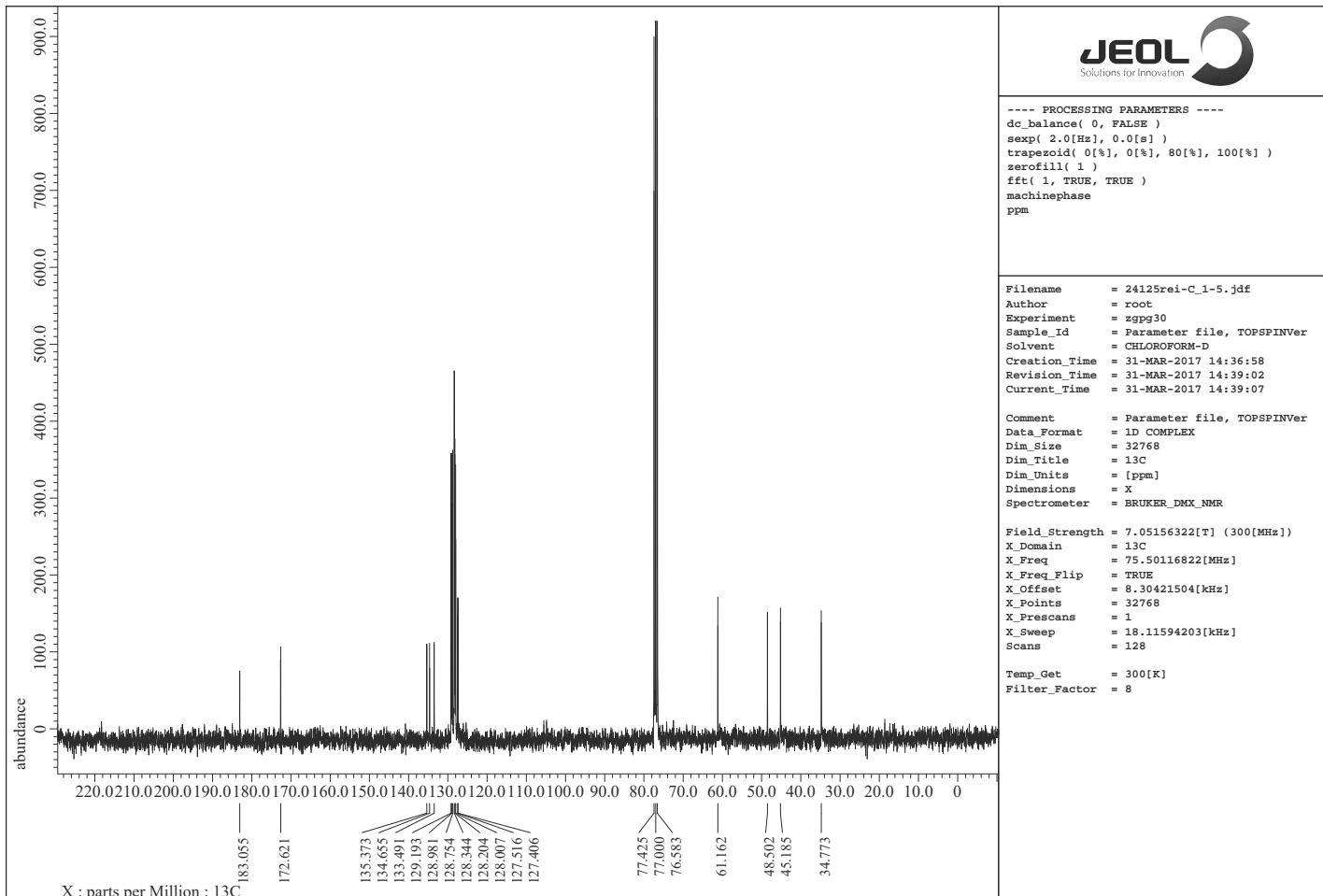
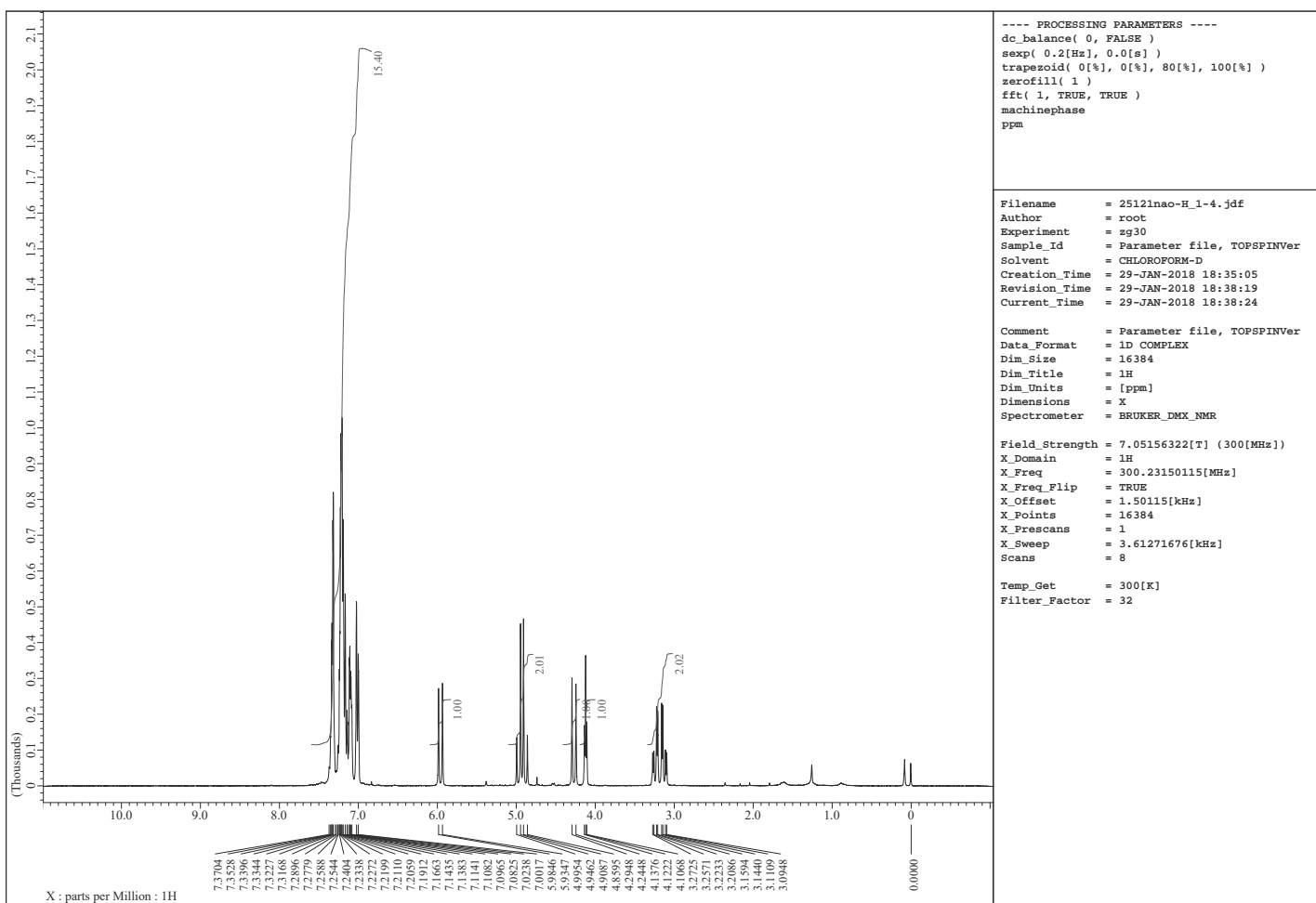


Figure S33. ^1H and ^{13}C NMR spectra of **3f**

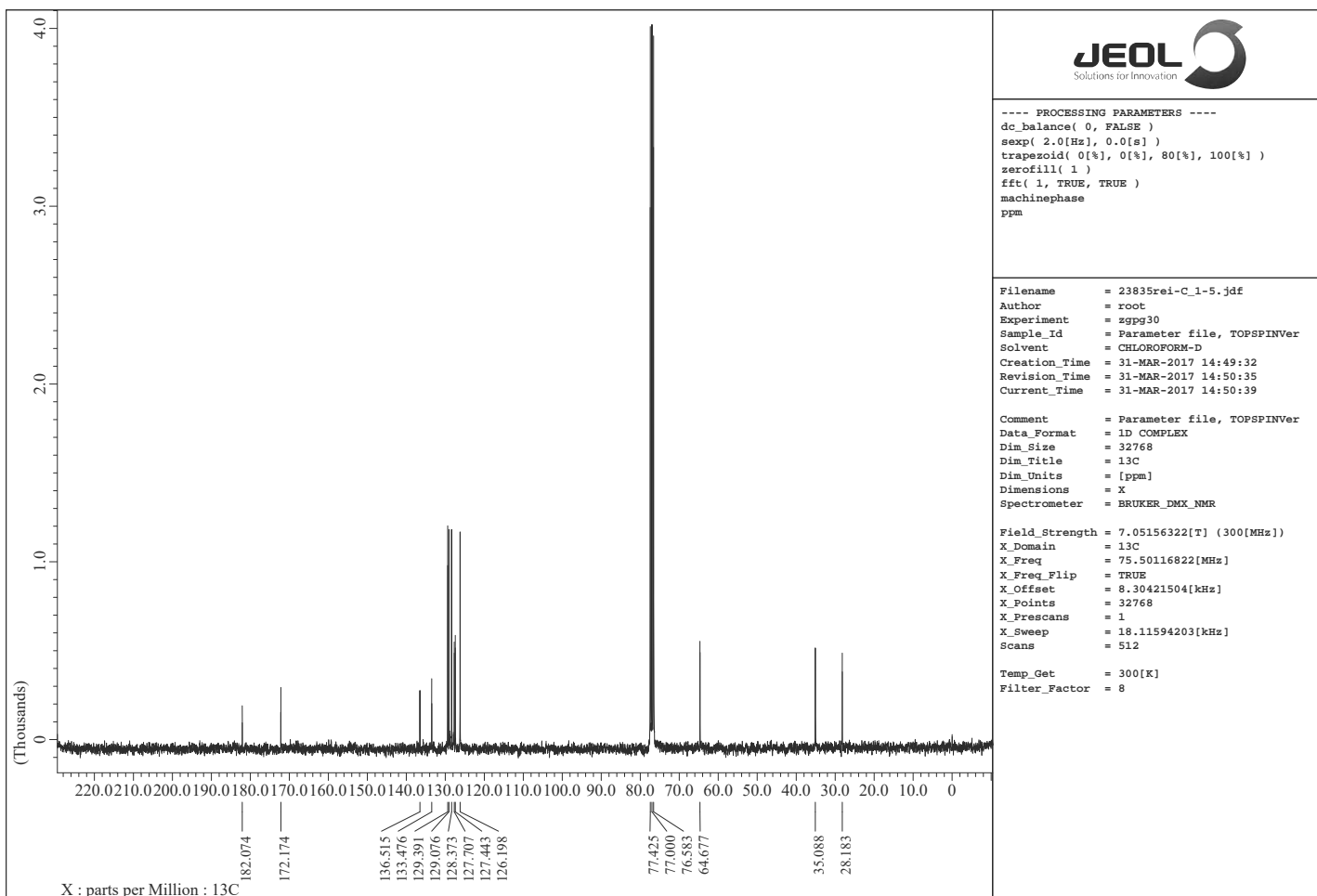
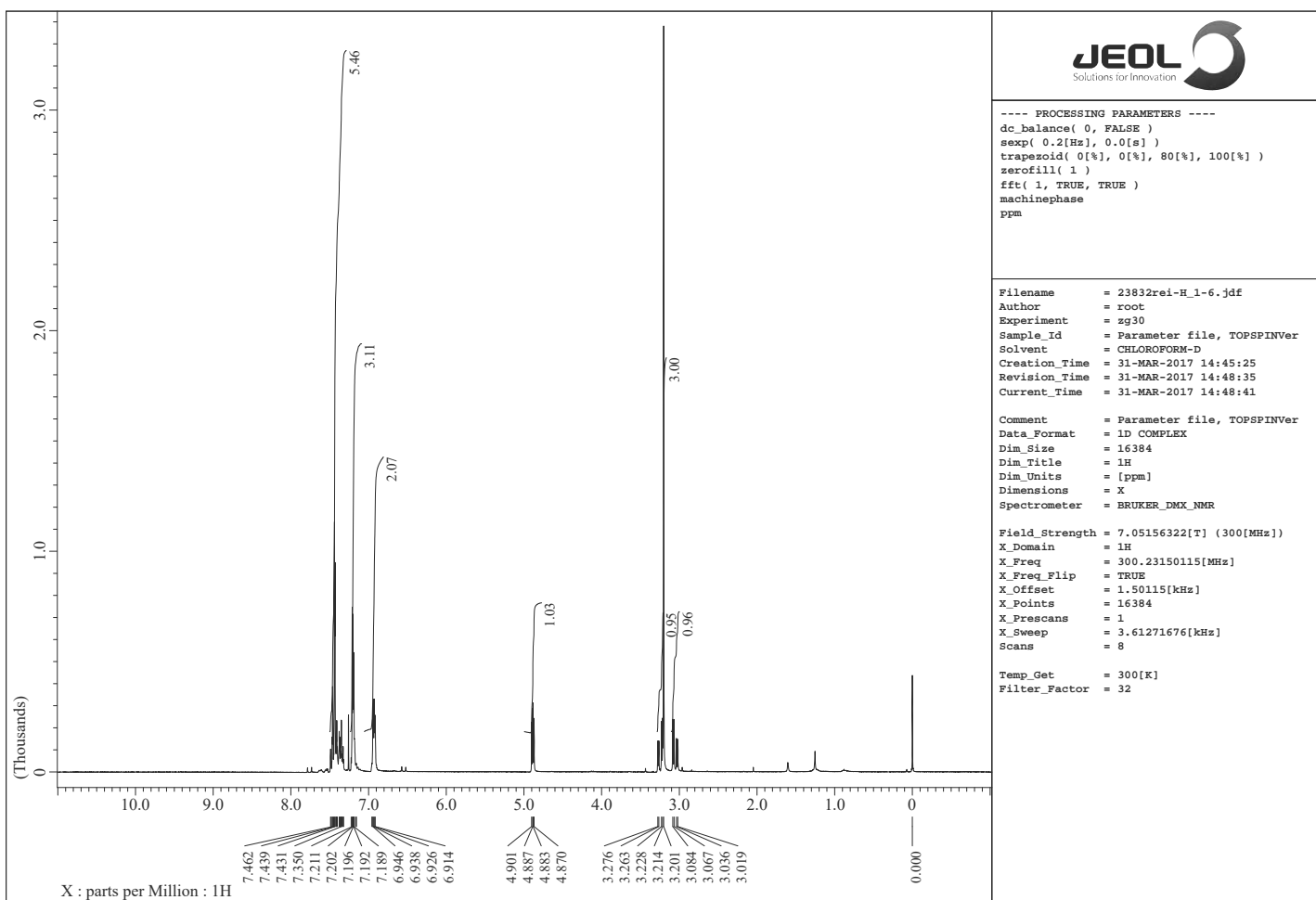


Figure S34. ^1H and ^{13}C NMR spectra of **3g**

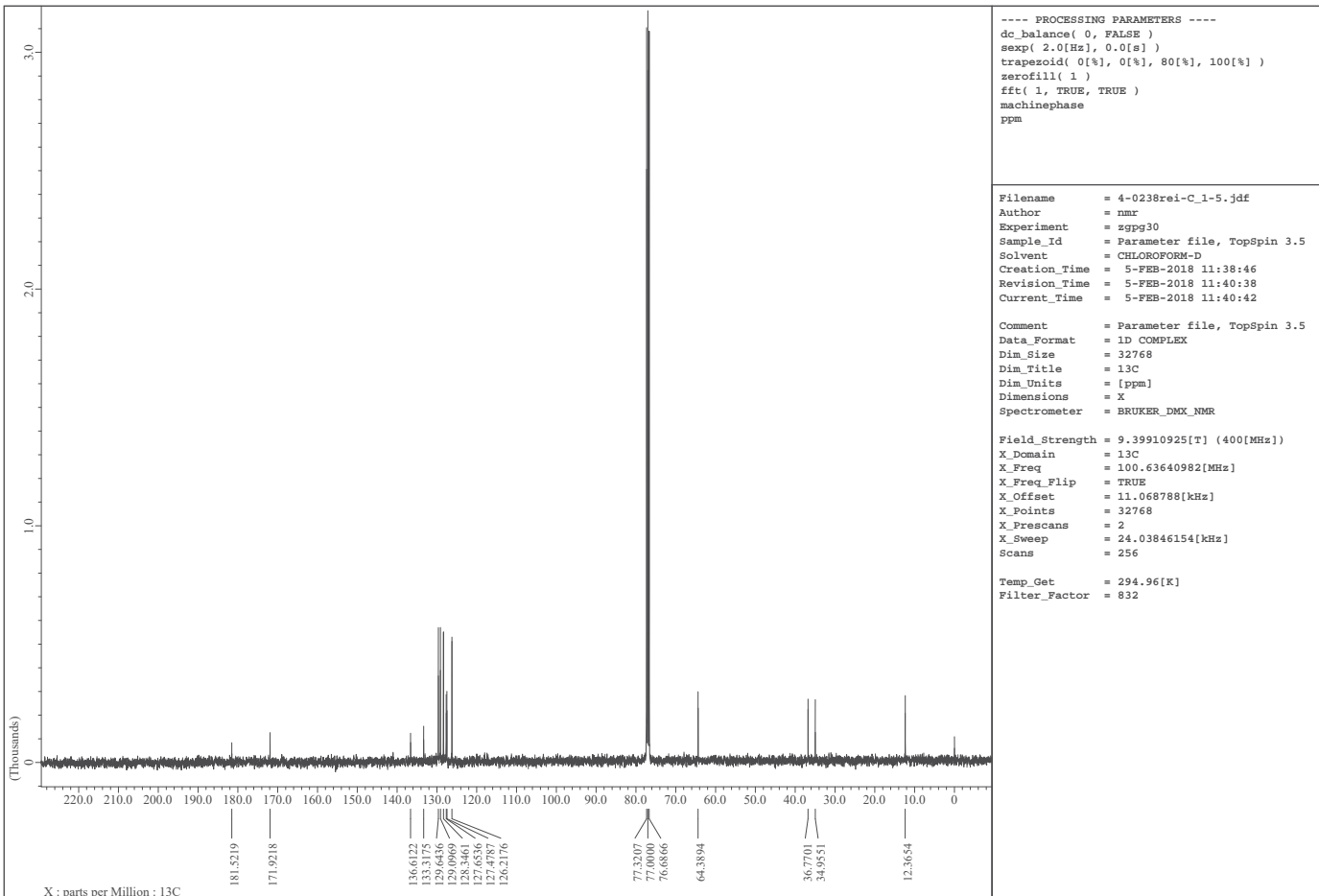
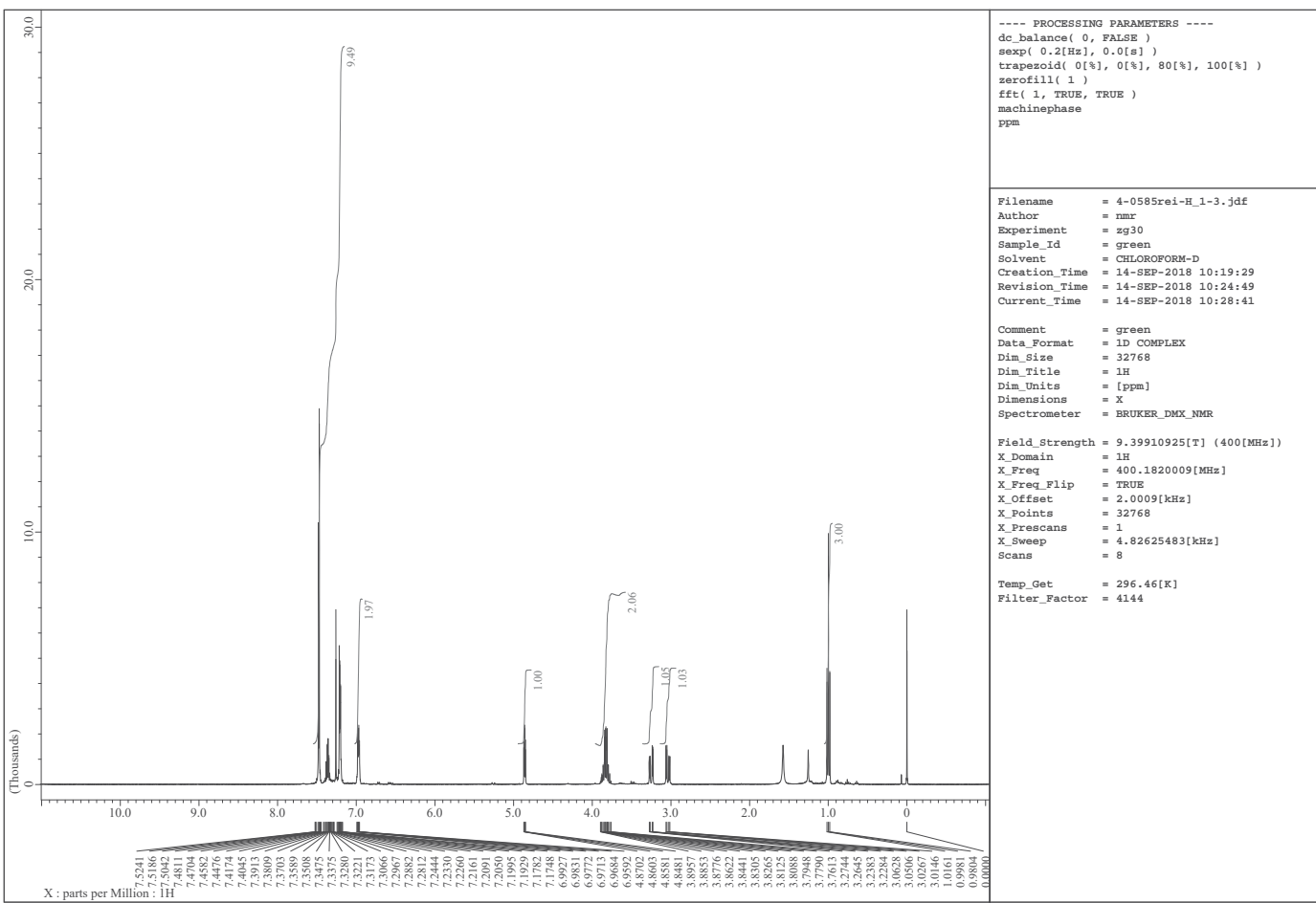


Figure S35. ^1H and ^{13}C NMR spectra of **3h**

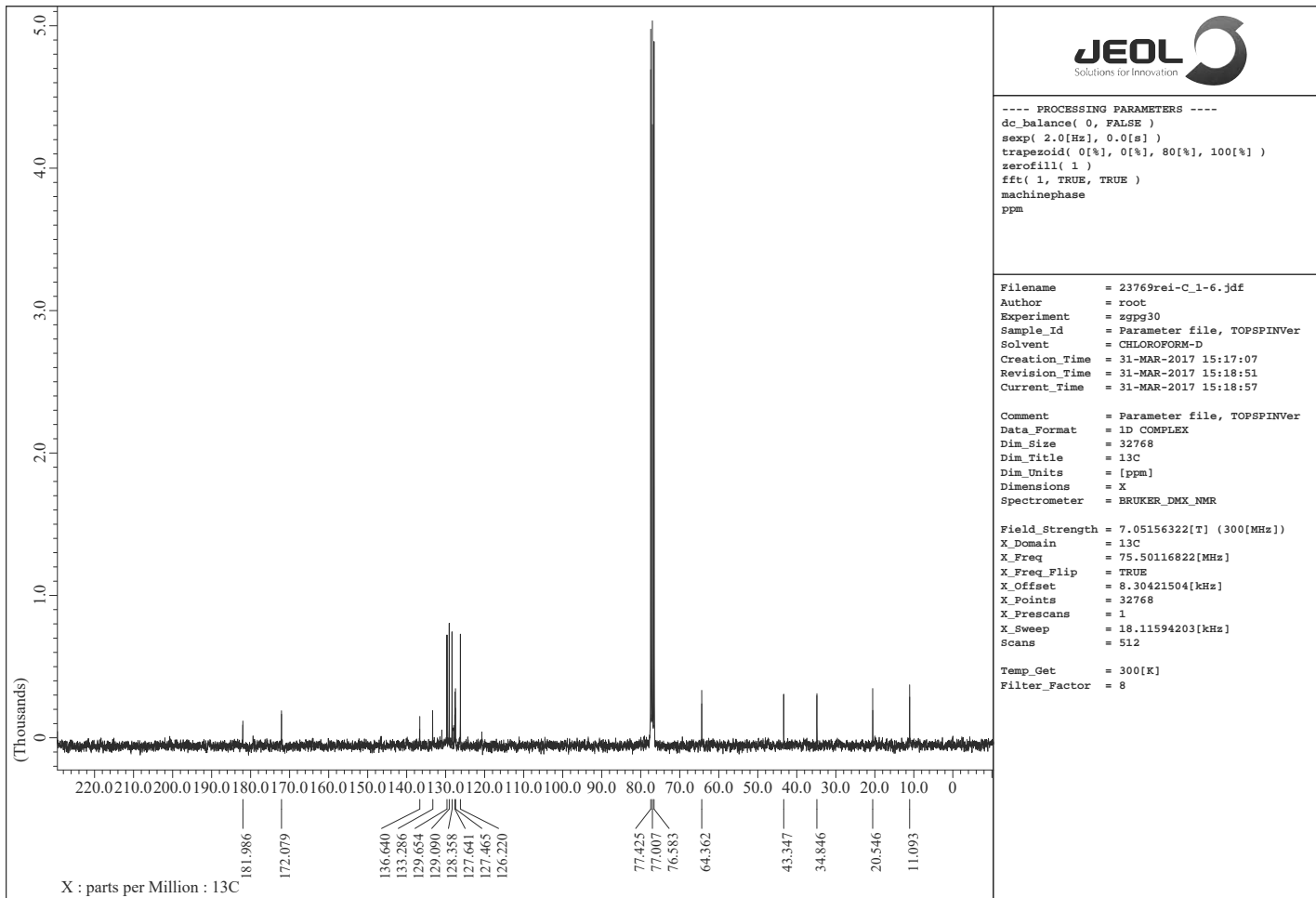
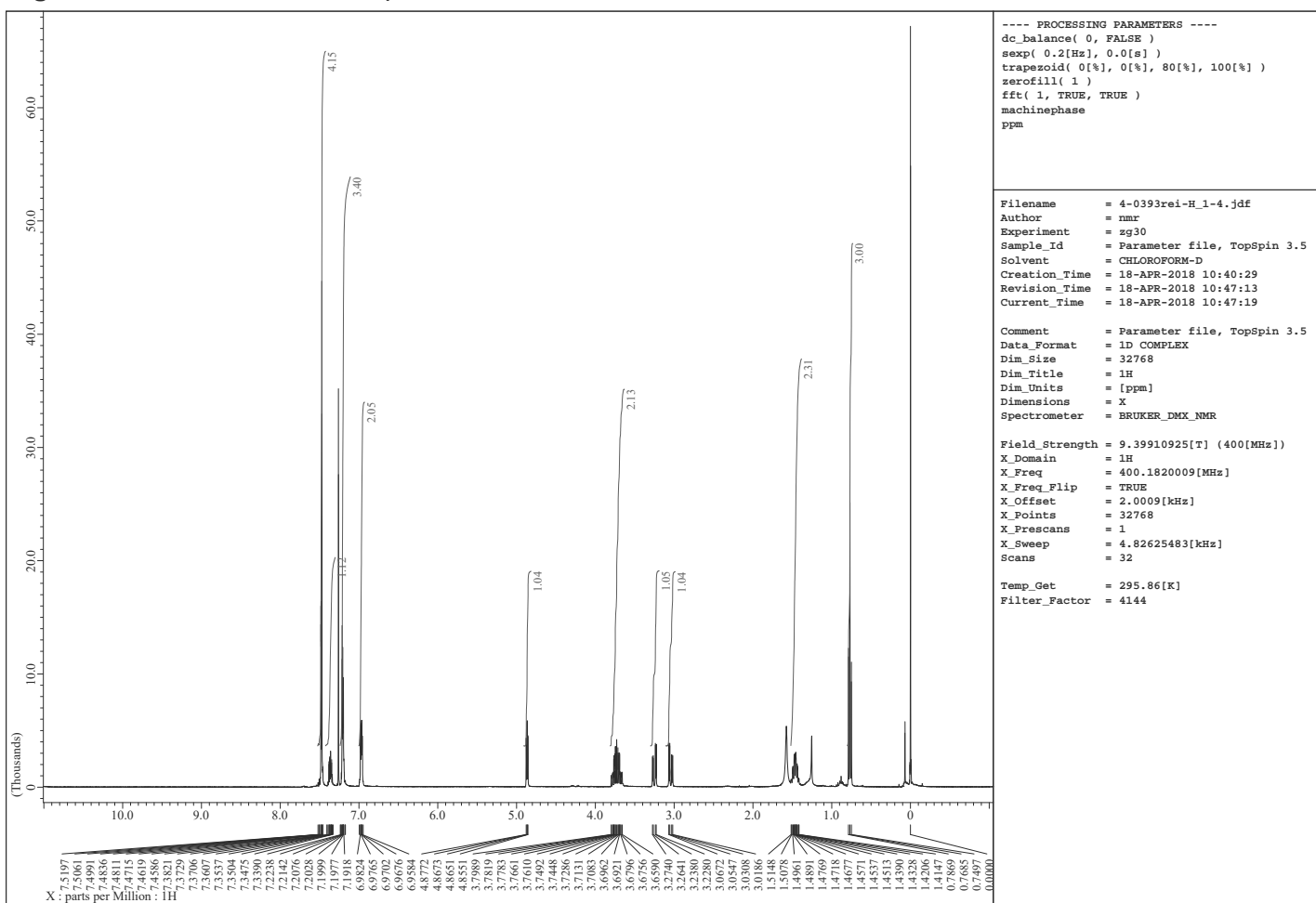


Figure S36. ^1H and ^{13}C NMR spectra of **3i**

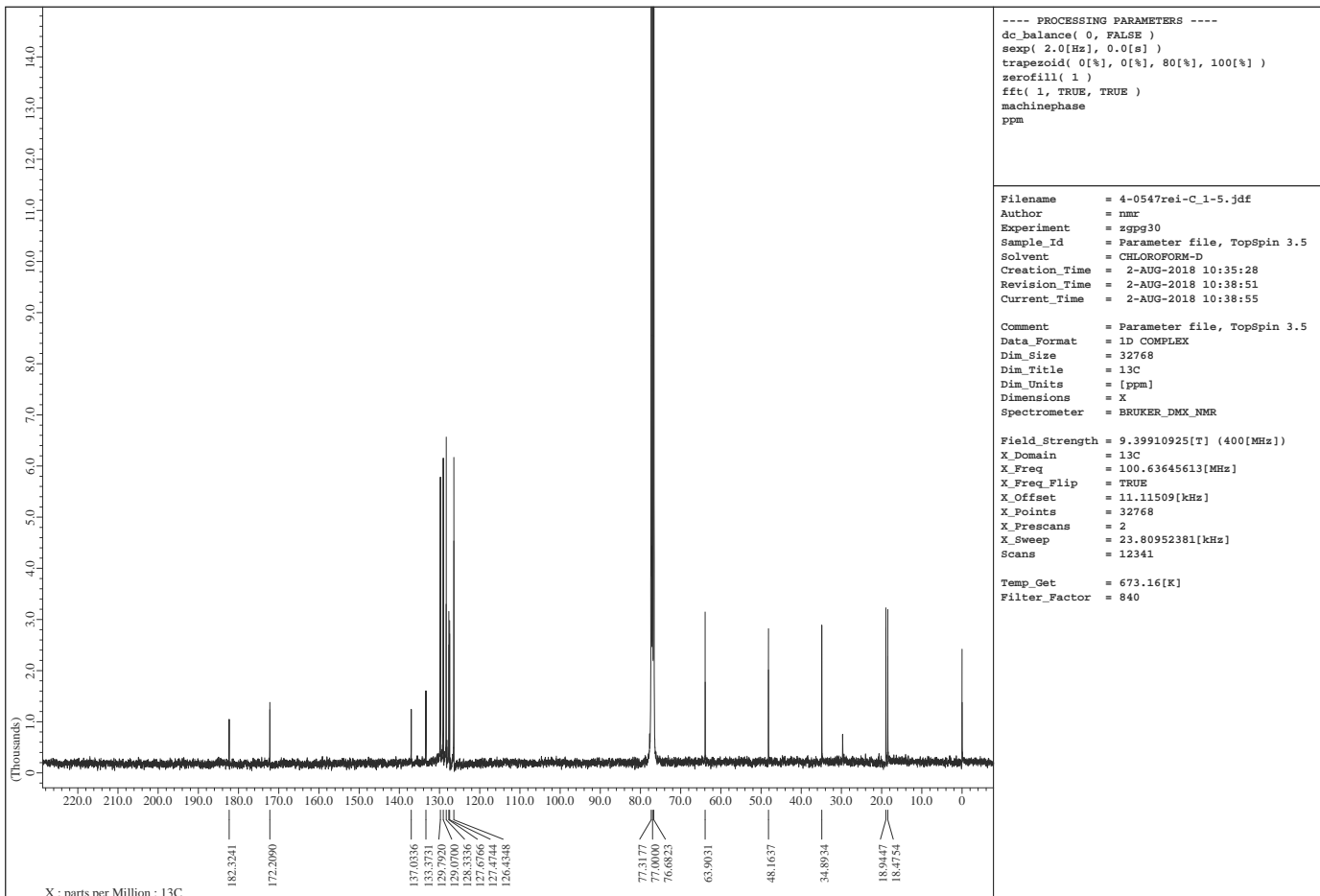
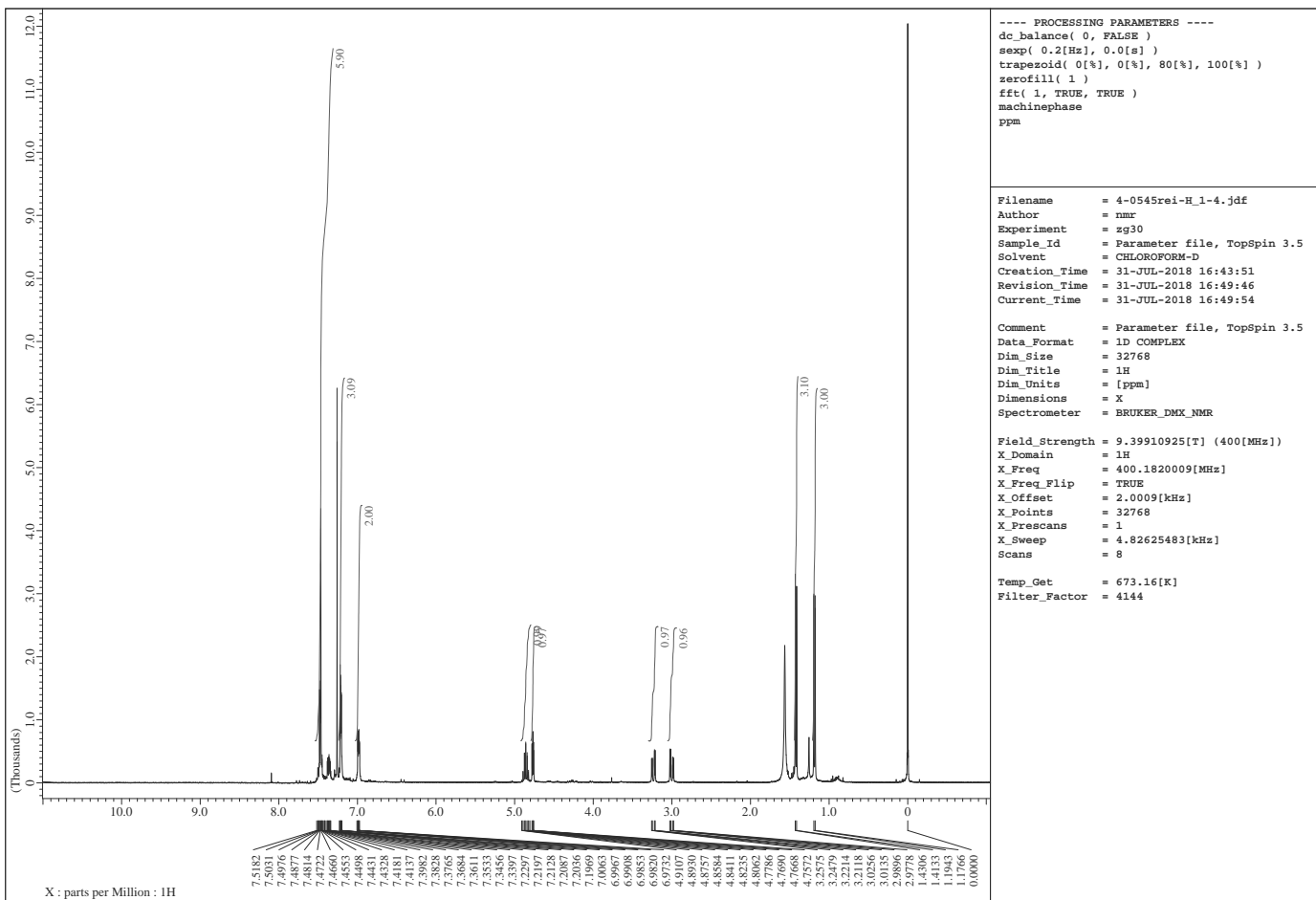


Figure S37. ^1H and ^{13}C NMR spectra of **3j**

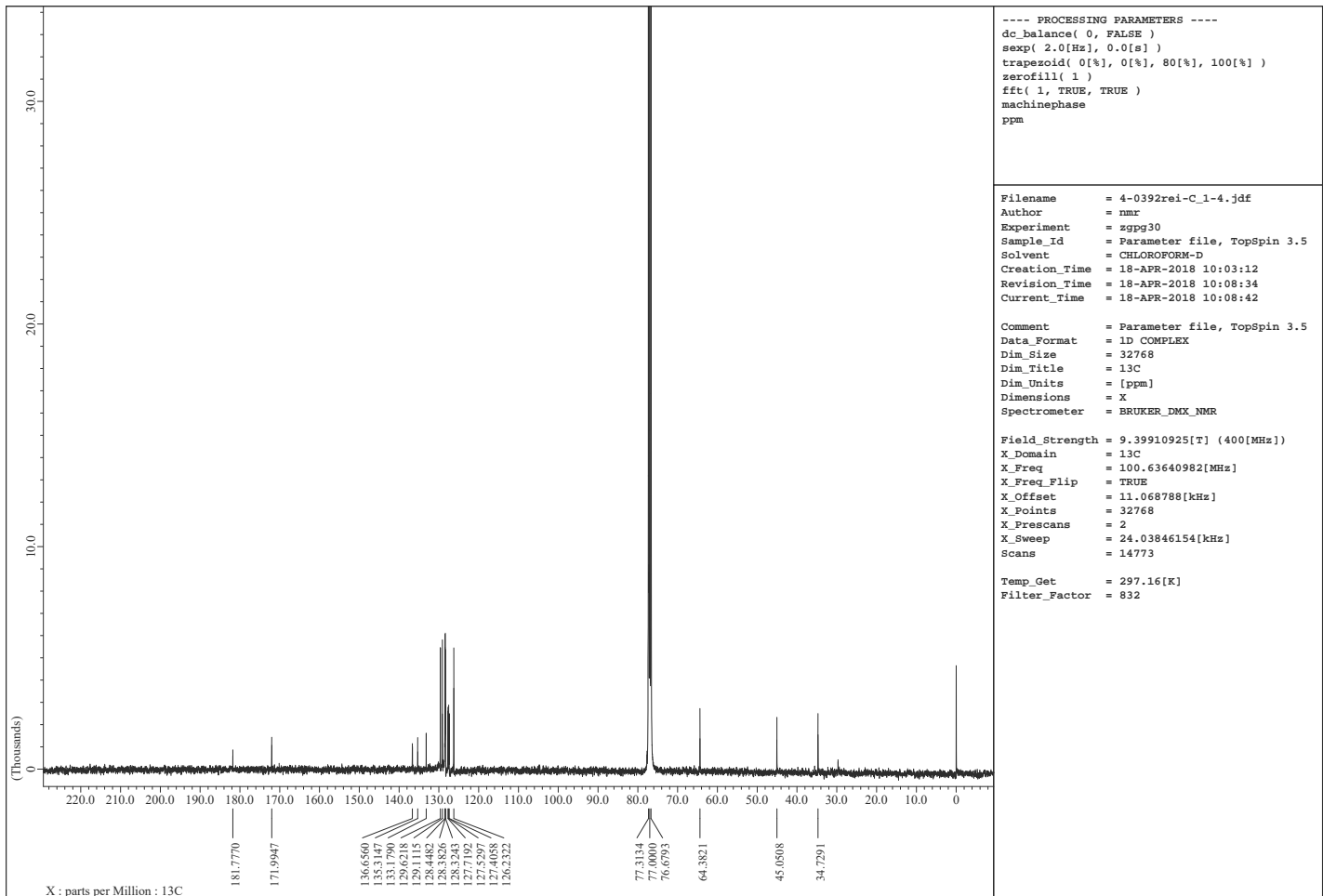
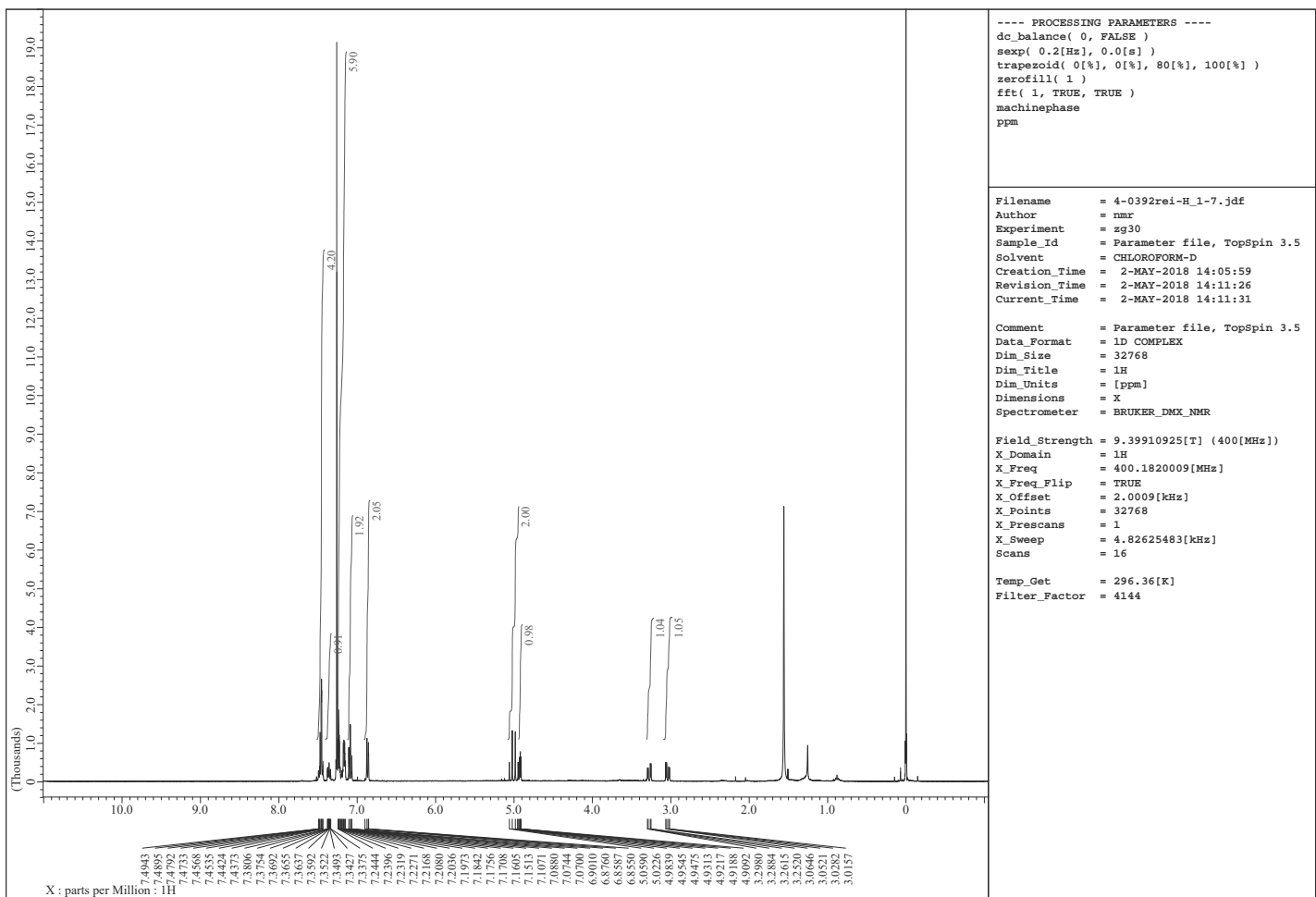


Figure S38. ^1H and ^{13}C NMR spectra of **4d**

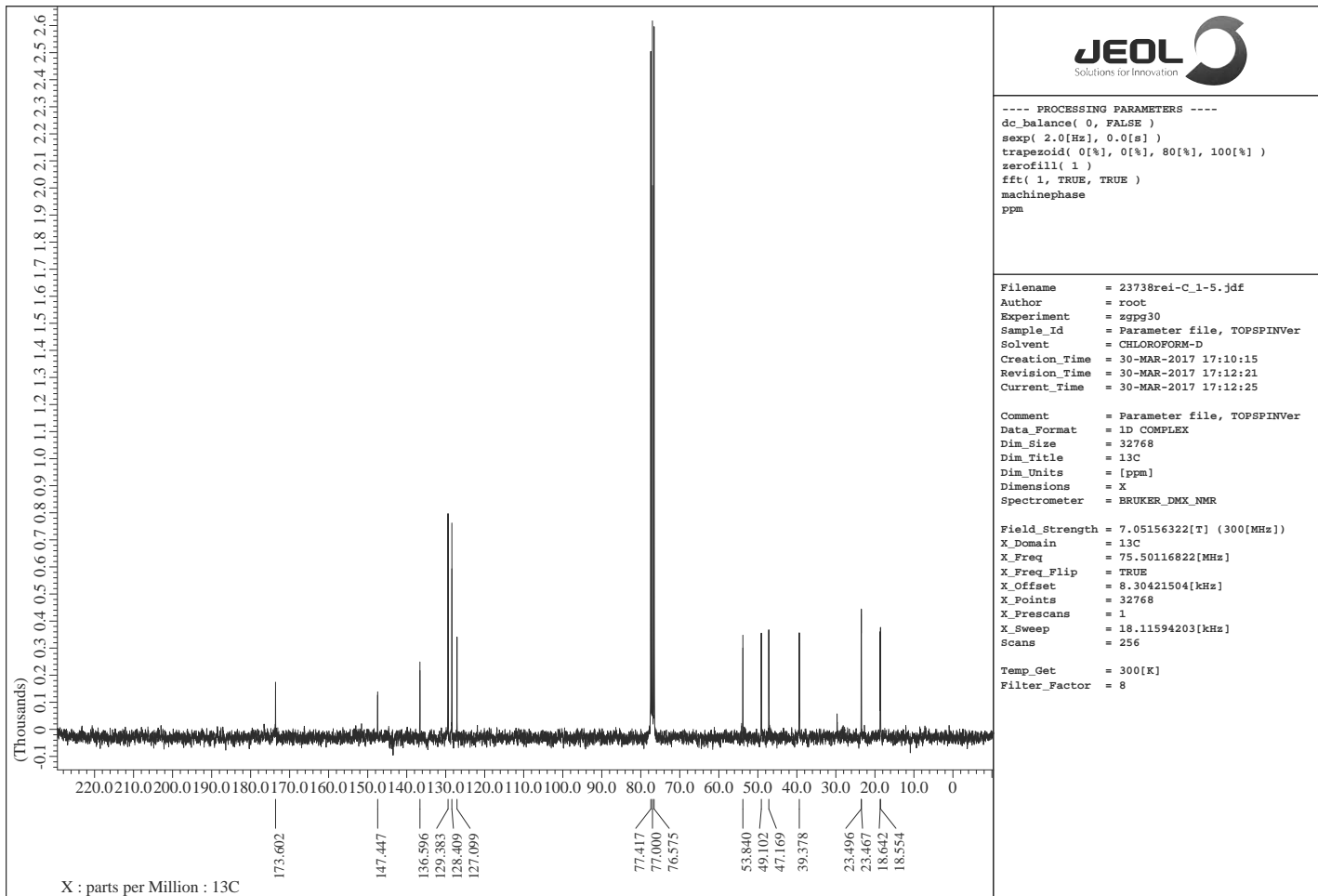
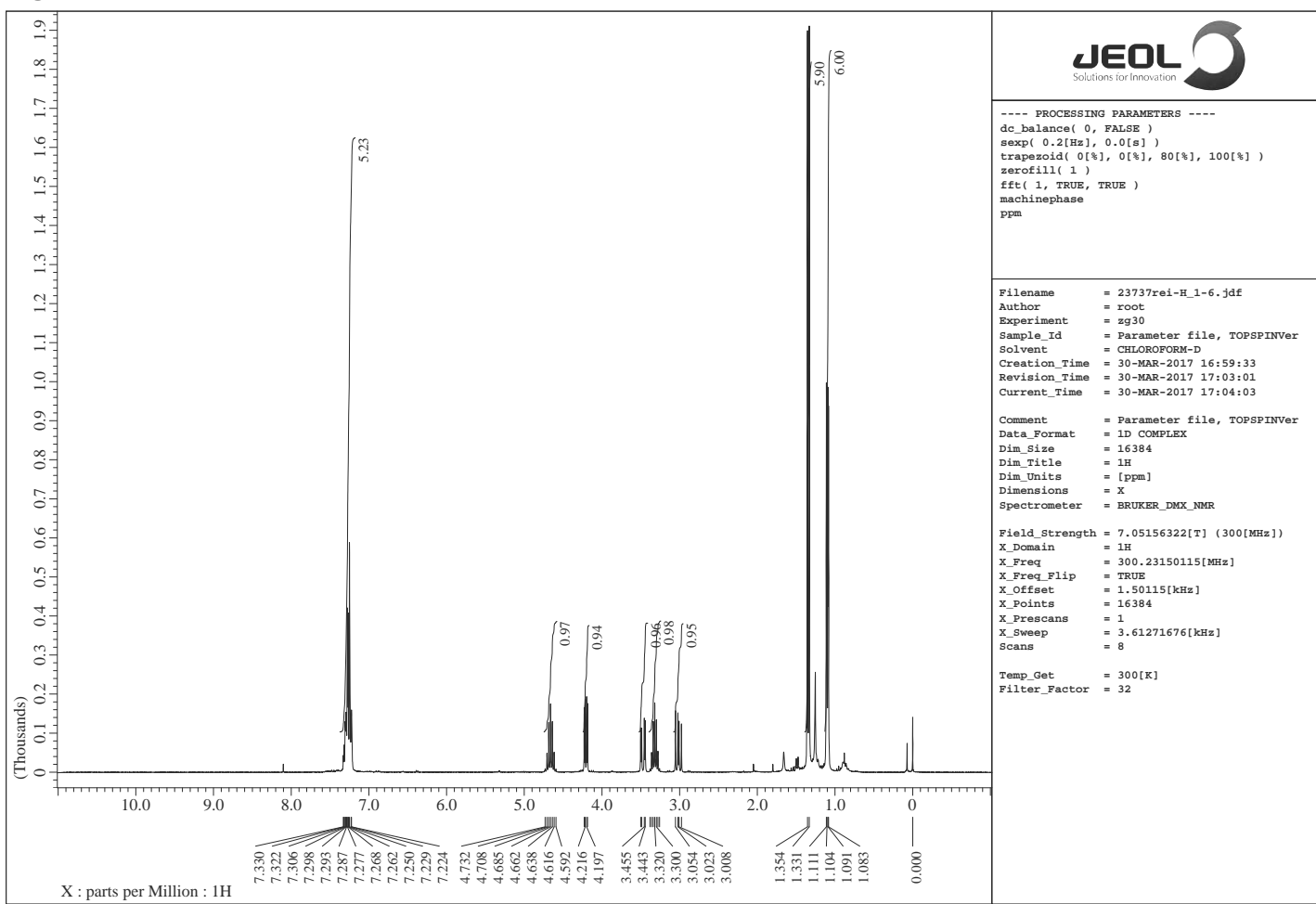


Figure S39. ^1H and ^{13}C NMR spectra of **4f**

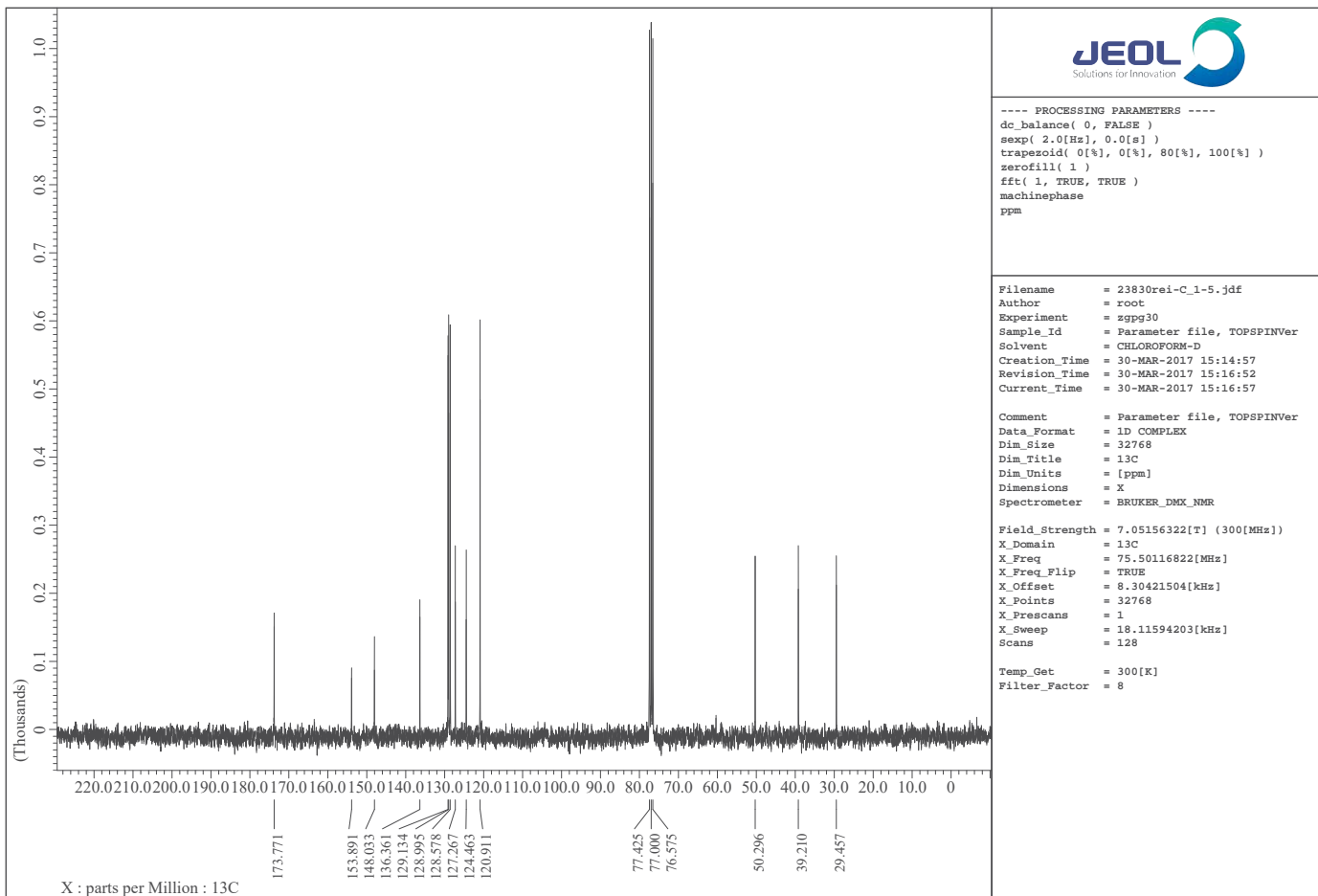
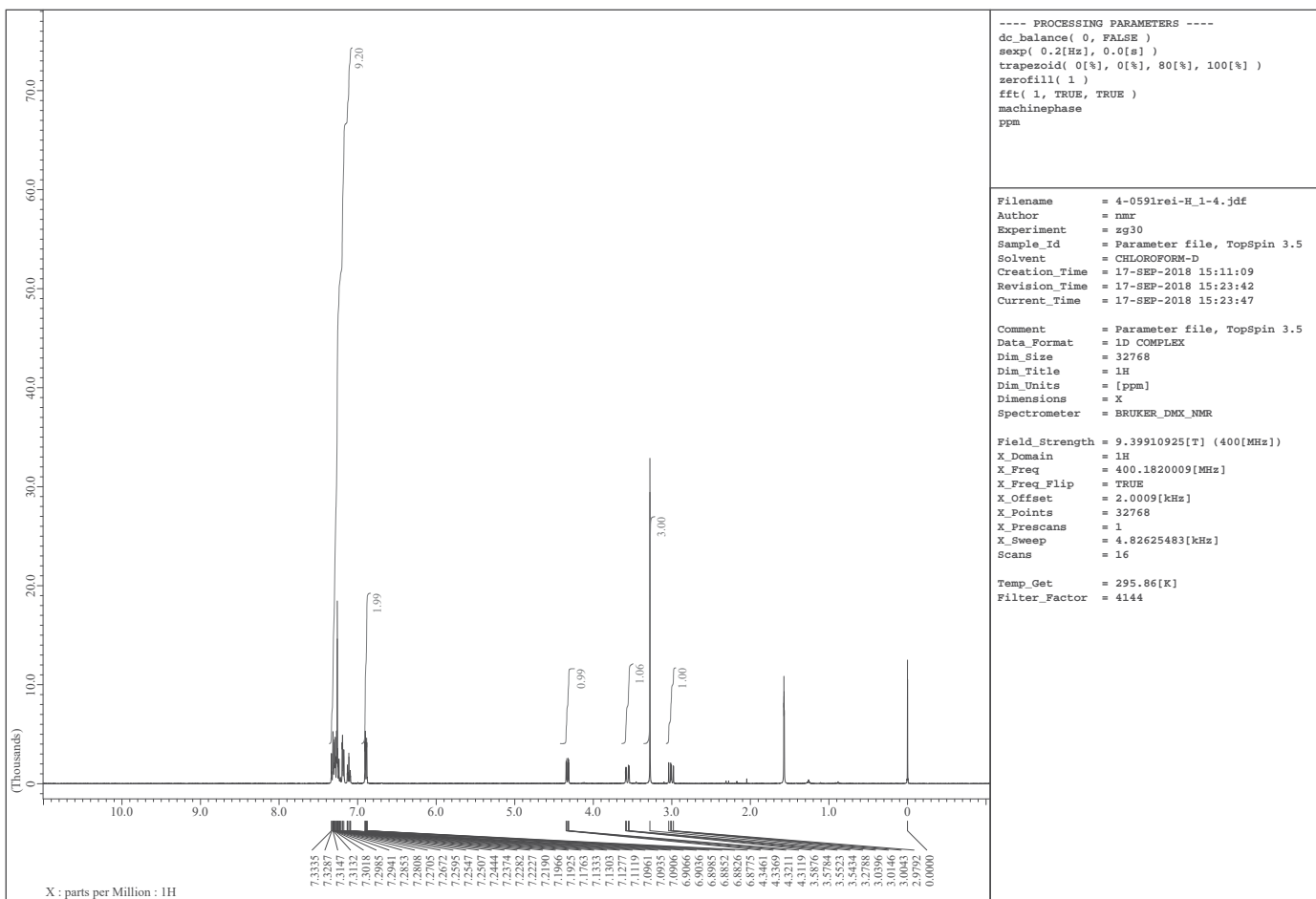


Figure S40. ^1H and ^{13}C NMR spectra of **4g**

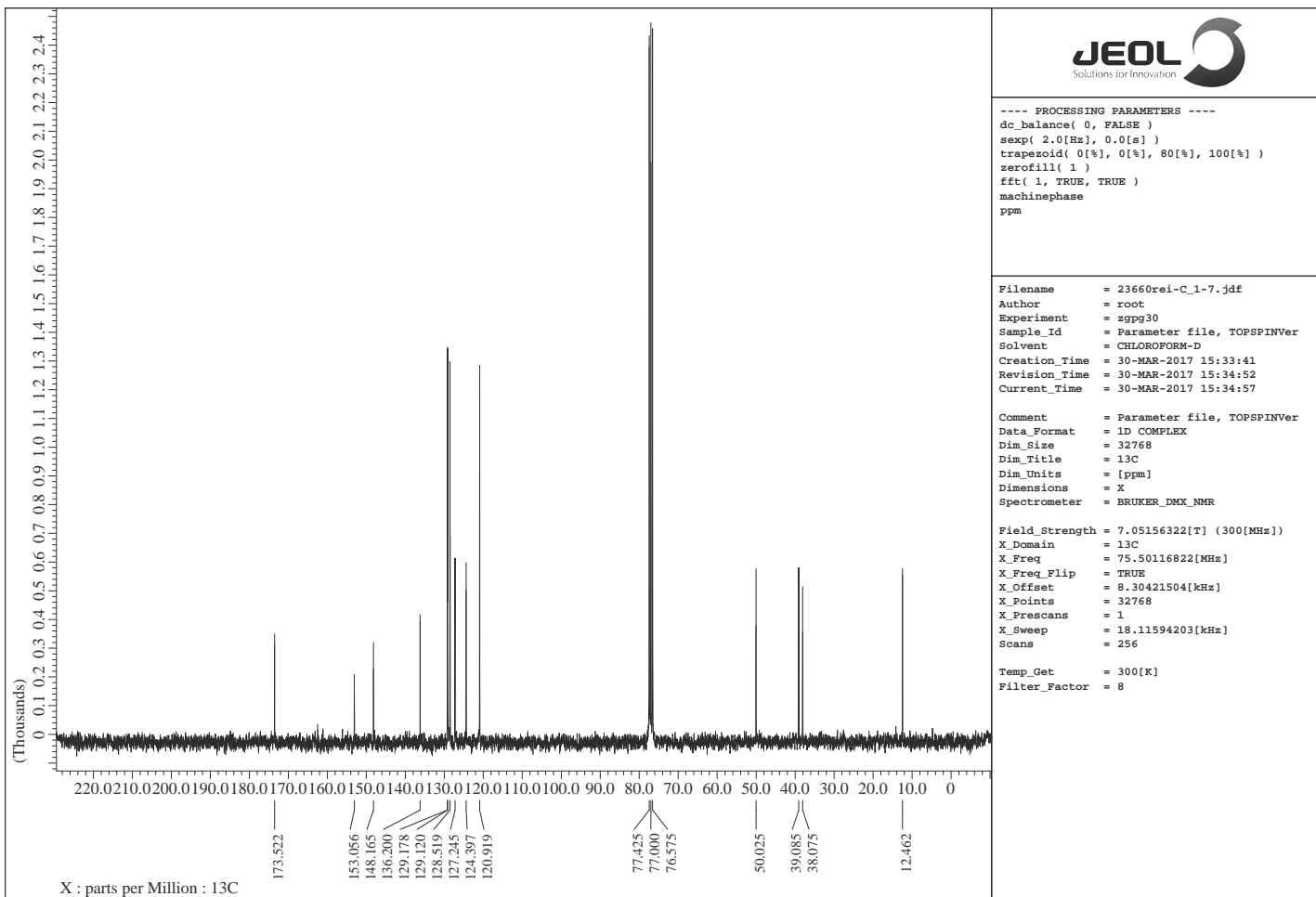
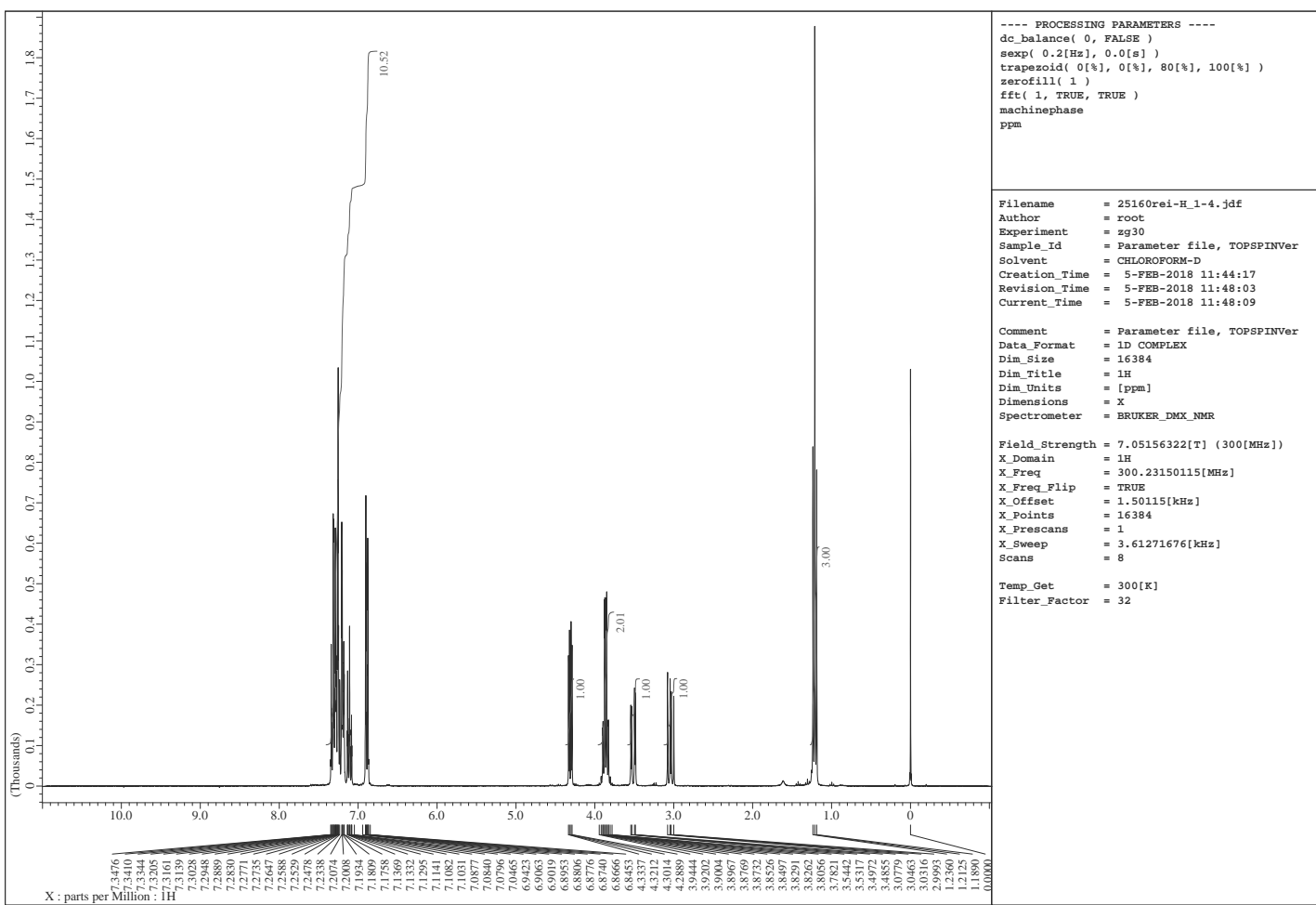


Figure S41. ^1H and ^{13}C NMR spectra of **4h**

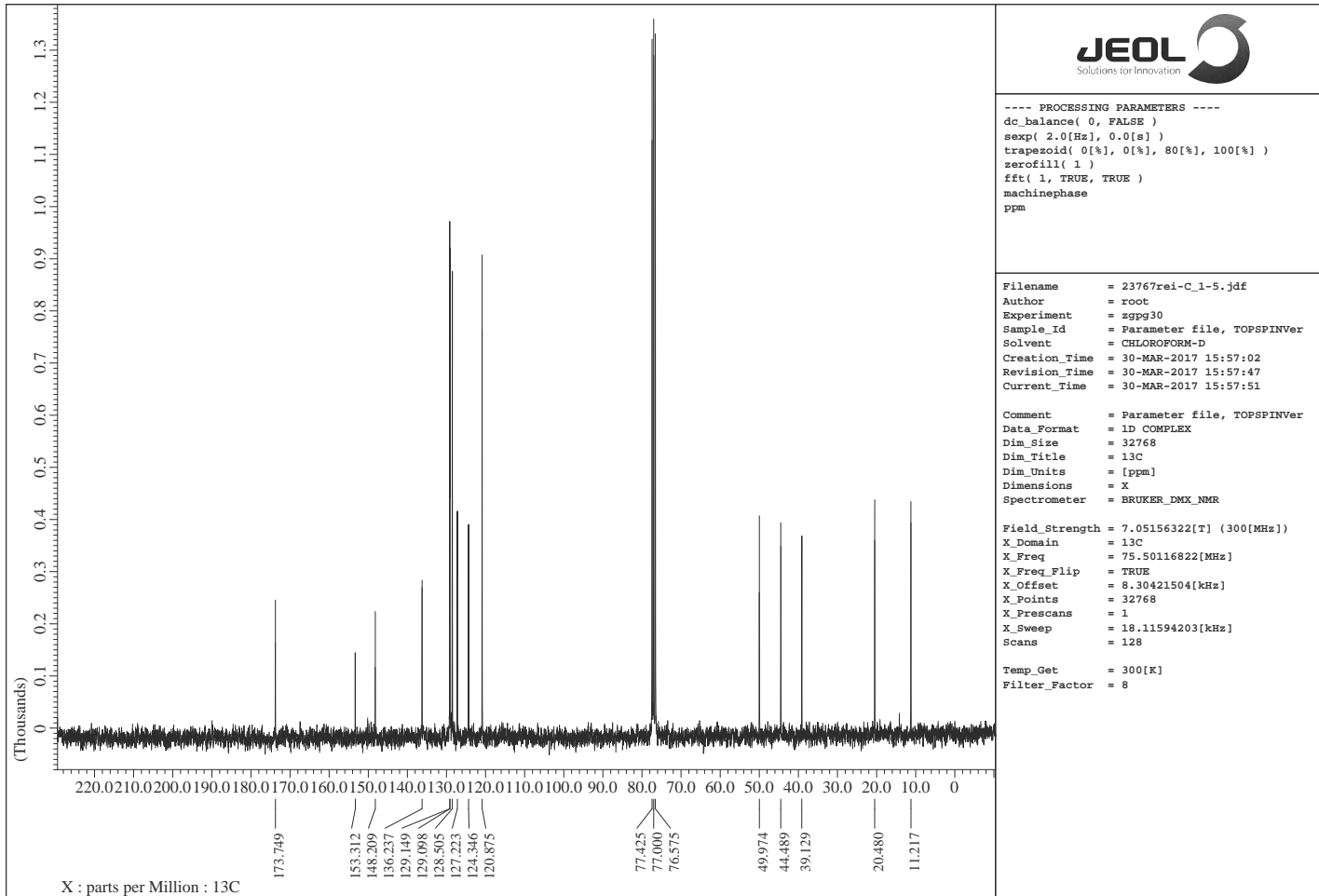
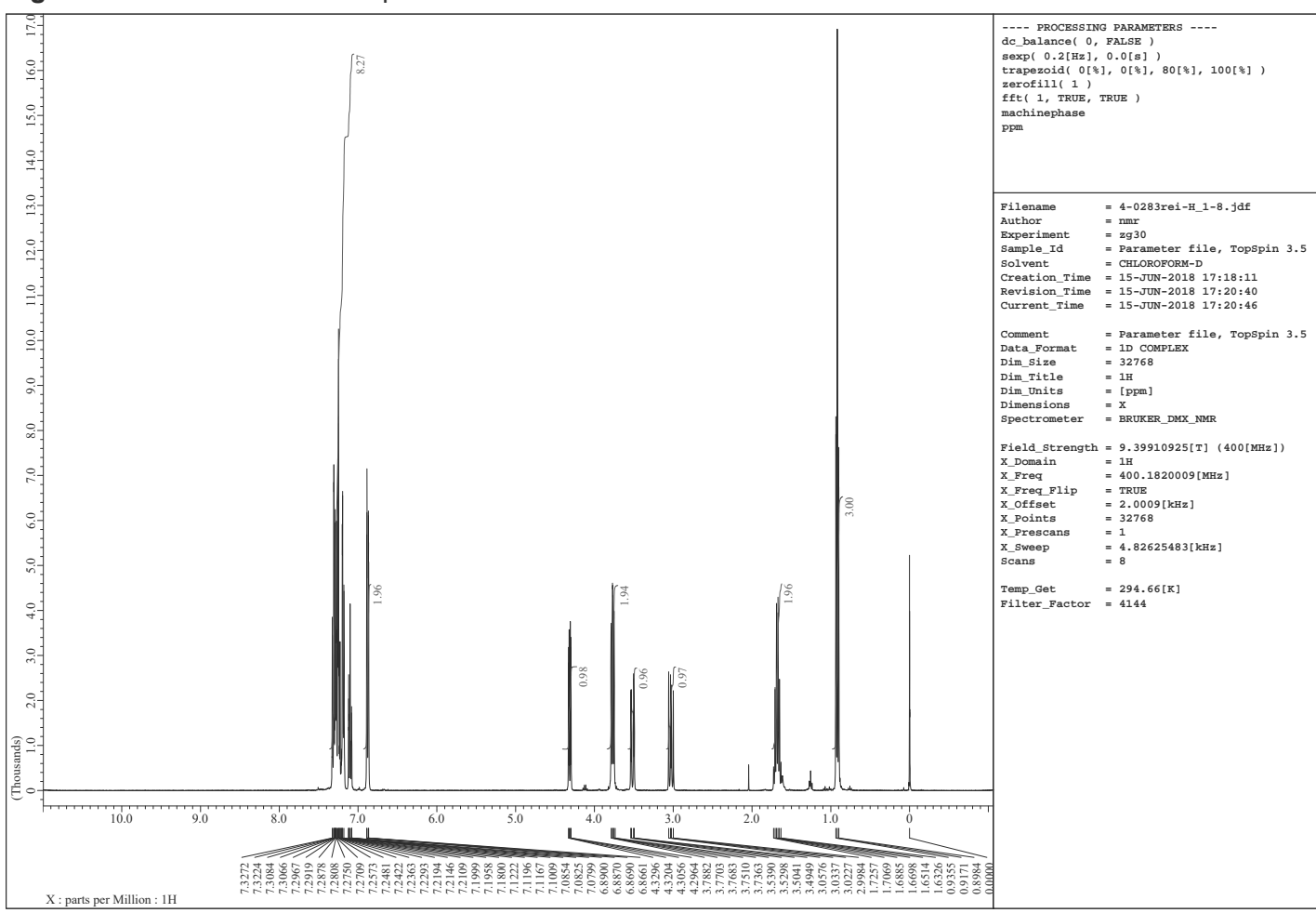


Figure S42. ^1H and ^{13}C NMR spectra of **4i**

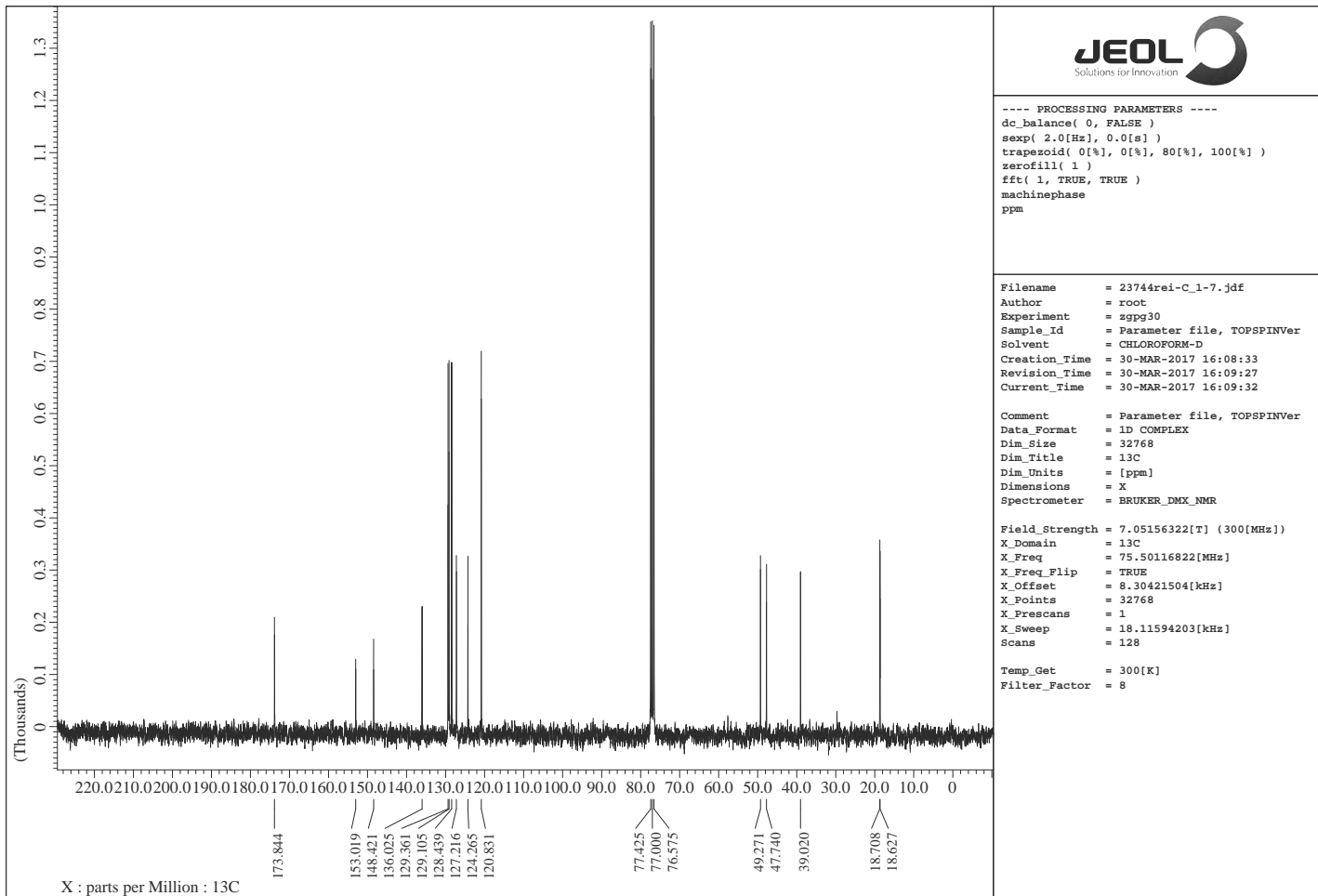
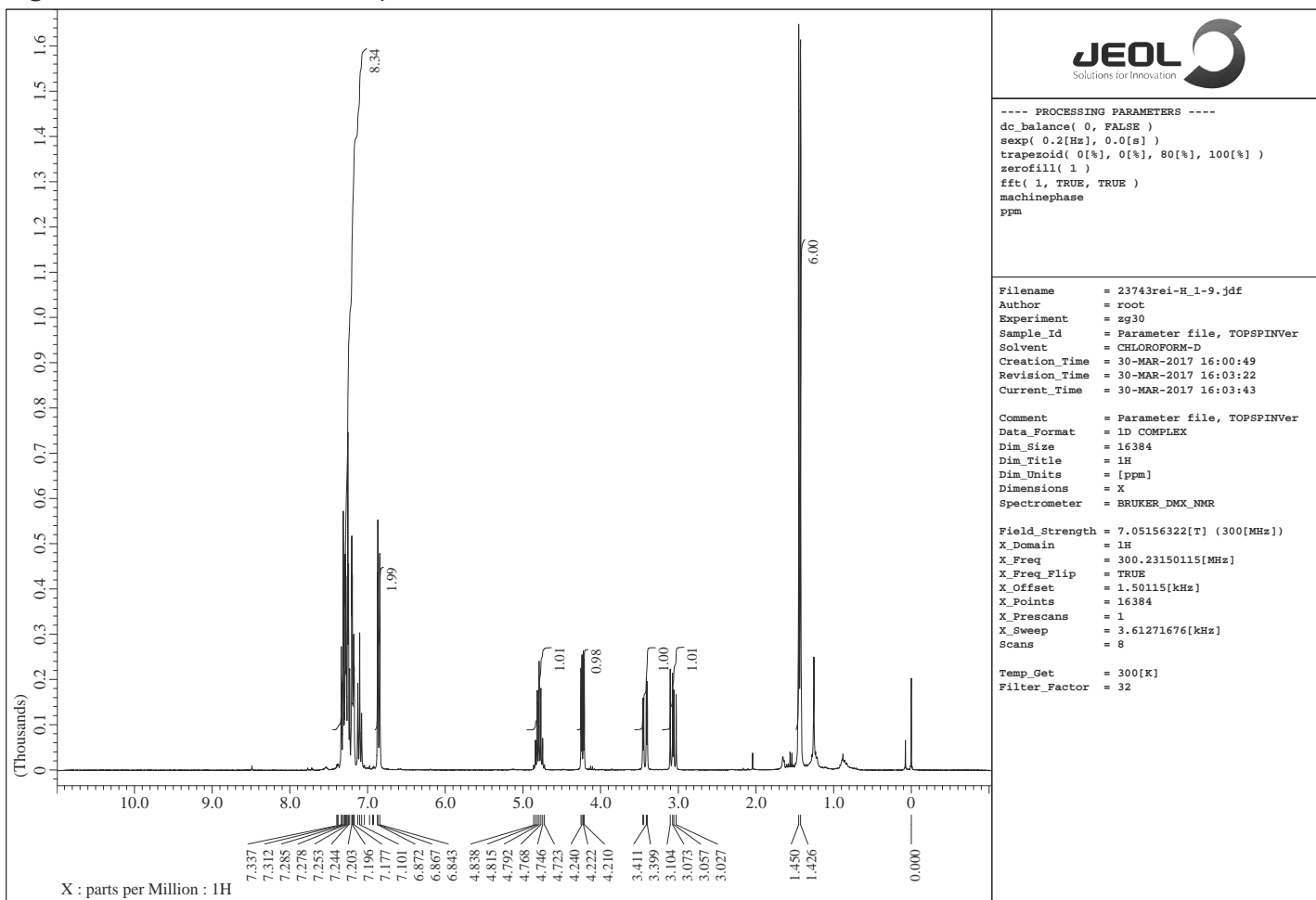


Figure S43. ^1H and ^{13}C NMR spectra of **4j**

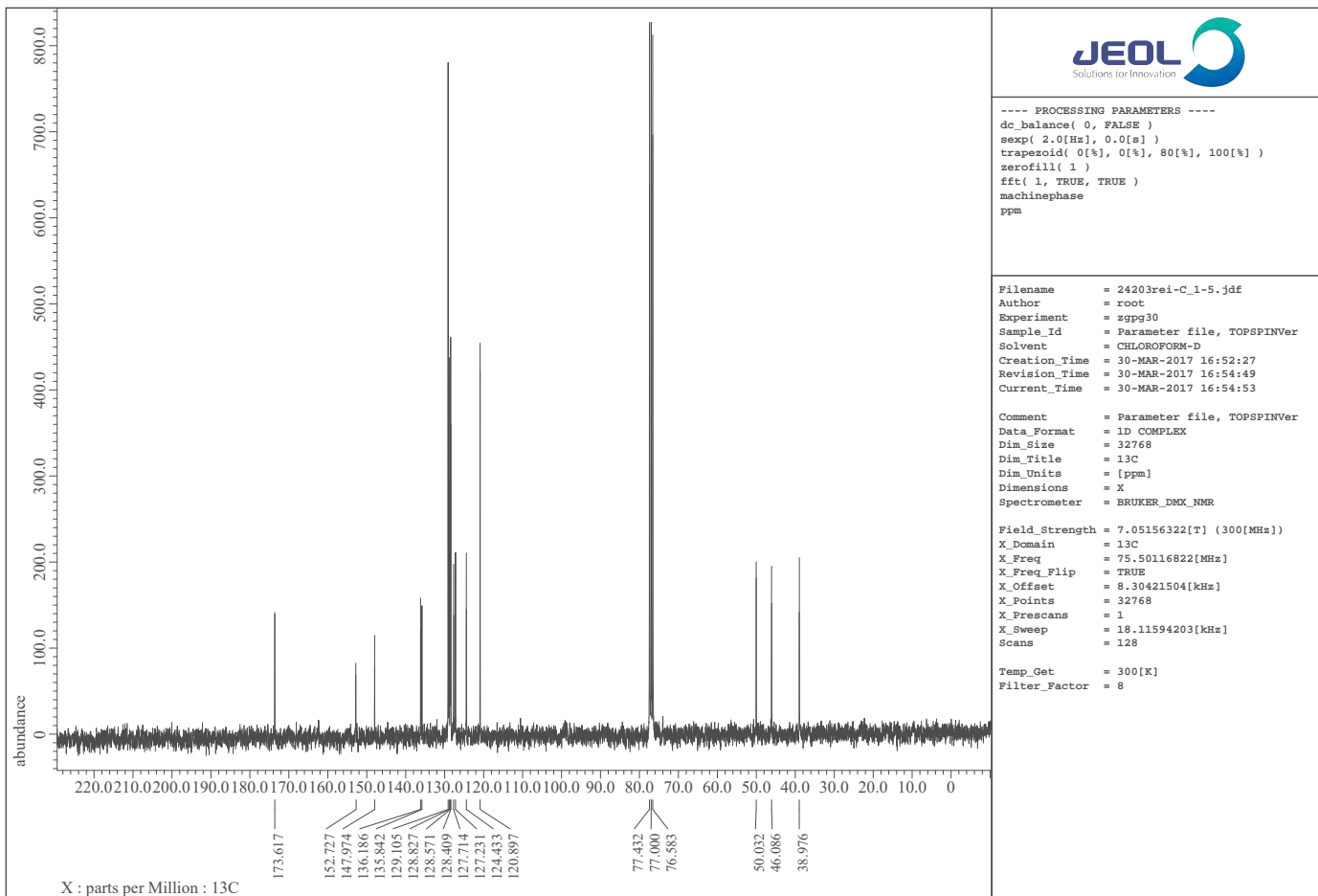
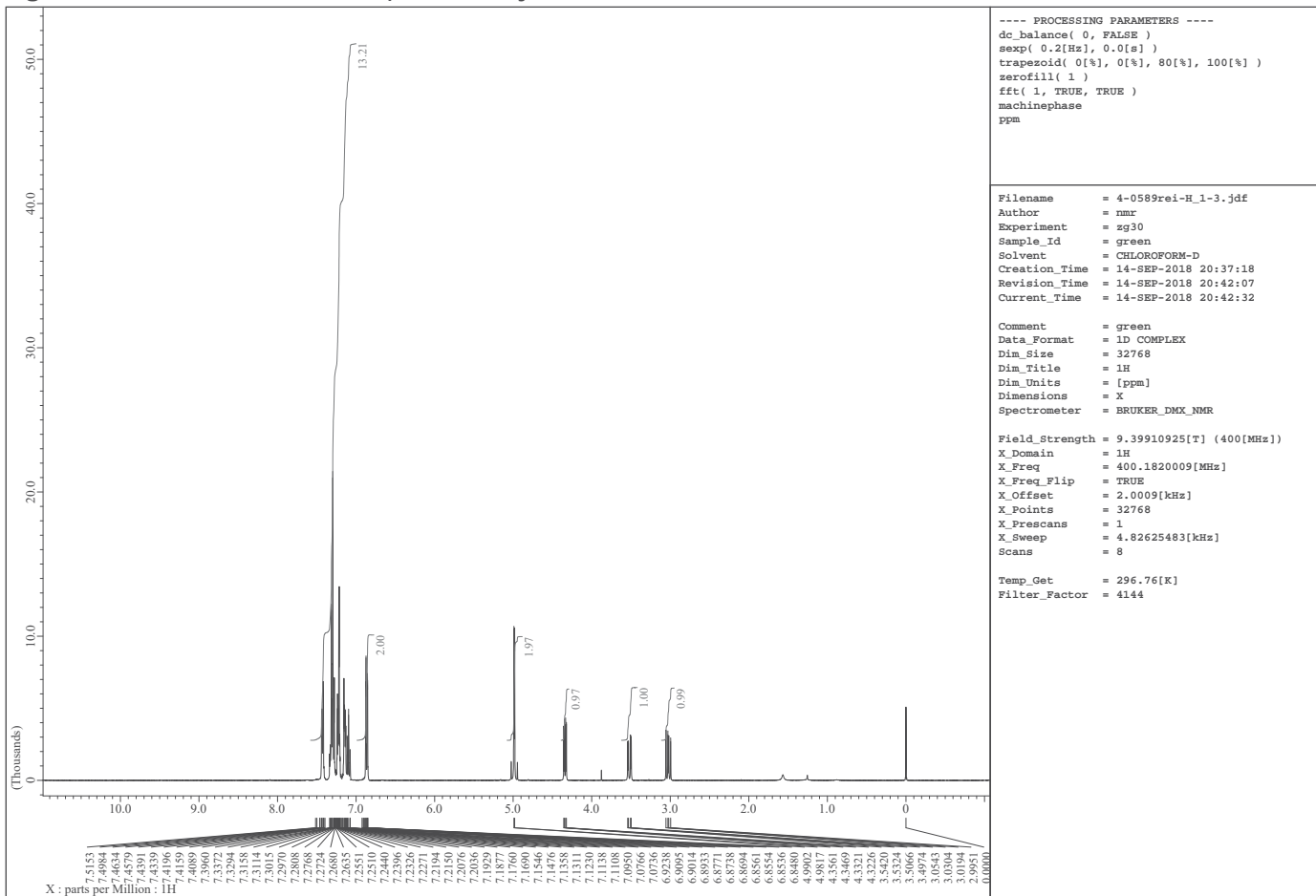


Figure S44. ^1H and ^{13}C NMR spectra of **5b**

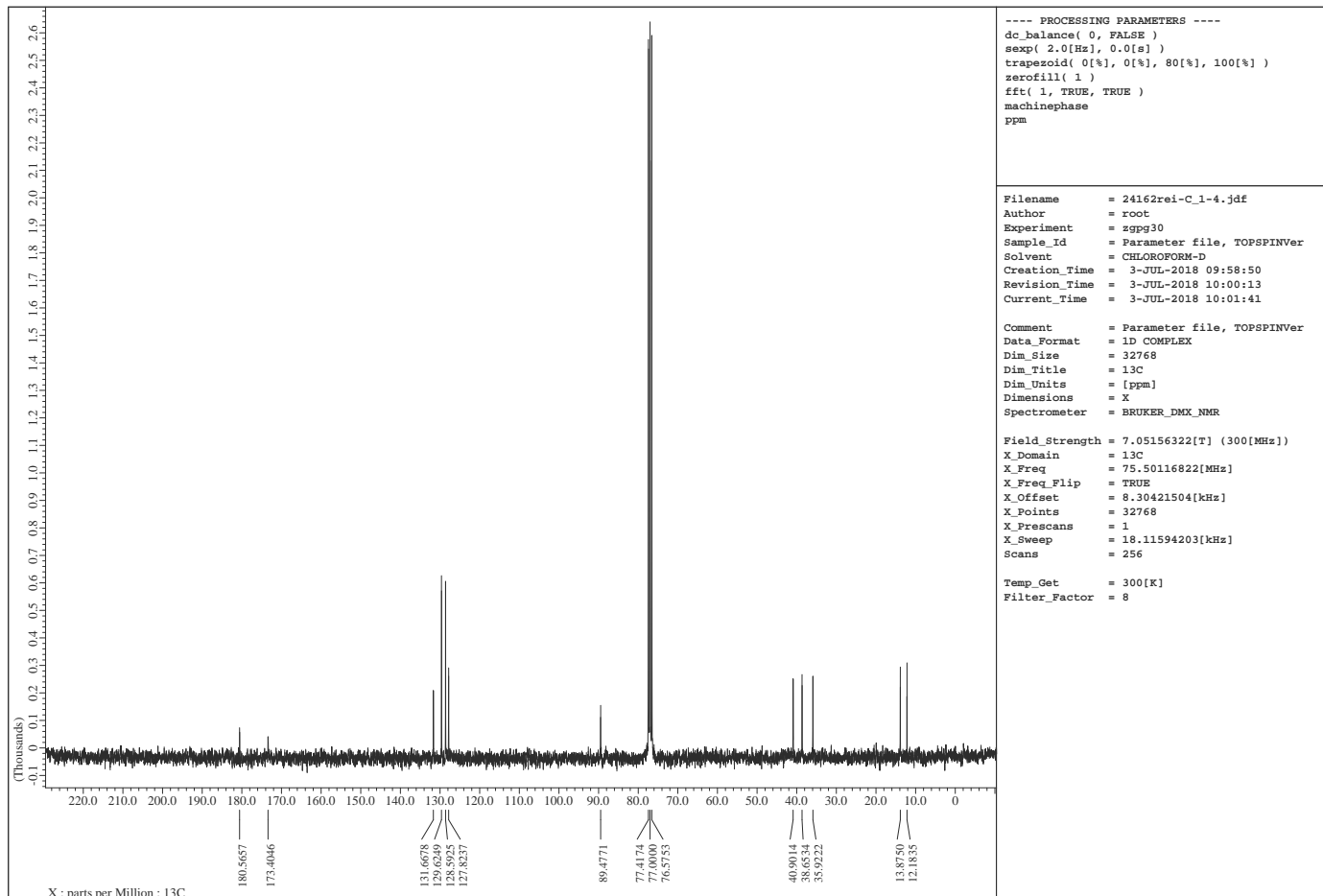
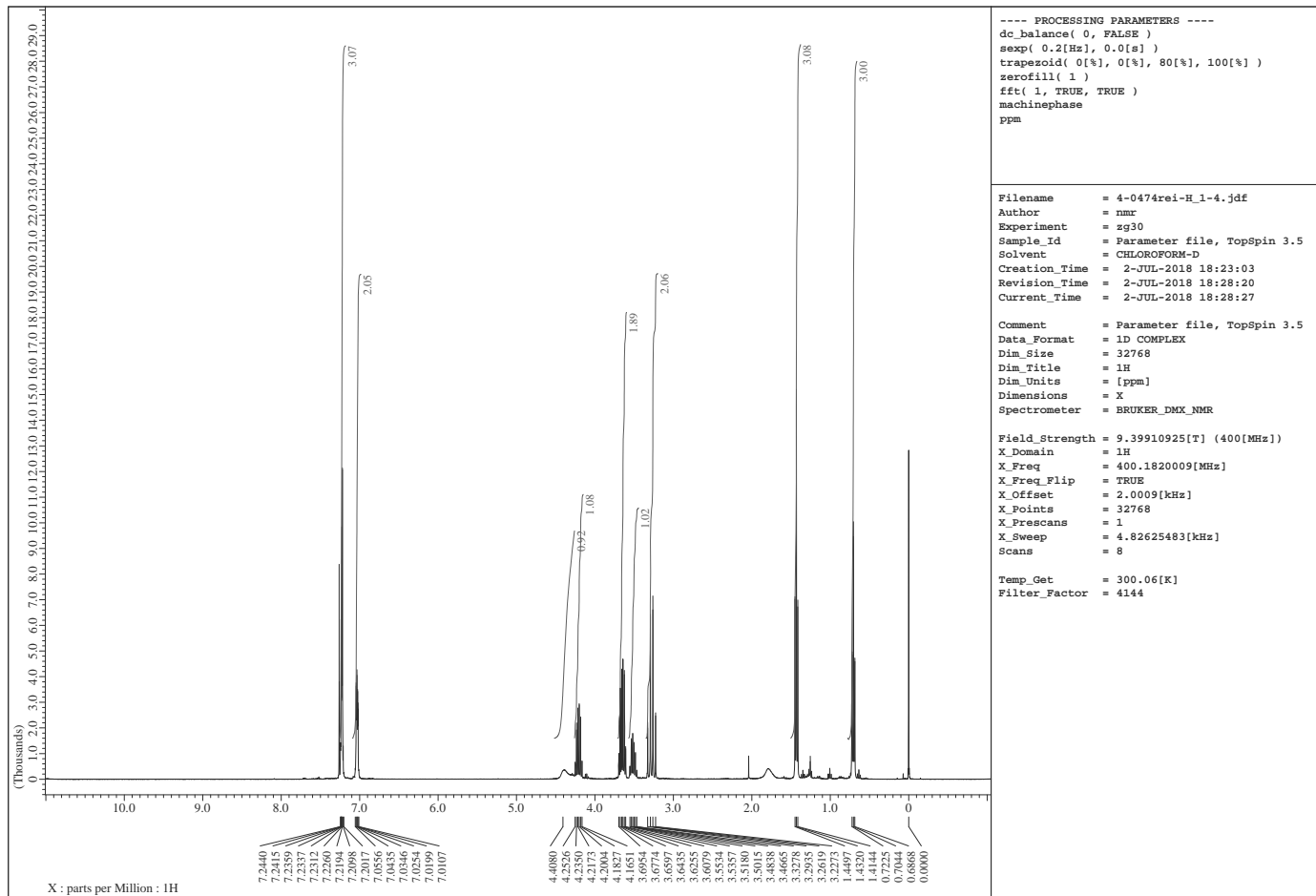


Figure S45. ^1H and ^{13}C NMR spectra of **5c**

